Filarial infection and filarial antigen administration promotes glucose tolerance in diet-induced obese mice

Dissertation

zur

Erlangung des Doktorgrades (Dr. rer. nat.)

der

Mathematisch-Naturwissenschaftlichen Fakultät

der

Rheinischen Friedrich-Wilhelms-Universität Bonn

vorgelegt von

AFIAT BERBUDI

aus

Jakarta, Indonesien

Bonn, 2015

Angefertigt mit Genehmigung der Mathematisch-Naturwissenschaftlichen Fakultät
der Rheinischen Friedrich-Wilhelms-Universität Bonn

1. Gutachter: Prof. Dr. Achim Hörauf
2. Gutachter: Prof. Dr. Sven Burgdorf

Tag der Promotion : 20.10.2015
Erscheinungsjahr : 2015

Title :

Filarial infection and filarial antigen administration promotes glucose tolerance in diet-induced obese mice

Table of Contents

Table of Figures

Summary

Excess of energy intake combined with reduced physical activity leads to accumulation and expansion of adipose tissue. Imbalance between adipose tissue expansion and oxygenation during a high fat diet results in adipocytes stress and defects to store excessive energy. Pro-inflammatory mediators produced by stressed adipocytes and infiltrated classically activated macrophages eventually trigger low grade and chronic inflammation. Several studies highlighted that obesity-induced chronic inflammation is a critical factor that triggers insulin resistance and alters the cellular composition within the adipose tissue.

Given that parasitic helminths are well known immunoregulators of host immune responses which induce a suppressive, regulatory immune response via the induction of regulatory T cells, AAM, anti-inflammatory cytokines, and induce a type 2 immune response, the aim of this thesis was to investigate whether the tissue–invasive rodent filarial nematode *Litomosoides sigmodontis* (*L.s.*) mediates protection against insulin-resistance in diet-induced obese (DIO) mice by counter-regulating inflammatory immune responses during a high fat diet.

In order to study whether *L.s*. infection has a beneficial impact on high fat diet-induced insulin resistance, 6 week old male BALB/c mice were fed with a high fat diet and a subgroup was infected 2-4 weeks later with *L.s*.. Following 8-10 weeks on high fat diet, mice were evaluated for glucose tolerance and immune responses. In separate experiments, daily injections of LsAg for 2 weeks were performed in male DIO C57BL/6 mice after 7-12 weeks of high fat diet feeding. DIO mice were evaluated for glucose tolerance and immunological studies afterwards.

This thesis demonstrates that both *L.s.* infection and LsAg administration improved glucose tolerance in DIO mice. This improvement was associated with increased eosinophil and AAM frequencies within the stromal vascular fraction of the epididymal adipose tissue (EAT) during *L.s.* infection and LsAg administration. Absence of eosinophils abrogated the beneficial impact of *L.s*. infection as was shown with eosinophil deficient dblGATA mice, suggesting that improved glucose tolerance by *L.s.* infection was dependent on eosinophils.

Further analysis showed reduced total numbers of B cells, but an increased frequency of the B1 subset in the adipose tissue of *L.s.*-infected DIO mice compared to uninfected DIO controls. Accordingly, pathogenic IgG2a/b levels were lower in *L.s.*-infected animals compared to uninfected DIO controls. qPCR array analysis of EAT further revealed an induction of genes related to insulin signaling, cell migration, suppressive immune responses as well as a reduced expression of genes related to adipogenesis in *L.s.*-infected DIO mice. Our in vitro experiments using the 3T3-L1 pre-adipose cell line confirmed that LsAg treatment suppressed the differentiation to mature adipocytes.

Multiple gene expression analysis of EAT from DIO mice that obtained LsAg administrations further revealed an induction of type 2 immune responses, as well as an upregulated expression of genes-related to insulin signalling and genes-related to fatty acid uptake in LsAg-treated DIO mice. Two weeks of daily LsAg administration in DIO mice further improved body temperature tolerance under cold exposure, which was accompanied by an increased expression of *Ucp1* in EAT, suggesting that LsAg administration promotes browning of white adipose tissue and increased energy expenditure.

In conclusion, this thesis demonstrates that both *L.s.* infection and LsAg administration reduces diet-induced EAT inflammation, improves insulin signaling, and glucose tolerance. The findings of this thesis suggest that helminth-derived products may offer a new strategy to ameliorate diet-induced insulin resistance.

1. Introduction

1.1 Diabetes – a major health problem in the world

Diabetes is a tremendous health problem throughout the world. It is a chronic metabolic disease that is characterized by high blood glucose levels which are either due to the insufficient insulin production by the pancreas or an impaired insulin sensitivity [1]. Generally, diabetes is divided into 2 main types, type 1 diabetes (T1D) and type 2 diabetes (T2D).

Diabetes leads to a risk of several other diseases as a result of the macro- and microvascular blood vessel damage and affects many organs such as eyes, brain, heart, and kidney [2]. Recent studies further reported that diabetes is also associated with an increased risk to develop cancer and dementia [3,4]. Insulin therapy reduces the risk of these co-morbidities, but becomes more difficult over time and represents a major cost factor.

According to the International Diabetes Federation (IDF), around 387 million people in the world suffered from diabetes in 2014 [5]. Diabetes incidence is still increasing both in developed and developing countries worldwide (Fig.1). Without collective effort, the number of diabetes patients was predicted to increase by more than 55% by 2035 to a total of 592 million patients [2]. In 2014, it was reported that 4.9 million people died due to diabetes and US $612 billion were spent for diabetes healthcare [5].

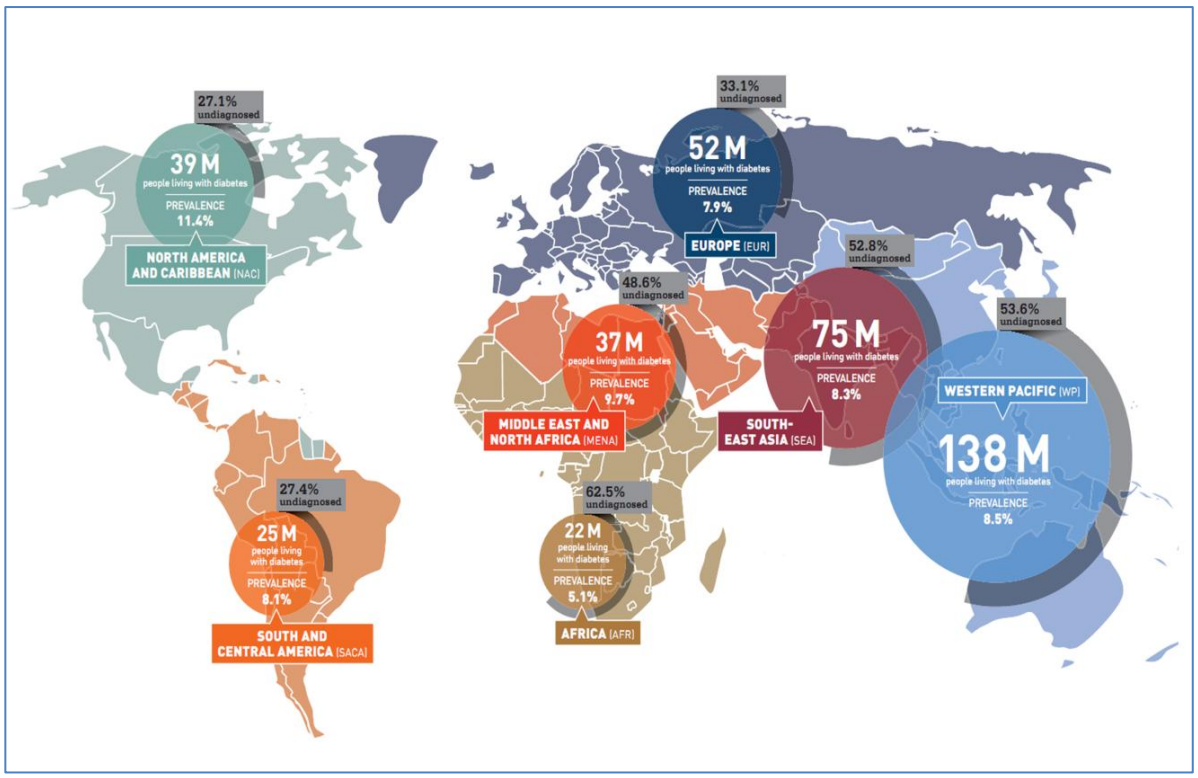

Figure 1. Worldwide number of people (20-79 years) suffering from diabetes in 2014.

Source: IDF Diabetes Atlas 6th edn. 2014 update [5].

1.1.1 Type 2 Diabetes

In most populations, 90% of all diabetes cases are due to T2D [6]. In this type of diabetes, insulin production by the pancreatic beta (ß)-islet cells still occurs but is insufficient to compensate the insulin resistance of insulin target tissues and results therefore in increased blood glucose levels. In other words, T2D can be defined as a metabolic disorder that is characterized by high blood glucose levels in the context of insulin-resistance and relative insulin deficiency. Insulin resistance is associated with obesity, ageing and physical inactivity [1]. In order to compensate the insulin resistance pancreatic islets initially enhance their cell mass and insulin secretion [7] and T2D develops when the functional expansion of β-islet cells fail to compensate for the degree of insulin resistance [7]. Exogenous insulin is required to control blood glucose levels if diet control or anti-hyperglycemic medication cannot maintain the normal blood glucose levels anymore. More than 50% of T2D patients require insulin

therapy due to an additional dysfunction of β-islet cells 10 years after the onset of insulin resistance [8,9].

1.1.2 Insulin and its role in energy metabolism

Glucose is an essential energy source for the body, especially for the brain. In order to be converted into energy, glucose has to be taken up by cells. Insulin is a peptide hormone produced and secreted by β-cells in the islets of the pancreas. Binding of insulin with its receptor allows glucose to enter the cells. Increased glucose levels in the blood stimulate the release of insulin from the ß-cells in pancreas [10].

Excess of glucose can be stored as glycogen in the liver. Between meals, when no glucose is supplied from the outside, these stores can be used to provide glucose for the brain. Skeletal muscle can also store large quantities of glucose in the form of glycogen when glucose is abundant. In contrast to the liver, it cannot release glucose to the blood to provide it as energy source for the brain [11].

Once Insulin binds to its receptor at the extra-cellular binding domain, the receptor will be activated, and induce tyrosine kinase activity in the intracellular part to phosphorylate tyrosine residues not only residing in the receptor itself but also in the insulin receptor substrate (IRS) molecules. Phosphorylated IRS binds and activates other proteins. In muscle and adipose tissue, the insulin cascade leads to the translocation of glucose transporter (GLUT)-4 from the intracellular compartment to the cell membrane [12]. Since GLUT-4 has a high affinity for glucose, it facilitates glucose transport into the cells effectively. In general, increased GLUT-4 expression on the cell membrane of muscle and adipose cells parallels the increased capacity of these cells to take up glucose.

In addition, receptor activation by insulin also activates the mitogen-activated protein kinases (MAPK) pathway [13]. Activated MAPK enters the cell nucleus, activates transcription factors of specific genes that are related to anabolic activity and activates the protein synthesis which results in an increased amino acid entry into the cells. Thus, insulin also reduces amino acid levels in the plasma.

Unlike in the adipose and muscle cells, the glucose transport into liver cells is facilitated by GLUT-2, but the presence of GLUT-2 is not influenced by insulin. Nevertheless, the fate of glucose in liver cells is regulated by insulin. Insulin activates glucokinase, an enzyme which phosphorylates incoming glucose to be incorporated into glycogen. In contrast, catabolic activity like glycogenolysis and gluconeogenesis is inhibited by insulin [14].

In addition, insulin enhances liver glycolysis and promotes lipogenesis, the formation of fat in the liver, by stimulating the synthesis of fatty acids from glucose. These fatty acids are then incorporated into triglyceride (TG) after esterification with glycerol and stored as lipid droplets or are exported to the blood as very low density lipoproteins (VLDL) [15].

1.1.3 Insulin action in adipocytes

The main function of adipocytes is to store excess fatty acids in the form of TG. If required, adipocytes can release fatty acids as energy substrate for other tissues like skeletal muscle. The majority of the fatty acids reach the adipose tissue as TG in two types of lipoproteins, chylomicrons from the intestine and VLDL from the liver. Adipocytes secrete an enzyme, lipoprotein lipase (LPL), which functions on the luminal surface of the capillary endothelial cells to hydrolyze TG from lipoproteins into fatty acids and glycerol. After hydrolization by LPL, the liberated fatty acids are taken up into adipocytes. Insulin can enhance the supply of fatty acids to adipocytes by inducing the expression of LPL in adipocytes.

In the fed state, insulin stimulates the translocation of GLUT-4 to the plasma membrane and activates glycerolphosphate acyl transferase for the TG synthesis in adipocytes. In addition, insulin also inhibits lipolysis that releases fatty acids from TG by activating phosphodiesterase (PDE) to reduce cellular cyclic Adenosine Monophosphate (cAMP) levels [16]. In the insulin resistant state, lipolysis is increased and leads to fatty acid release into the circulation.

1.1.4 Obesity, inflammation and insulin resistance

Excessive food intake in combination with reduced physical activity initiates the imbalance between energy input and energy expenditure [17]. The extra energy will be stored as reserved energy source in the form of glycogen in liver and muscle as well as lipid in adipose tissue [17]. As professional storage, adipose tissue has an almost unlimited capacity to store excessive energy. The diameter of a normal adipocyte is in the range of 50µm. Lipid droplet formation in the adipocytes continuously increase the storage of excessive energy and leads to lipid accumulation and adipocyte enlargement called hypertrophy [18]. In this condition, the diameter of adipocytes increases up to 100µm. This eventually expands the body fat tissue in whole, especially in subcutaneous and visceral adipose tissue (VAT) and results in obesity.

Obesity is a major risk factor to develop T2D and is associated with low grade chronic inflammation. Adipocyte hypertrophy and tissue expansion in obesity leads to an impaired oxygenation of cells due to the imbalance between increase of oxygen demand and supply by blood innervations [19,20]. Overtime, adipocytes suffer from hypoxia and undergo oxidative stress which initiates inflammatory cytokine production and apoptosis [19,20]. This leads to the infiltration and accumulation of classically activated macrophages (CAM) into the adipose tissue, resulting in low grade inflammation and changes in the cellular composition (Fig. 2).

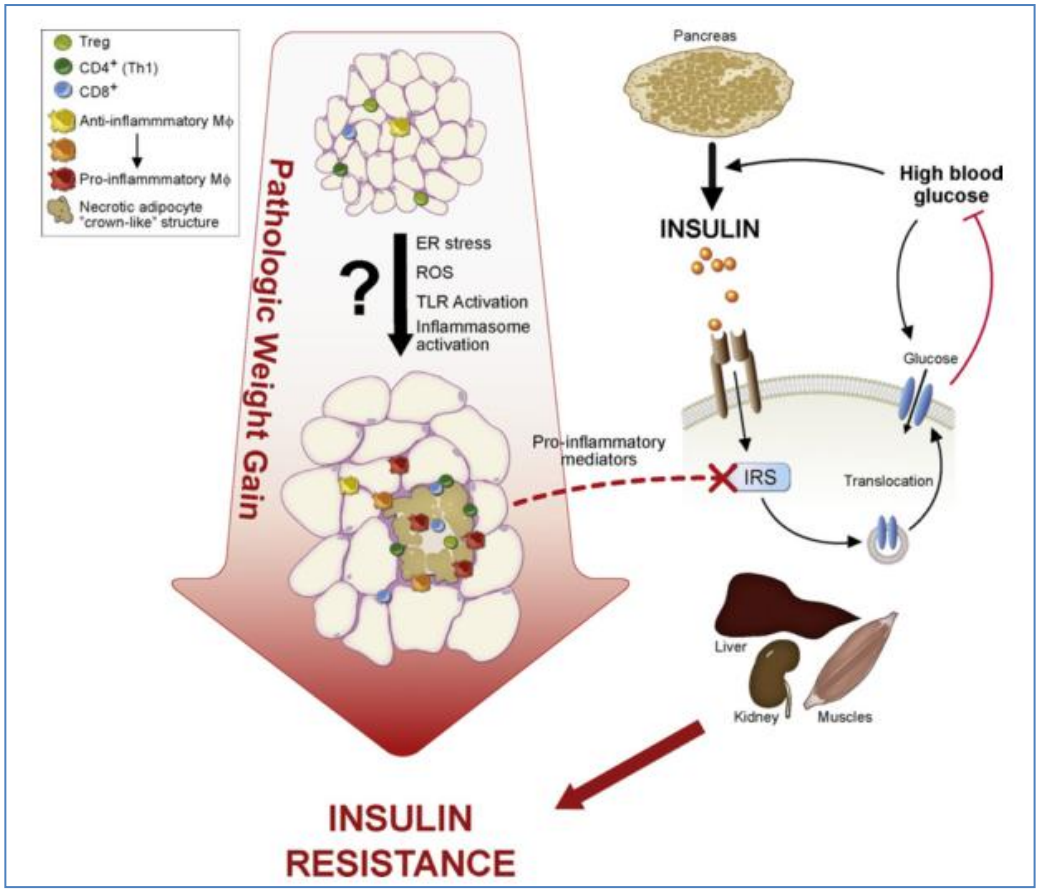

Figure 2. Obesity leads to adipocyte apoptosis and macrophage infiltration into adipose tissue. Several inflammatory responses including Toll-like receptor (TLR) and inflammasome induction, reactive oxygen species (ROS) release, and endoplasmic reticulum (ER) stress lead to pro-inflammatory cytokine production which impairs insulin signaling in adipose tissue, muscle, liver, and kidney, resulting in elevated blood glucose levels.

Source : Cipolletta D, Kolodin D, Benoist C, Mathis D. Tissular T(regs): a unique population of adipose-tissue-resident Foxp3+CD4+ T cells that impacts organismal metabolism. Semin Immunol. Elsevier Ltd; 2011;23: 431–7 [21].

1.1.5 Mechanisms of insulin resistance

Several cytokines and chemokines, such as monocyte chemotactic protein (MCP)-1, the chemokine (C-C motif) ligand (CCL)-2, interleukin (IL)-6, IL-1β, macrophage migration inhibitory factor (MIF), and tumor necrosis factor-alpha (TNFα), can be released by both stress adipocytes and macrophages [22–24].

Elevated levels of pro-inflammatory cytokines as mentioned above was evidenced in obesity and is associated with insulin resistance [25]. In addition, C-reactive protein (CRP), IL-6, plasminogen activator Inhibitor (PAI-1) and many other inflammatory mediators were reported to be increased in the plasma of obese mice [24,26]. TNFα, FFA, diacylglyceride (DAG), ceramide, reactive oxygen species (ROS) and hypoxia activate intracellular signaling pathways such as IκBα kinase β (IKKβ) and c-Jun N-terminal kinase (JNK)-1 in adipose tissue and liver [27] and result in the inhibition of IRS-1 [28–30]. Moreover, TNFα leads to insulin resistance via the inhibition of the peroxisome proliferator-activated receptor gamma (PPARγ) function [31,32]

IKKß activation phosphorylates Iκßα, induces Iκßα ubiquitination and its degradation in the proteosome results in the translocation of nuclear factor kappa B (NFκß) into the nucleus to induce the expression of various genes involved in inflammation and other immune responses. IKKß also inhibits insulin signaling through phosphorylation of serine residues of IRS-1 in adipocytes [29,33]. JNK activation also inhibits insulin signaling by phosphorylation of IRS-1 in response to TNFα [30,34] (Fig. 3).

Alternatively, insulin signaling is inhibited through the Janus kinase / signal transducer and activator of transcription (JAK/STAT) pathway. Tyrosine phosphorylation of STAT by JAK kinases induces dimerization and translocation of STAT to the nucleus [35] and leads to IRS-1 phosphorylation at Serine (Ser)636 and Ser307 [36].

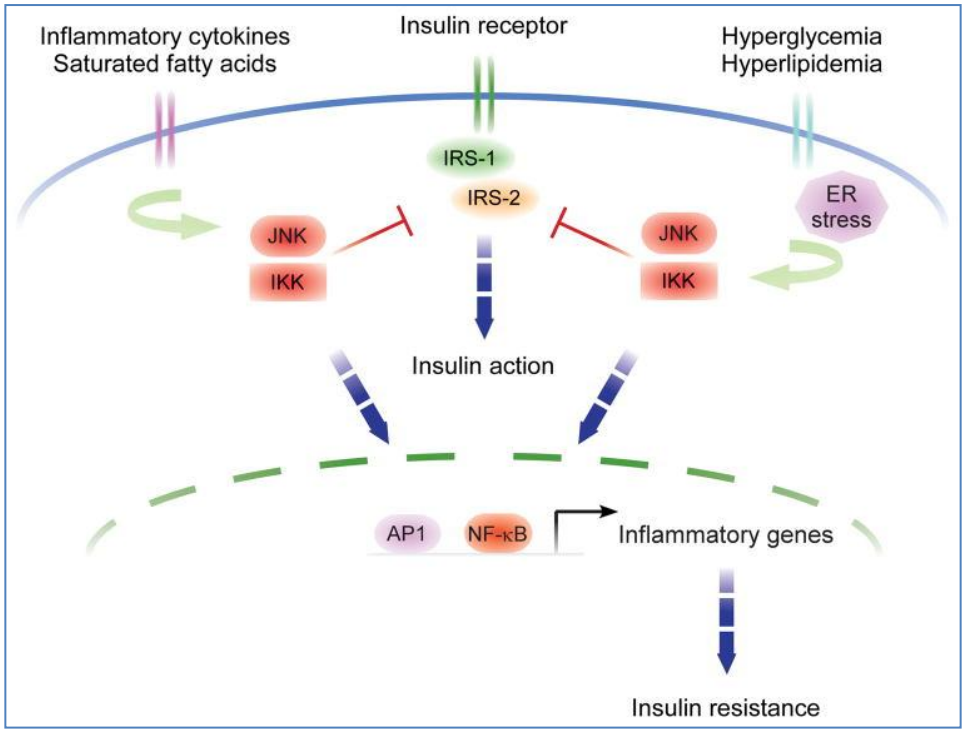

Figure 3. Intracellular mechanisms of inflammatory insulin resistance. Insulin signaling is transmitted from the cell surface to cytoplasmatic and nuclear responses via tyrosine phosphorylation of insulin receptor substrate (IRS)-1 and -2. Nevertheless, insulin action is inhibited through serine phosphorylation of IRS substrates by IKKβ and JNK1, the mediators of stress and inflammatory responses. In addition, JNK1 and IKKβ induce the transcriptional activation of inflammatory genes, resulting in insulin resistance in an autocrine and paracrine manner in tissues. Furthermore, during obesity, influx of free fatty acids (FFA) and glucose also activate JNK1 and IKKβ signaling pathways.

Source: Odegaard JI, Chawla A. Alternative macrophage activation and metabolism. Annu Rev Pathol. 2011;6: 275–97 [37].

As a consequence of insulin signaling inhibition, glucose in the circulation cannot be uptaken into the cells and leads to high glucose levels in the blood plasma. Furthermore, insulin signaling inhibition impairs anabolic metabolism, and shifts the metabolism to catabolic states including breakdown of lipid storage (lipolysis) and results in elevated free fatty acids (FFA) in the blood circulation [38]. Subsequently, fatty acids from food intake further increases the TG levels in the blood. Given the

reduced ability of adipose tissue to store TG during insulin resistance, excessive TG are stored ectopically in the liver, leading to fatty liver (hepatosteatosis) [17]. In addition, ectopic lipid storage also occurs in muscle tissue [39]. The accumulation of lipid intermediates such as DAG in non-adipose tissue results in cellular dysfunction and cell death and is termed lipotoxicity. By inducing phosphorylation of IRS at serine residues, DAG leads to the inactivation of IRS and triggers lipotoxicity-induced insulin resistance [40]. On the other hand, along with increasing levels of inflammatory cytokines and chemokines, systemic FFA trigger the inflammation of insulin target organs like liver and muscle via Toll-like receptor (TLR)-4 [41–43]. Taken together, both inflammatory mediators and hyperlipidemia can trigger insulin resistance.

1.1.6 Alteration of cellular composition during obesity

Low grade inflammation during obesity is associated with the alteration of the cellular composition in the adipose tissue [21]. Infiltration of immune cells into the inter-space of adipocytes within the adipose tissue changes the cellular composition within the adipose tissue and leads to the formation of “crown-like structures”. Those changes include the loss of eosinophils, alternatively activated macrophages (AAM) and regulatory T (Treg) cells and increases accumulation of classically activated macrophages (CAM) and B-cells [44–47].

1.1.6.1 Eosinophils

Eosinophils are induced by type 2 immune responses and may function as effector cells, antigen–presenting cells (APC) [48] and were recently reported to be involved in tissue homeostasis, modulation of adaptive immune responses and innate immunity to certain microbes [49].

Eosinophils are well known for their function during helminth infection and allergic diseases [48]. Eosinophils are able to produce type 1, type 2 as well as immunoregulatory cytokines and are involved in the regulation of type 2 immune responses [49]. Furthermore, eosinophils can produce molecules that are implemented in protective immune responses against parasitic filarial nematodes

as was sown for eosinophil peroxidase (EPO) and major basic protein (MBP) [50–52].

Interestingly, recent studies revealed that eosinophils are also involved in the metabolic homeostasis and regulation of energy expenditure. Wu et al. reported that in adipose tissue, eosinophils are present in low numbers and decline during obesity in mice. They also demonstrated that IL-4 producing eosinophils play a role in maintaining AAM in visceral adipose tissue and promote glucose tolerance in diet-induced obese (DIO) mice [44]. Conversely, the absence of eosinophils impairs glucose tolerance in DIO mice [44,53]. In this context they further demonstrated that infection with the intestinal nematode *Nippostrongylus brasiliensis* increased eosinophil numbers in the adipose tissue of mice.

Eosinophils were also linked indirectly to energy expenditure through their role in sustaining AAM in adipose tissue by secreting IL-4. Under cold exposure, AAM produce catecholamine which can induce the browning of adipose tissue, thus increasing energy expenditure [54,55]. A recent study further reported that meteorin-like (Metrnl), a new protein which is produced in muscles during exercise and adipocytes during cold exposure, has been identified as an inducer of IL-4 expressing eosinophils in adipose tissue [56]. Hence, eosinophils may have a role to ameliorate insulin resistance via suppression of inflammatory immune responses and by increasing energy expenditure.

1.1.6.2 Macrophages

Macrophages have an important role in immune responses and tissue homeostasis. Numerous studies reported that various stimulations activate macrophages to release cytokines, chemokines, and metabolic enzymes in distinct patterns that ultimately generate the variation of functions seen in inflammatory and non-inflammatory settings. In general, CAM promote inflammation and AAM suppresses inflammation [57,58]. CAM are characterized by high levels of IL-12, inducible nitric oxide synthase (iNOS or NOS2), and major histocompatibility complex (MHC) class II expression [57,58]. During obesity, CAM infiltrate into the

adipose tissue (49), causing low grade inflammation by production of TNFα and other pro-inflammatory cytokines (50). Polarization of CAM are induced by LPS and interferon (IFN)γ [59].

Unlike CAM, polarization of AAM are induced by IL-4 and IL-13 [57], which can be produced by eosinophils and Th2 cells during type 2 immunity [41]. AAM produce anti-inflammatory IL-10, arginase, and Resistin-Like Molecule alpha (RELMα) [35,60]. In addition, arginase, an enzyme expressed in AAM blocks iNOS activity through a variety of mechanisms, including competition for arginine which is required for nitric oxide (NO) production [61].

Thus, AAM are believed to suppress inflammatory responses and promote tissue repair [62]. In addition, recent studies demonstrated that IL-4–mediated AAM polarization is associated with the activation of transcription factors that are involved in the lipid oxidative metabolism including PPARγ and PPARγ coactivator 1β (PGC-1β) [63].

1.1.6.3 Regulatory T-cells

Tregs are a subset of T lymphocytes that constitute 5–20% of the cluster of differentiation (CD)4+ T-cell population [64]. They mediate immune suppression in the contexts of autoimmunity, allergy, inflammation, infection, and tumorigenesis [65,66]. Tregs regulate other T cell populations and influence innate immune cell activity [67–69]. Treg cells are marked by expression of the forkhead–winged-helix transcription factor-3 (Foxp3) as well as CD25.

Based on their origins, Tregs are divided into two main groups: thymus derived natural Tregs (nTreg) and inducible Tregs (iTreg). Natural Tregs circulate in the blood in the absence of pathogens or tissue damage while inducible Tregs (iTreg) have a regulatory function after pathogen or neoplasm exposure. In parasitic infection, induction of Tregs is believed as a strategy used by the helminths to modulate the host's immune response, facilitating their long term survival.

Tregs are present in the visceral adipose tissue and are associated with improved insulin sensitivity. In lean mice, frequency of adipose tissue Tregs is 20-30% of CD4+ T-cells, while in obese mice, the frequency of Treg drops by 70% compared to lean mice. Induction of Tregs by injecting anti-CD3 specific antibodies to diet-induced obese (DIO) mice was demonstrated to improve glucose tolerance [64,70]. The exact mechanisms by which regulatory CD4+ T cells promote insulin sensitivity require further study, but it is suggested to rely on the induction of IL-10–secreting AAM [70].

1.1.6.4 B-cells

During high fat (HF) diet-induced obesity, total B cell populations increase in visceral adipose tissue and peak by 3–4 weeks after the initiation of HF diet [46,71]. B cells consist of distinct subsets including B-1 and B-2 cells. B-1 cells dominate in mucosal tissues and pleural/peritoneal cavities while B-2 cells are dominant in secondary lymphoid organs [72]. B-1 cells are further classified as B-1a cells which produce natural Immunoglobulin (Ig)-M antibodies and B-1b cells which respond to T-cell-independent antigens in adaptive humoral immune responses [73]. B-2 cells are the most common B cells and are generated in the bone marrow. B-2 cells respond to T-cell dependent antigens and are responsible for the adaptive humoral immunity. IL-10 producing B cells, called B-10 cells, form part of a broader subset of regulatory B cells [74].

Winer et al. demonstrated that B cell numbers increase during HF diet in DIO mice [46]. In DIO mice, B cell accumulation in VAT is linear to the occurrence of insulin resistance. The negative impacts of B cells on glucose metabolism are linked to the activation of pro-inflammatory macrophages and T cells and the production of pathogenic IgG antibodies. After several weeks on HF diet, class switching from IgM^+ IgD^- to IgG^+ increases, especially to pro-inflammatory IgG2c in VAT [46], leading to increased levels of IgG2c in spleen and serum of obese mice. Accordingly, treatment with a B cell–depleting CD20 antibody attenuates disease, whereas transfer of IgG from DIO mice rapidly induces insulin resistance and glucose intolerance in an fragment crystallizable (Fc) -dependent manner [46].

1.2 The Hygiene Hypothesis

Epidemiological studies reported that there are increased rates of disease-related allergies such as asthma, rhinitis and dermatitis in developed countries compared to developing countries [75]. Numerous cohort studies further showed an inverse correlation between helminth infections and allergies, e.g. in children who are infected with *Schistosoma haematobium* [76,77] and *Schistosoma mansoni* [78–80]. In contrast, clearance of helminth infection increases skin test reactivity in children [81,82]. Therefore, increased incidence of allergies has been correlated with improved hygiene in developed countries and a lower incidence of childhood infections. This lack of infection may lead to a dysregulated immune system which facilitates the development of allergies and led to the concept of the hygiene hypothesis.

Antihelminthic treatment during pregnancy in a population endemic for schistosome and hookworm infections increased the incidence of atopic eczema in the offspring [83,84]. In addition, studies in Ecuador and Vietnam have reported that the prevalence of skin allergic and allergen skin sensitization were increased in children who received long term antihelminthic treatment [81,85]. In line with this, a cross sectional study in a poor sanitation area in Vietnam has reported that prevalence of allergen skin test sensitization is reduced in a population of children with a high prevalence of hookworm infection [86].

The ‘hygiene hypothesis’ was later postulated not only to explain the inverse correlation between the incidence of infections and the rise of allergic diseases but also autoimmune diseases. Accordingly, Zaccone et al. reported that the incidence of T1D is positively correlated with hygiene conditions [87] (Fig. 4).

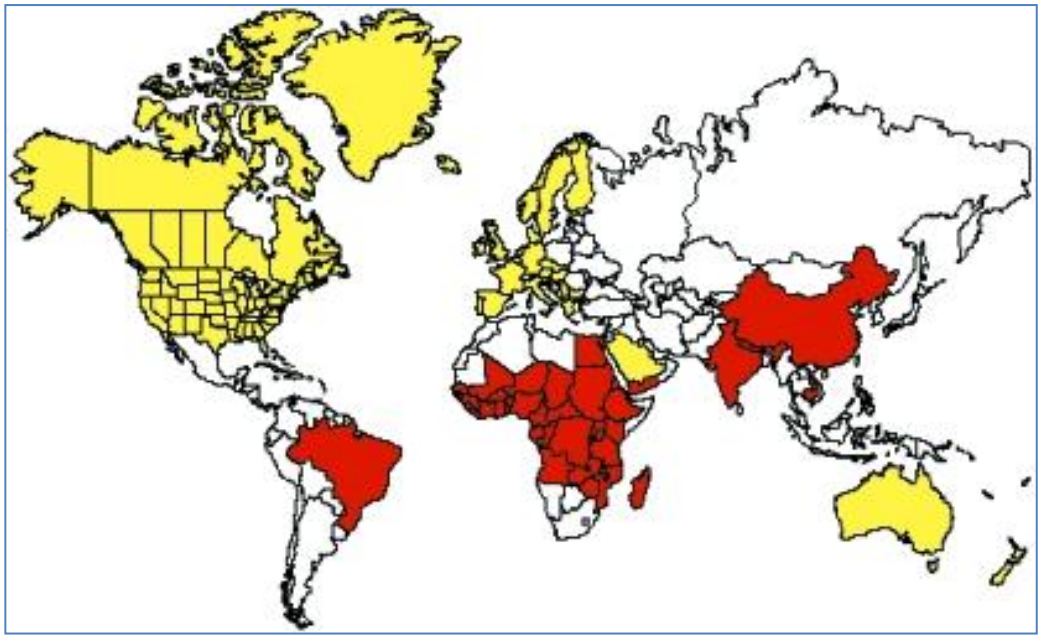

Figure 4. Inverse correlation between Type 1 Diabetes (T1D) incidence and neglected infectious diseases. Red areas represent endemic regions for at least 6 neglected diseases (filariasis, leprosy, onchocerciasis, schistosomiasis, soil-transmitted helminths, and trachoma). Yellow areas indicate countries with a high incidence of T1D (> 8 per 100 000/year).

Source: Zaccone P, Fehervari Z, Phillips JM, Dunne DW, Cooke a. Parasitic worms and inflammatory diseases. Parasite Immunol. 2006;28: 515–23 [87].

Mutapi et al. further reported that autoantibody levels of schistosome-infected individuals are lower than in infection-free individuals. They also revealed that levels of autoantibodies increased in infected individuals after clearance of schistosome infection by praziquantel treatment [76]. In another study, it was reported that multiple sclerosis (MS) prevalence was inversely correlated with the prevalence of *Trichuris trichiura* infection [88]. Furthermore, a cohort study by Correale et al. demonstrated that helminth-infected MS patients show a significantly lower progression of MS compared to uninfected individuals [89].

By now, a number of studies demonstrated that helminth infections prevent or ameliorate autoimmune diseases like T1D, rheumatoid arthritis, chronic inflammatory bowel disease, and MS [87,90–93]. Studies in clinical trials are

currently testing the beneficial effect of *Trichuris suis* ova treatment on autoimmune diseases.

1.3 Helminth infections and its beneficial impact on diabetes

1.3.1 Impact of helminths on type 1 diabetes

Hübner et al. demonstrated that infection with the filarial nematode *Litomosoides sigmodontis* (*L.s*.) prevents the onset of T1D in non obese diabetic (NOD) mice. Interestingly, the protection was not only given by living worm infection, but also by administration of crude worm extract (*L.s*. antigen). This protection was associated with a type 2 immune shift and induction of $FoxP3^+$ Treg cells [92]. Using IL-4 deficient NOD mice, which failed to develop a type 2 immune response during *L.s.* infection, Hübner et al. demonstrated that *L.s*.-infected NOD mice were still protected from T1D development. In contrast, depletion of the anti-inflammatory cytokine transforming growth factor beta (TGF-β), but not blockade of IL-10 signalling in immunocompetent NOD mice, prevented the protective effect of helminth infection on diabetes, suggesting that TGF-β is required to provide protection by *L.s.* infection [93].

In addition, Cooke et al. demonstrated that *Schistosoma mansoni* infection or administration of *S.mansoni* eggs or soluble worm antigen (SWA) or eggs antigen (SEA) protect NOD mice from onset of T1D [94–96]. This protection was elucidated by induction of Th2 immune response and Foxp3 expressing Tregs [95,96].

1.3.2 Impact of helminths on type 2 diabetes

Although a beneficial impact of helminth infections is well known for autoimmune diseases like T1D, its impact on the metabolic diseases like insulin-resistant T2D is less well studied.

Epidemiological studies suggested a beneficial effect of helminth infections on metabolic diseases. Aravindhan et al. (2010) observed a significant decrease in the prevalence of lymphatic filariasis among diabetic subjects in an area that is endemic for lymphatic filariasis. Decreased prevalence of lymphatic filariasis among diabetic

subjects was further associated with a diminished pro-inflammatory cytokine response [97].

A study in a rural area in China with a high prevalence of *Schistosoma* infections showed significant lower TG levels in people that had a history of schistosomiasis compared to people who were never infected [98]. In addition, people with previous schistosome infections had significantly lower levels of adjusted fasting blood glucose, postprandial blood glucose, and glycated hemoglobin (Hb)-A1c levels indicating that helminth infection may prevent ß-islet cell destruction by reducing metabolic factors such as FFA and hyperglycemia [98].

In line with epidemiology studies in India and China, a recently study in Flores Island, Indonesia, has reported an improvement of insulin sensitivity in individuals with soil transmitted helminth (STH) infections. The lower body mass index of individuals with STH was associated with improvement of insulin sensitivity as indicated by a decreased homeostatic model assessment for insulin resistance (HOMAIR) [99].

In addition to epidemiological studies, some experimental studies demonstrated an improvement of glucose tolerance in DIO mice that were either helminth-infected or treated with helminth-derived products. Wu, et al. initially demonstrated that *Nippostrongylus brasiliensis* infection improves glucose tolerance in DIO mice. This improvement was associated with increased frequencies of eosinophils in perigonadal / epididymal adipose tissue (EAT) and a reduced body weight and fat mass [44].

Using the same model, Yang et al. highlighted that glucose tolerance improvement in *N. brasiliensis*-infected DIO mice was associated with a decreased body weight gain and upregulation of AAM markers in EAT [100].

Subsequently, Bhargava et al. demonstrated that administration of soluble egg antigen of *S. mansoni* (LewisX-containing LNFPIII) improves glucose tolerance and insulin sensitivity in DIO mice. These effects were associated with increased IL-10 production in bone marrow-derived macrophages and dendritic cells [101].

The last evidence was shown by Hussaarts et al., who reported that *Schistosoma mansoni* infection and soluble egg antigen (SEA) administration in DIO mice improve glucose tolerance and promote type immune responses, eosinophilia, and AAM in EAT [102].

1.4 Helminth infection and immune regulation

Helminth parasites infect almost one-third of the world's population, primarily in tropical and sub-tropical regions [103,104]. Most helminth infections cause no or only mild pathology and only a subset of patients develop severe pathologies. The maintenance of an asymptomatic state during helminth infection is due to the immunoregulatory capacity of the helminths which involves the induction of multiple regulatory cell types and cytokines; while a breakdown of this regulation may cause pathology [105].

Helminths are well known to modulate the immune system by inducing type-2 immunity which is characterized by T helper (Th) 2 cells and their associated cytokines, increased frequency of tissue eosinophils, mucosal mastocytosis, and enhanced production of IgE [106]. In addition, helminth infections induce regulatory responses via regulatory T cells (Treg) that secrete the suppressive cytokines IL-10 and TGF-ß [107] and express molecules such as cytotoxic T-lymphocyte-associated protein 4 (CTLA-4) or glucocorticoid-induced TNF receptor (GITR) that are involved in the suppression of immune responses [65]. Helminth infections have also been associated with regulatory B cells (Breg), which can release IL-10 [108].

This immunomodulation by helminths may not only enable the long-term survival of the parasite in the host, but may also affect the response to bystander antigens.

1.4.1 Th2 immune response

Generally, helminth parasites induce in their hosts type 2 immune responses which are characterized by increased levels of IL-4, IL-5, IL-9, IL-13 cytokines that are in general thought to mediate protective responses against helminth parasites [109–115].

Th2 immune responses were also proposed to promote wound healing and tissue regeneration which can limit the damage due to helminth parasites during their trafficking through host tissues [116–119].

In filarial infection, Th2 differentiation from naïve T cells is initiated after contact with live larvae (L)-3 of *Brugia pahangi* and *L.s.*[120]. Nevertheless, during filarial infection, Th1 immunity is also induced by endosymbiontic *Wolbachia* bacteria, which are present in most human pathogenic filariae, as well as *L.s.,* that can be released after the death of filariae [121,122]. At ~ 12 days post infection (dpi), *L.s.* infection induces Th2 responses with increased levels of IL-5 and IL-4, which are important for filarial elimination and control patency [120,122].

IL-4 and IL-13 are further suggested to promote wound healing by stimulating innate and adaptive immune cells to secrete cytokines, growth factors and angiogenic factors that promote fibroplasia and angiogenesis and inhibit classical inflammation [119,123].

L.s. infection was demonstrated to increase the numbers of AAM in their hosts [124]. To identify AAM, several markers have been used including cell surface IL-4 receptor-a (IL-4Ra) and the mannose receptor CD206 in flow cytometriy [125] or immunohistology [109]. Gene expression of Arginase-1 (*Arg1*), *Fizz* (found in inflammatory zone) family member proteins (ChaFFs), including: *Fizz1*/ *Relmα*, *Ym1*, and acidic mammalian chitinase (*AMCase*) are upregulated during nematode infection [60]. AAM are activated through IL-4/IL-13 stimulation via the IL-4Rα receptor and STAT6 [126]. Through Th2 cytokines induction, several helminth antigens were demonstrated promote AAM polarization [127–130].

1.4.2 *Wolbachia* and its role in immune regulation

An endosymbiotic bacteria of the genus *Wolbachia* was identified in the 1970s as an unusual body in the hypodermis of filarial nematodes [131]. These bacteria are found in all developmental stages and are abundant in adult worms [132]. The majority of filarial species including the major filarial parasites of humans: *Wuchereria bancrofti, Onchocerca volvulus* and *Brugia malayi* as well as the

murine filarial nematode *L.s.* harbor *Wolbachia* [132]. However, some filarial nematodes including the rodent filaria *Acanthocheilonema viteae* and the deer parasite *Onchocerca flexuosa* are free from *Wolbachia* [132]. Similarly, the human pathogenic filaria *Loa loa* does not contain *Wolbachia* [133]. As an endosymbiont, *Wolbachia* are essential for worm fertility, reproduction, larval molting and survival. Depletion of *Wolbachia* prevents filarial development, fertility and viability, which offers a novel approach for treating filarial diseases using antibiotics such as doxycycline [134,135].

The presence of *Wolbachia* in filarial nematodes can provoke inflammation in the filariae-infected host [136–138] through TLR-2/6 activation [138], resulting in increased production of IL-6, TNFα, and IL-1β [139]. The *Wolbachia* surface protein of *B. malayi* induced increased frequencies of Th17 cells and Th1 cytokines like interferon-γ (INFγ) and IL-2 and reduced the frequency of Tregs, Th2 cytokines like IL-4 and anti-inflammatory IL-10 and TGF-β levels in culture supernatants of splenocytes [140]. Therefore, classical antihelminthic treatment (e.g. diethyl carbamazine /DEC) could induce adverse drug reactions due to the *Wolbachia* release from dying filariae [139].

Depletion of *Wolbachia* by doxycycline does not only eliminate adult filarial worms and microfilariae, but was also shown to improve lympangiogenesis, lymphatic endothelial proliferation, and dilation of lymphatic vessels [141].

1.5 Helminth-derived products

Several immunomodulatory helminth-derived molecules have been described over the past decade [142]. Studies about those molecules have two beneficial aspects: (1) since those molecules are used by parasites to enable their survival—their neutralization would be a strategy to eliminate helminth infections [143] and (2) their potential immunosuppressive effect could be used to counter inflammatory disorders.

Different helminth-derived products have recently been demonstrated to prevent the development of inflammatory diseases in mouse models. Such a molecule is ES-62, a

glycoprotein from the filarial nematode *Acanthocheilonema viteae* which modulates cellular activity via TLR4 [144–146]. Administration of this molecule prevents the development of collagen-induced arthritis, oxazolone-induced contact sensitivity and ovalbumin-induced airway hypersensitivity in mice through the inhibition of B-2 cell proliferation and the induction of B-1 cell-dependent IL-10 secretion. In addition, ES-62 promotes type 2 anti-inflammatory responses through TLR4-dependent activation of APCs. This molecule also inhibits mast cell degranulation and inflammatory mediator release via TLR4-dependent activation [146].

Cystatin, a cysteine protease inhibitor (CPI) from helminths is another well studied immunomodulatory molecule, which attenuates Ovalbumin airway hypersensitivity as well as Dextran sulfate sodium (DSS)-induced colitis [147]. Nematode cystatins inhibit proteases involved in antigen processing and presentation and therefore reduce T cell responses. Nematode cystatins were further described to promote IL-10 and Th2 cytokine secretion by macrophages [147,148].

In addition, administration of a crude extract from *L.s.* (LsAg) induced type 2 immune responses and triggered IL-10 production in NOD mice and delayed diabetes onset when administered at 6 weeks of age [92].

Given that helminth-derived products have been shown to modulate immune responses, the study of those molecules may provide new candidates for treatment of inflammatory disorders including obesity-induced insulin resistance.

1.6 The *L. sigmodontis* mouse model

The rodent filarial nematode *L. sigmodontis* is an excellent model to investigate immune responses during filarial infections. While human-pathogenic filariae like *Brugia spp*. and *Oncocerca spp*. do not develop in immunocompetent wildtype (WT) mice [149–151], *L. sigmodontis* is able to complete its life cycle in immunocompetent BALB/c mice, where the infection results in patent infections with circulating microfilariae [149,152]. The infection with *L. sigmodontis* in BALB/c mice mimics hereby immune responses as they occur during helminth infections in humans. Thus,

L. sigmodontis is an ideal model for filarial infection in humans and induces type 2 immune responses [149,153], Tregs and IL-10 [62,113,114].

1.6.1 *L. sigmodontis* life cycle

The life cycle of *L.s.* is illustrated in Fig. 5. The tropical rat mite *Ornithonyssus bacoti* transfers with its blood meal infectious L3 larvae, which migrate from the entrance site in the host skin via the lymphatic vessels to the pleural cavity.

Approximately 60% of the inoculated L3 larvae are eliminated before they reach the pleural cavity which occurs 2-6 dpi [149]. The L3 which reach the pleural space develop into L4 larvae around 8-12 dpi and molt into adult worms around 30dpi. After mating of male and female adult worms, filarial embryos develop in the female filariae. Starting around day 50 to 55 post infection, microfilariae (Mf) circulate in the peripheral blood (Hoffmann, Petit et al. 2000).

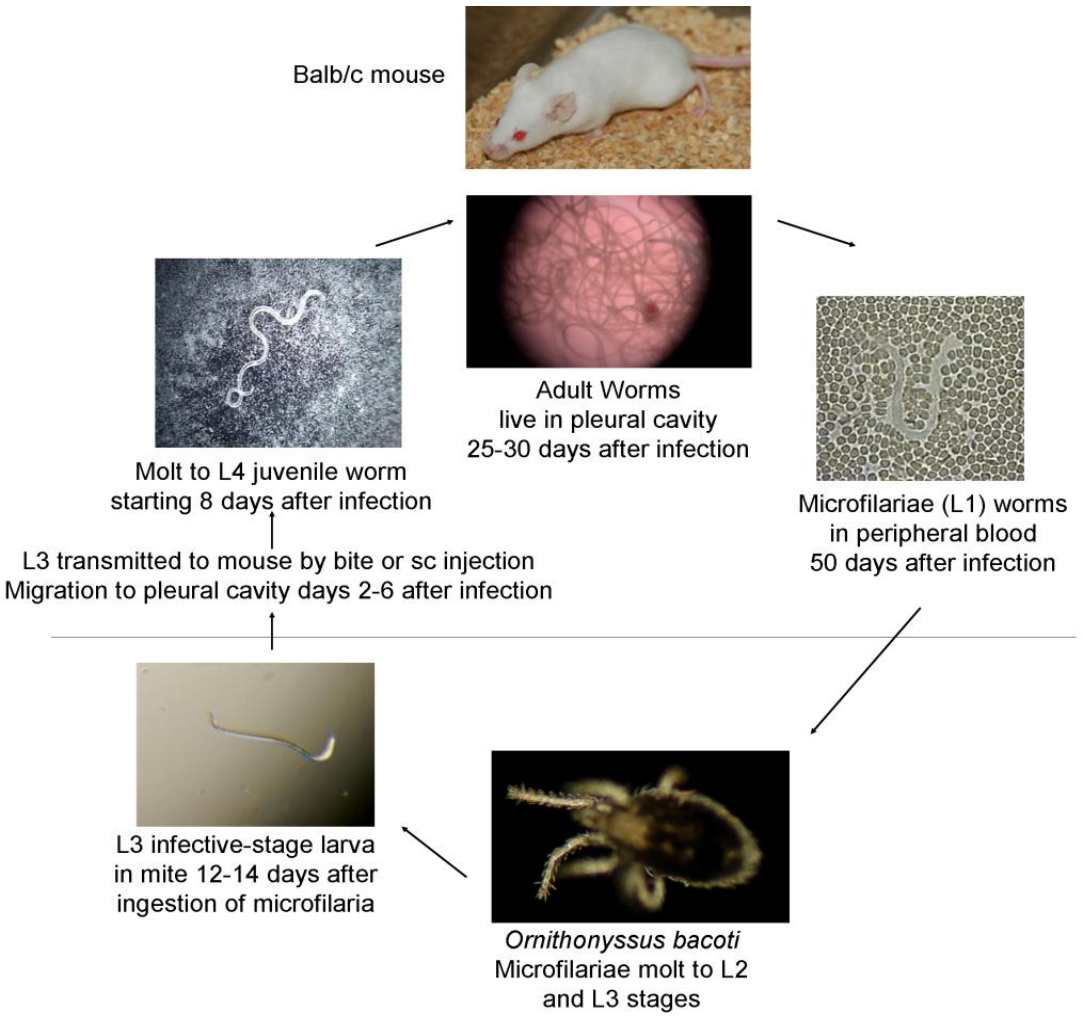

Figure 5. Life cycle of *Litomosoides sigmodontis*: during natural infection mice are infected with L3s by the bite of infected tropical rat mites (O*rnithonyssus bacoti*). After infection, L3 larvae migrate via the lymphatic system to the pleural cavity within 2-6 days post infection (dpi). In the pleural cavity, L3 larvae molt into the L4 stage between 8-12 dpi, become adults after another molt at 25-30 dpi. After mating, female adult worms start to release microfilariae which circulate in the peripheral blood by 50 dpi.

Source: Hübner MP, Torrero MN, McCall JW, Mitre E. Litomosoides sigmodontis: a simple method to infect mice with L3 larvae obtained from the pleural space of recently infected jirds (Meriones unguiculatus). Exp Parasitol. 2009;123: 95–8[154].

1.7 Aims and Objectives of this work

Although a protective role of filarial infections is well accepted for autoimmune diseases like T1D, it is not known whether filarial infections impact the development of metabolic diseases like insulin-resistant in T2D.

Despite first epidemiological and experimental studies that investigated the impact of helminth infections on the metabolic syndrome, experimental studies using filarial nematodes have not been conducted yet and the protective mechanism mediated by helminth infection is still insufficiently understood. The major aim of this thesis was therefore to investigate whether infection with the tissue–invasive rodent filarial nematode *L. sigmodontis* and administration of LsAg protect against HF diet-induced insulin resistance in DIO mice and to elucidate the protective mechanism. As pro-inflammatory cytokines and CAM are important for the induction of insulin resistance in mice fed on a HF diet, we hypothesized that filarial infection and its derived product reduces the pro-inflammatory immune response and maintains the frequency of AAM in adipose tissue, thus ameliorating insulin resistance. Since eosinophils have been previously shown to play a key role in maintaining AAM to improve insulin sensitivity, an additional aim of this study was to address whether eosinophil and AAM are required to improve insulin sensitivity in *L.s*. infected DIO mice.

Since accumulation of B cells in VAT of DIO mice promotes insulin resistance through pathogenic IgG production, we further hypothesized that *L.s.* infection promotes insulin sensitivity by modulating B cells in VAT of DIO mice, which should be addressed using flow cytometry.

As excessive adipose tissue mass in obesity is a major risk factor for initiating insulin resistance, the impact of *L.s.* infection and LsAg administration on adipogenesis was planned to be investigated.

Furthermore, over the past few years, brown adipocytes became a new target to counter obesity and metabolic-related diseases by its capacity to control energy homeostasis by dissipating chemical energy and increasing energy expenditure [155–157]. Interestingly, recent studies reported that helminth-associated features such as eosinophils, AAM and type 2-associated cytokines are correlated with browning of white adipose tissue [54,55,158]. Thus, the hypothesis that *L.s.* infection and LsAg administration promote browning of adipose tissue and increase energy expenditure was to be analyzed.

To obtain a better understanding regarding the molecular mechanism by which *L.s.* infection and LsAg administration impact insulin signaling, multiple gene expression analyses of EAT were supposed to be performed using polymerase chain reaction (PCR) array.

Thus, the overall aim of this thesis was to investigate whether *L.s*. infection and/or LsAg treatment improve insulin sensitivity in DIO mice and to analyze several potential protective mechanisms.

2. Materials and Methods

2.1 Animals and animal care

All mice used in this study were maintained at the animal facility of the Institute for Medical Microbiology, Immunology and Parasitology, University Hospital of Bonn. Mice were housed in individually ventilated cages at a 12-hour day/night cycle with free access to food and water. The experiments in this thesis were performed using male BALB/c, ΔdblGATA on a BALB/c background and C57BL/6J mice. BALB/c and C57BL/6J mice were purchased from Janvier Labs (La Genest St. Isle, France). ΔdblGATA mice were originally obtained from Jackson Laboratory (Bar Harbor, ME, USA) and bred and housed at the central animal facility of the University Hospital of Bonn (Haus für Experimentelle Therapie). HF diet which provides 60% of calories from fat was purchased from Research Diets, Inc., Brogaarden, Denmark. HF diet feeding was started at 6-8 weeks of age. All protocols were approved by the Landesamt für Natur, Umwelt und Verbraucherschutz, Cologne, Germany.

2.1.1 Glucose tolerance test

Six hours before the glucose tolerance test (GTT), food was removed from the cages. After 6 hours of fasting, blood glucose levels were measured from the tail vein using a standard blood glucose meter (Accu-Check Advantage, Roche Diagnostics GmbH, Mannheim, Germany) to determine fasting glucose. For glucose challenge, mice were injected intraperitoneally (i.p.) with 2g glucose monohydrate (Merck, Darmstadt, Germany) solution per kg body weight [159]. At 15, 30, 60, 90, and 120 minutes post glucose injection, blood glucose levels were measured from the tail vein.

2.1.2 Insulin tolerance test

Before the insulin tolerance tests (ITT) were performed, the food was removed from the cages. The first glucose measurements were taken immediately before the insulin injection. Glucose levels of mice were determined from blood taken from the tail vein using surgical scissors. After the baseline glucose level measurement, insulin (0.001unit/g body weight) was injected i.p. [159]. The blood glucose levels were

observed overtime at 15, 30, 60, 90, and 120 minutes using a standard blood glucose meter (Accu-Check Advantage, Roche Diagnostics GmbH, Mannheim, Germany).

2.1.3 Cold tolerance test

For cold tolerance test, mice were placed in a 5^{o}C temperature room for a maximum of 4 hours. The body temperature was measured from the mid-dorsal body surface using a ThermoScan thermometer (PRO 4000, Braun, Kronberg, Germany) as described previously [160]. The measurement was performed before, 1, 2, 3 and 4 hour(s) of cold exposure.

2.1.4 Euthanasia of mice

At the determined time point of experiment, euthanasia was performed. Mice were anesthetized per isoflurane (Abbot, Wiesbaden, Germany) inhalation. Blood was then taken from the retro-orbital vein using micro-haematocrit capillaries (Brand, Wertheim, Germany) and transferred into 1ml disodium ethylenediaminetetraacetic acid (EDTA)-containing tubes (Kabe Labortechnik, Nümbrect-Elsenroth, Germany).

Afterwards, mice were killed using an overdose per inhalation of isoflurane and were fixed on a surgical board. The skin and peritoneum were gently dissected and the EAT was removed from the intra abdomen. Subcutaneous adipose tissue (ScAT) was collected by dissecting fat under the dorsal skin. For brown adipose tissue collection, interscapular brown adipose tissue was taken. Adipose tissues for Fluorescence-Activated Cell Sorter (FACS) analysis were collected in DMEM-low glucose medium (Gibco, life technologies, US) containing 1g/L D-glucose, 4mM L-Glutamine, 25mM HEPES, 1g/ml BSA and 1% penicillin-streptomycin. For quantitative PCR (qPCR) analysis, small tissue parts were collected and immediately snap frozen in liquid nitrogen. Finally, the thoracic cavity was opened to confirm the presence of adult worms.

2.1.5 *L.s.*infection

L.s. infection was performed by natural infection as was previously described [161]. If not stated otherwise, mice were infected at 8-10 weeks of age, 2 weeks after the

onset of HF diet. During natural infection, infective L3 larvae are transmitted with the blood meal of infected *O. bacoti* mites and migrate to the thoracic cavity where they molt into adult worms (~30dpi). At the time of necropsy, infection status of mice was confirmed by screening for adult worms in the thoracic cavity.

2.2 LsAg preparation

L.s. adult worms were harvested from the pleural cavity of *L.s.*-infected-cotton rats and transferred into a glass potter. By adding phosphate buffer saline (PBS), worms were homogenized until a suspension was obtained. This suspension was centrifuged for 10 minutes at 3200g and 4°C. The supernatant was collected and the protein concentration was measurement by BCA Protein assay kit (Thermo scientific, Rockford, USA). Those procedures were performed under sterile conditions.

2.3 Helminth-derived product administration

At the determined time, each group of DIO mice were injected i.p. with 2µg/mouse of ES-62, CPI, or LsAg. DIO controls were injected with PBS. *Achanthocheilonema vitae* derived ES-62 was kindly provided by Prof. Dr. William Harnett (University of Strathclyde, UK). *Litomosoides sigmodontis* derived CPI and Abundant Larva Transcript (ALT) were kindly provided by Dr. Simon Babayan (University of Glasgow, UK).

2.4 Isolation of the stromal vascular fraction

Epididymal fat pads from male mice fed a normal chow diet or HF diet were excised and minced in DMEM-low glucose (Gibco, life technologies, US) containing 1g/L D-glucose, 4mM L-Glutamine, 25mM HEPES, 1g/ml bovine serum albumin (BSA) and 1% penicillin-streptomycin. Minced tissue was transferred to 2ml medium containing 1.5mg/ml Collagenase-P (Roche, Mannheim) and then incubated at 37°C for 20-30 minutes with continuous shaking. After incubation, the tissue suspension was washed with DMEM-low glucose (without supplements) and was centrifuged at 300*g* for 5 minutes to remove the collagenase and separate floating fraction from the stromal vascular fraction (SVF) pellet. After retaining SVF, the floating fraction were digested for a further 10 minutes in medium containing collagenase, and the SVF were pooled

through the filter for FACS analysis. After centrifugation, the SVF pellet was incubated for flow cytometric analysis in 1ml 1x red blood cell lyses buffer (eBioscience) for 5 min and was afterwards washed with DMEM-low glucose (without supplement). The cells were blocked with anti-CD16/anti-CD32 antibodies in FACS buffer (1X DPBS without Ca^{2+} and Mg^{2+}, 2mM EDTA, and 1% FCS) at a final concentration of 0.5-1 µg/10^6 cells for 30 minutes. Before antibody staining, the cell suspension was filtered through a 100µm filter, and the volume was adjusted to obtain 1 million cells per FACS tube.

2.5 Flow cytometry

To analyze the cell composition in SVF of EAT, cell surface markers were stained for 30 minutes at 4°C with rat anti-mouse F4/80 PerCP-Cy5.5, CD4 FITC, CD11c APC, CD19 PE, CD23 FITC, CD5 PE-Cy-7-A, Gr1 PerCP-Cy5.5 (all eBioscience), and Siglec-F PE (BD Bioscience). To identify intracellular proteins, cells were fixed with fixation/permeabilization buffer (eBioscience) overnight, washed and blocked in PBS containing 1% BSA (PAA) and rat Ig (1µg/ml, Sigma, St. Louis, MO, USA). For RELMα staining, fixed cells were incubated in permeabilization buffer (eBioscience) and were stained with rabbit-anti-mouse RELMα (Peprotech, Rocky Hill, NJ, USA). After a washing step, cells were stained with a secondary antibody (goat anti-rabbit Alexa488, Invitrogen, Carlsbad, CA, USA). Tregs were analyzed after overnight fixation and permeabilization and staining with CD4 FITC and Foxp3 PE (all eBioscience). Data were acquired using a BD FACS Canto and analyzed with BD FACS DIVA software.

2.6 IgG2a measurement by Enzyme-linked immunosorbent assay (ELISA)

IgG2a (BD Pharmingen) concentrations were measured by sandwich ELISA according to the manufacturers direction. Polysorb ELISA plates (Nunc, Roskilde, Denmark) were first coated with primary antibodies in PBS or coating buffer (Na2HPO4 0.1M, Merck, in distilled aqua pH 7.0) for overnight at 4 ^{o}C. Plates were then blocked with PBS/1% BSA for a minimum of 2 hours at RT and washed three times with PBS/0.05% Tween 20 (Sigma-Aldrich). 50µl of blood serum were added for a minimum of 2 hours at RT or at 4°C overnight. The detection antibody was added for 2 hours. Following 20 minutes of incubation with horseradish peroxidase (HRP)-streptavidin (R&D Systems)

and tetramethylene benzidine (TMB) (Carl Roth GmbH, Karlsruhe, Germany), the color reaction was stopped with 1M H_2SO_4 (Merck) and optical density (OD) was measured at 450nm using the SpectraMAX 340 microplate reader and data was analyzed with the Softmax Pro software (both Molecular Devices, Sunnyvale, CA, USA).

2.7 Adipose tissue histology staining

Adipose tissue was fixed in 4% paraformaldehyde (Otto Fischar GmbH, Saarbrücken, Germany) for at least 24 hours. After fixation, tissue was dehydrated with ethanol and then embedded in paraffin for cutting. The paraffin block was cut using a microtome. The cut sections of 5µm thickness were placed on warm water to flatten out and were then transferred to glass slides. For dewaxing, sections were dipped into xylol and then dipped into a series of 100%, 90%, 80%, 70%, and 50% ethanol. Afterwards, the tissue sections were dyed with hematoxylin solution for 10 minutes, and then washed under tap water for 10 minutes. Subsequently, tissue sections were dipped into distilled water and dyed using 0.1% eosin for 3 minutes afterwards. The stained tissue was dipped in 96% ethanol and 100% xylol respectively. To make the section permanent, the stained section was mounted.

2.8 Ribonucleic acid (RNA) isolation and Real-time PCR

To extract RNA from tissues, about 30mg of epididymal fat pads were collected, snap frozen in liquid nitrogen and stored at -80°C until RNA isolation. RNA was extracted from adipose tissue using Trizol (Invitrogen, US) in combination with the RNeasy mini kit (Qiagen, Hilden, Germany). Frozen adipose tissues were transferred into 2ml innuSPEED Lysis Tubes W (Analytik-Jena) containing Trizol. Tissues were disrupted with the Precellys homogenizer for 10 seconds (6000rpm). Tissue suspensions were then transferred into new tubes and were washed with 70% ethanol (1:1). Subsequent procedures used RNeasy mini columns following standard protocols of the RNeasy mini kit from Qiagen. Quality of extracted RNA was assessed by spectrophotometric determination of the OD260/OD280 ratio. Template-RNA was quantified by the OD260 value. At least 4.2µg/ml of total RNA was reverse transcribed with an Omniscript RT Kit

(Qiagen, Hilden, Germany) according to the manufacturer's instructions with oligo-d(T) primers (Roche, Mannheim). Real Time PCR was performed in a 20µl reaction volume containing 2µl 10x reaction buffer, 5mM Deoxynucleotide (dNTP) mix, 0.2µl SYBR green (diluted 1:1000), 0.1µl Hotstar Taq and 2µl complementary deoxyribonucleic acid (cDNA), and a standardized concentration of Mg^{2+} and primer, using a Rotorgene cycler (Corbett life science). For gene expression quantification, a relative quantification method was used (ΔΔCt). List of primer sequences are presented in Table S4.

2.9 PCR array

Deoxyribonucleic Acid (DNA)se treatments were performed to avoid DNA contamination of the RNA isolate. Before cDNA syntheses were performed, RNA integrities were checked using RNA StdSens chips from Experion (Bio-Rad, US). RNA quality indicator (RQI) $\geq$7 was recommended and used to be continued for PCR array performance. cDNA synthesis was performed as described with the RT^2 PreAMP cDNA Synthesis Kit (Qiagen, Hilden, Germany) protocol. After cDNA was obtained, 27µl preamplified cDNA template was diluted to 111µl by adding 84µl of destilled H_2O. For PCR amplification reaction, 1275µl 2x SABioscience RT^2 qPCR SYBR Green master Mix, 102µl diluted preamplified cDNA and 1173 destilled H_2O were mixed. For PCR running, 20µl of PCR amplification reactions were pippeted into 100-well Disc formats of the Mouse Diabetes PCR Array (PAMM-023, Qiagen) or Mouse Insulin Resistance PCR Array (PAMM-156Z Qiagen), and were run with the following real-time thermal cycle program: 95^{o}C, 10 min; 40 cyles (95^{o}C, 15s; and 60^{o}, 60s). PCR array data were analyzed using the online software of RT^2Profiler PCR Array Data Analysis version 3.5. The CT values were normalized to glyceraldehyde 3-phosphate dehydrogenase (GAPDH) and beta-2-microglobulin (B2m).

2.10 3T3-L1 cell culture and treatment

3T3-L1 cells, a murine fibroblast/pre-adipocyte cell line, were obtained from the German Diabetes Centre, Düsseldorf, and the Institute of Pharmacology and Toxicology, University Hospital of Bonn. Cells were seeded in 96 well plates with

Dulbecco's modified Eagle's medium (DMEM)-high glucose (PAA) containing 10% calf serum (PAA), 1% penicillin/streptomycin and 1mM Natrium pyruvat (PAA). Differentiation was induced 2 days after reaching 100% confluence (d0). For induction of differentiation, 100µL DMEM-high glucose medium containing isobutyl-methylxanthine (0.5mM), dexamethasone (1µM) and insulin (10µg/ml) (all from Sigma Aldrich) were added to the 3T3-L1 cells. Every other day (at d2, d4, d6, d8), medium was exchanged with insulin medium (DMEM-high glucose containing 10% calf serum, 1% penicillin/streptomycin, 1mM sodium pyruvate and 10µg/ml insulin). Positive adipogenesis controls were made by adding troglitazone (10µmol/L) at d0. Treated cells received 0.25µg LsAg /100µl at d0, d2, d4, d6, d8. At d9, adipogenesis assays were performed.

2.11 Oil Red O staining

Lipid droplet formation in cells was analyzed by Oil Red O (Sigma) staining. At d8, culture medium was removed and cells were fixed for at least 1h with 10% formaldehyde. After fixation, cells were stained with Oil Red O solution (a mixture of three parts of 0.5% (w/v) Oil Red O in isopropanol and two parts of water) for 30 minutes at room temperature followed by washing with water. Cells were kept in PBS and were photographed. For analysis of lipid droplet formation, 100 µL 96% isopropanol was added per well and cells were incubated on a shaker (300 rpm) at room temperature for 30 minutes. Absorbance was measured using SpectraMAX 340 microplate reader at 540nm and data was analyzed with the Softmax Pro software (both Molecular Devices, Sunnyvale, CA, USA).

2.12 Triglyceride assay

The triglyceride assay was performed using the adipogenesis assay kit from Sigma. In brief, at d11, the 3T3-L1 murine pre-adipocyte cells were seeded in 96 well-plates. After differentiation and treatment, medium was removed and cells were washed once with PBS at room temperature. 100 µL of Lipid Extraction Buffer was added to the culture wells and the plate was incubated for 30 minutes at 90–100°C to extract lipids from the cells. The plate was then placed at room temperature and shaken for 1

minute to homogenize the solution. 5–50µL of the lipid extracts were transferred to a new 96 well plate and the Adipogenesis Assay Buffer was added to a 50µl final volume. To convert TG to glycerol and fatty acids, 2µL of Lipase solution was added to each sample and standard well, and the plate was incubated for another 10 minutes at room temperature. As final step, 50µl of the master mix reaction were added to each well. After 30 minutes of incubation at room temperature with shaking, the absorbance was measured at 570nm wavelength to measure TG levels using a SpectraMAX 340 microplate reader. The data was analyzed with Softmax Pro software (both Molecular Devices, Sunnyvale, CA, USA).

2.13 MTT assay

Two days post confluence, cells were treated with 0.25µg/100µl LsAg, 10µmol/l troglitazone (Sigma) and PBS as control. After 2 days of incubation, the medium was discarded and cells were washed with PBS. Cells were then incubated in insulin medium containing 0.5mg/ml Thiazolyl (Carl Roth GmbH) at 37°C for 3-4 hours. After incubation, medium was aspirated. For analysis, formazan was dissolved by adding 100µL Dimethyl sulfoxide (DMSO) (Sigma) and the absorbance was read at 490nm after an incubation of 5 minutes. Percent viability data was calculated for each well by normalizing to the median absorption of PBS-treated control cells (set to 100% viability).

2.14 Statistics

Data were analyzed for statistical significance using GraphPad Prism software Version 5.03 (GraphPad Software, San Diego, CA, USA). Mann-Whitney-U-test was applied to test differences between two unpaired groups for statistical significance. For comparison of more than two groups, differences were tested for statistical significance using the Kruskal–Wallis test, followed by Dunn's post hoc multiple comparisons test. P values of < 0.05 were considered as significant. PCR array data analyses were performed using the online software provided by SABioscience (Frederick, USA). The p values were calculated based on a Student's t-test of the

replicate 2^(-Delta Ct) values for each gene in the control group and treatment groups, and p values < 0.05 were considered as significant.

2.15 Referencing methods

References in this thesis were managed using the Mendeley desktop version 1.13.8 software (Mendeley Ltd, London, UK), licensed for free.

2.16 Text processing

Word and tabular processing were performed with Microsoft Office 2013 (Microsoft, USA), licensed for private. This work is written, grammar and spell-checked in American English.

2.17 Funding

I was supported by the German Academic Exchange Service (DAAD). This work was funded by the German Research Foundation (HU 2144/1–1); intramural funding by the University Hospital of Bonn (BONFOR, 2010–1–16 and 2011–1–10); and the People Programme (Marie Curie Actions) of the European Union's Seventh Framework Programme FP7/2007–2013 under Research Executive Agency Grant GA 276704.

All funders had no role in study design, data collection and analysis, decision to publish, or preparation of the manuscript.

3. Results

3.1 *L.s.* infection improves glucose tolerance in diet-induced obese mice

Low grade chronic inflammation in visceral adipose tissue due to obesity plays an important role in the induction of insulin resistance [162]. In contrast, helminth infection is associated with type 2 suppressive immune responses and induces regulatory T-cells, eosinophils and AAM [163]. To investigate whether *L.s.* infection improves insulin sensitivity in DIO mice, experiments using *L.s.*-infected and uninfected BALB/c mice were conducted. Male BALB/c mice were maintained on a HF diet that provided 60% of calories from fat for 10 weeks to induce insulin resistance, and a subset of animals were infected with *L.s.* two weeks after the onset of HF diet (Fig. 6A).

During HF diet feeding, both *L.s.*-infected and control mice developed body weights exceeding 30g after 10 weeks on HF diet. At 7 and 8 weeks after the onset of HF feeding, the body weights of *L.s.*-infected mice were lower than of uninfected controls (Fig. 6B). However, in repeat experiments this difference was not observed and body weights in this experiment were not different at 9 and 10 weeks on HF feeding anymore (Fig. 6C).

A glucose tolerance test revealed that blood glucose levels of *L.s*.-infected DIO mice peaked 15 min post glucose injection while blood glucose levels in control mice reached their maximum after 30 minutes (Fig. 6D). At 60 minutes post glucose injection, blood glucose levels of *L.s*.-infected DIO mice declined, while blood glucose levels in uninfected DIO mice remained high, suggesting an improved glucose tolerance in *L.s*.-infected DIO mice (Fig. 6D). Blood glucose levels were significantly reduced in *L.s.*-infected DIO mice at all time points measured 15-120 minutes post glucose challenge. Accordingly, the area under the curve (AUC) of the glucose tolerance test in *L.s*.-infected DIO mice was significantly lower compared to uninfected DIO mice (Fig. 6E). Despite the improved glucose tolerance in *L.s*.-infected DIO mice, insulin tolerance was not significantly improved by *L.s.* infection. (Fig. 6F,G).

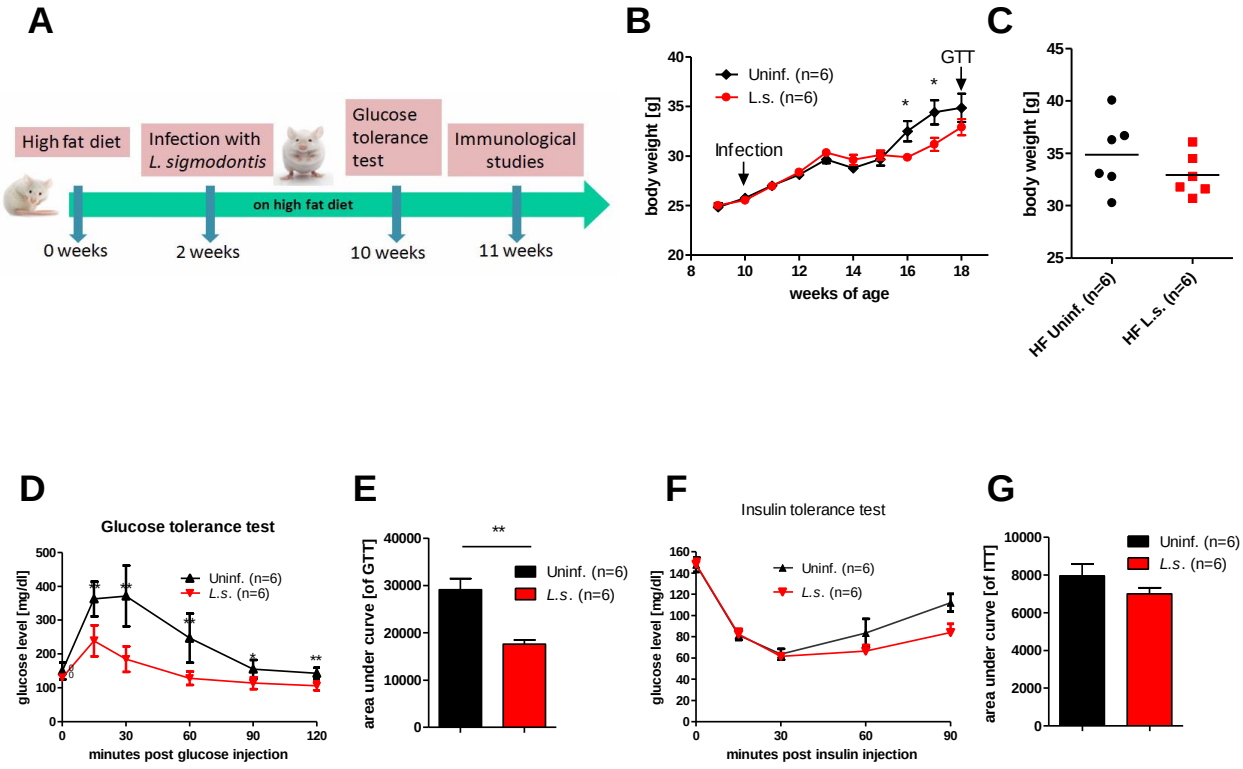

Figure 6. *L.s.* infection improves glucose tolerance in DIO mice. A) Schema of the experimental set up. B) Body weight development of *L.s.*-infected and control mice maintained on a 60% HF diet. C) Body weight of *L.s.*-infected and control mice before the glucose tolerance test. D) Blood glucose levels over time following i.p. glucose challenge (glucose tolerance test) in *L.s.*-infected BALB/c mice and uninfected controls that received a HF diet for 10 weeks. E) Area under the curve obtained from the glucose tolerance test. F) Blood glucose levels over time following i.p. insulin challenge (insulin tolerance test) in *L.s.*-infected BALB/c mice and uninfected controls that received a HF diet for 12 weeks. G) Area under the curve obtained from the insulin tolerance test. A-D, representative data of one out of three independent experiments with at least 6 animals per group. Statistical significance was determined using Mann-Whitney-U-test. Data are expressed as means ± SEM *p<0.05; **p < 0.01

3.2 *L.s.* infection increases the frequency of eosinophils and alternatively activated macrophages within EAT of DIO mice

During obesity, alterations of the cellular composition within the EAT occur [21,164,165]. Classically activated macrophages and B cells infiltrate into the EAT,

which is accompanied by the loss of AAM and eosinophils [41,44,46] and leads to low chronic inflammation and results in insulin resistance. Thus, we investigated whether *L.s.* infection alters the cellular composition in the SVF of EAT in DIO mice.

FACS analyses of the SVF from EAT showed that *L.s.*-infected DIO mice had a significant increased frequency of Siglec-F^{+} eosinophils (DIO controls: 2.84%, *L.s.*-infected DIO mice: 11.32%). RELMα mean fluorescence intensity as well as frequency of RELMα+ macrophages was increased in macrophages from *L.s.*-infected DIO mice compared to uninfected DIO controls (DIO controls: 10.57 %, *L.s.*-infected DIO mice: 24.78 %), while the frequency of macrophages per se did not change (Fig. 7A, B).

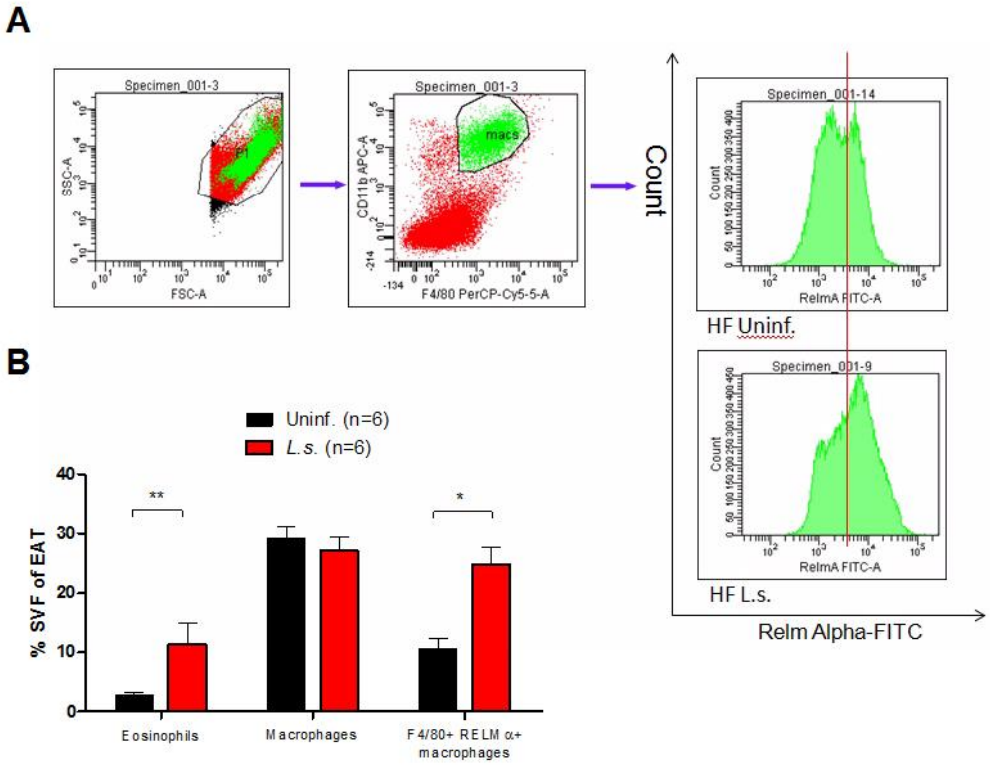

Figure 7. EAT of *L.s.*-infected DIO mice are characterized by increased frequencies of eosinophils and alternatively activated macrophages. A) Gating strategy to identify RELMα mean fluorescence intensity of F4/80+ macrophages and frequencies of RELMα+ macrophages. B) Frequencies of eosinophils, macrophages, and RELMα+ macrophages within the SVF of EAT of *L.s.*-infected and uninfected mice that received a HF diet for 10 weeks. Statistical significance was determined using Mann-Whitney-U-test. Data are expressed as means ± SEM. *p < 0.05; **p < 0.01.

3.3 *L.s.* infection restricts the frequency of B cells but increases B1 cell subsets in epididymal adipose tissue during HF diet

As described by Winer et al., B cells promote insulin resistance in DIO mice by producing pathogenic IgG2 antibodies [46]. B cell subsets were therefore analyzed in EAT of *L.s.*-infected DIO mice and DIO controls (Fig. 8A). As expected, *L.s.*-infected DIO mice had significantly reduced frequencies and total numbers of CD19+ B cells compared to uninfected DIO controls (Fig. 8B, C). Interestingly, the frequency of B cells that represent the B1 cell subset (CD19+ CD5+ CD23-) was higher in *L.s.*-infected DIO mice compared to DIO controls (Fig. 8D). In line with the reduction of B cells in EAT of *L.s.*-infected DIO mice, the level of potential pathogenic total IgG2a antibodies was significantly lower compared to uninfected DIO controls (Fig. 8E). Those results suggest that *L.s.* infection restores a cellular composition within EAT that is characterized by increased frequencies of eosinophils and AAM, while B cells are restricted, which may reduce inflammation and improve glucose tolerance.

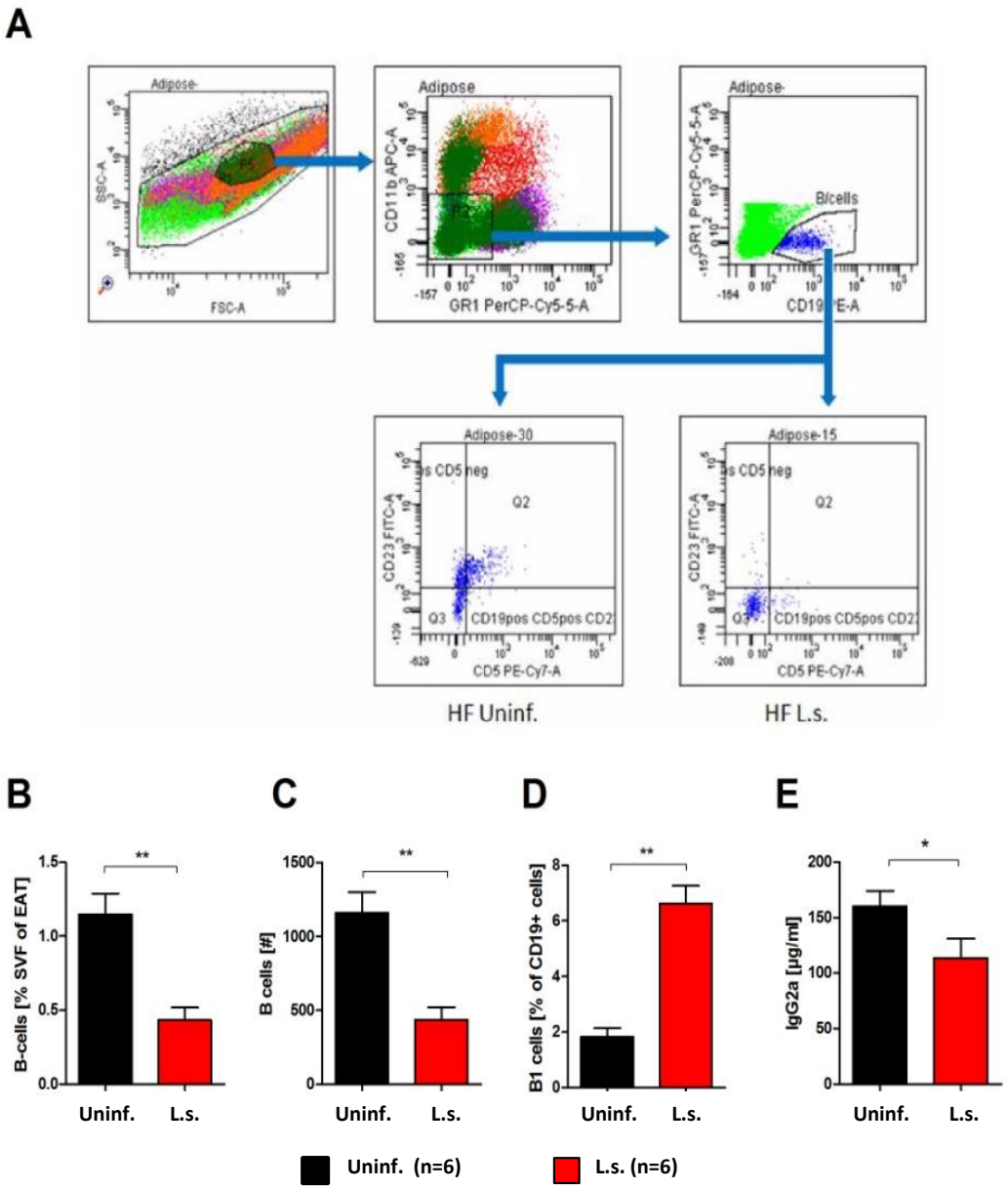

Figure 8. B cell frequency within EAT of *L.s.*-infected DIO mice are reduced compared to DIO controls. A) Gating strategy to identify B cells and B cell subsets. B) Frequency of B cells in SVF of EAT (C), total number of B cells and (D) frequency of B cells with B1 phenotype within the SVF of EAT of *L.s.*-infected BALB/c mice and controls after 10 weeks of HF diet. (E) Total IgG2a antibody levels in blood plasma. Statistical significance was determined using Mann-Whitney-U-test. Data are expressed as means ± SEM. *$p < 0.05$; **$p < 0.01$.

3.4 Absence of eosinophils impairs glucose tolerance improvement by *L.s.* infection

Davina Wu et al. demonstrated that eosinophils play a major role in the improvement of insulin sensitivity in DIO mice by maintaining AAM in the adipose tissue via IL-4 [44]. Since our earlier finding showed an increased number of eosinophils in EAT of *L.s.*-infected DIO mice (Fig. 6B), we investigated using eosinophil-deficient ΔdblGATA mice, whether the improvement of glucose tolerance in *L.s.*-infected DIO mice depended on eosinophils.

Glucose tolerance tests in both *L.s.*-infected and uninfected ΔdblGATA mice showed a worsened glucose tolerance in comparison to both infected and uninfected WT mice (Fig. 9A, B). While *L.s.* infection improved glucose tolerance in WT mice (AUC, p=0.055), this effect was not given in ΔdblGATA mice (Fig. 9A, B), suggesting that improvement of glucose tolerance by *L.s.* infection is dependent on eosinophils.

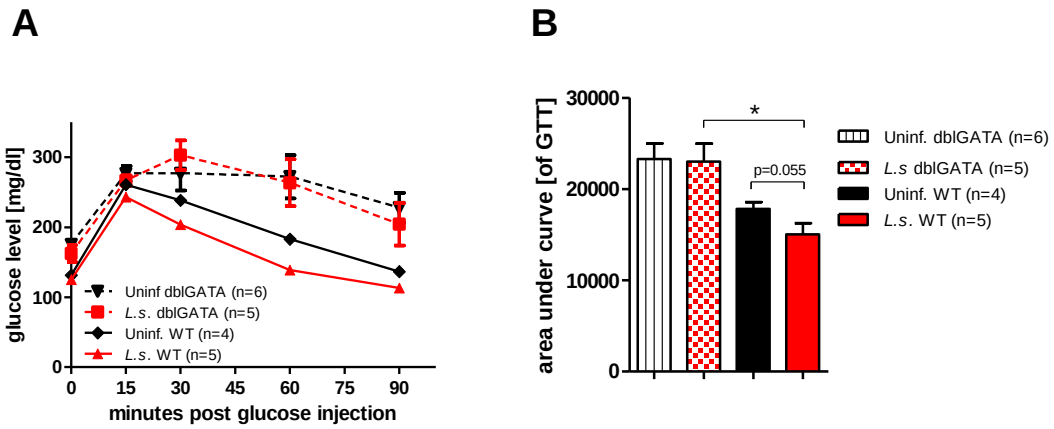

Figure 9. Improvement of glucose tolerance by *L.s.* infection is dependent on eosinophils. A) Kinetic of blood glucose levels after i.p. glucose challenge and B) area under the curve (AUC) from the glucose tolerance test (GTT) in *L.s.*-infected and uninfected ΔdblGATA mice and wild type (WT) controls after 14 weeks of HF diet. A and B show representative data of one out of two independent experiments. Statistical significance was determined using Kruskal-Wallis followed by Dunn's multiple comparisons test. Data are expressed as means ± SEM. *p<0.05.

3.5 The beneficial Impact of *L.s.* infection on glucose tolerance in diet-induced obese mice is dependent on the time point of infection

Although glucose tolerance was improved in *L.s.*-infected DIO mice at 8 weeks post infection (Fig. 6D,E), experiments at different time points of infection demonstrated that the glucose tolerance was not improved at all time points of infection. Given that the immune response to *L.s.* infection is influenced by the *L.s.* life cycle, GTTs were performed at several time points of infection from 7 to 16 weeks post *L.s.* infection. Interestingly, each time point of infection had unique patterns for the impact on glucose tolerance in DIO mice (Fig. 10 and 11). At 7-8 weeks post infection, immediately before the onset of microfilaremia, glucose tolerance was improved as was shown by reduced area under the curve levels of *L.s.*-infected and uninfected DIO mice (Fig. 11), while 9-10 weeks post infection did not give consistent improvements of glucose tolerance in *L.s.*-infected mice. However, the improvement of glucose tolerance in *L.s.*-infected mice consistently returned at 11 weeks post infection (Fig. 10 and 11). Nevertheless, we found that the improvement disappeared after 13 weeks of infection, with one exception found at 16 weeks post infection (Fig. 10, 11). These findings indicate that the beneficial impact of *L.s.* infection on glucose tolerance is dependent on the time point of infection, which provided at 7-8 wpi and 11 wpi the best improvements of glucose tolerance (Fig. 10 and 11).

Inflammatory immune responses caused by the release of microfilaria into the peripheral blood were suspected to be the reason for the vanished improvement of glucose tolerance at 9-10 wpi (63-70dpi), as pro-inflammatory immune responses can be induced by microfilariae [166]. However, no microfilariae were detected in the peripheral blood at 9-10 wpi (data not shown), suggesting that microfilaremia may be reduced during HF diet. Further investigation is required to understand the correlation between the time point of infection and glucose tolerance improvement and the underlying mechanism.

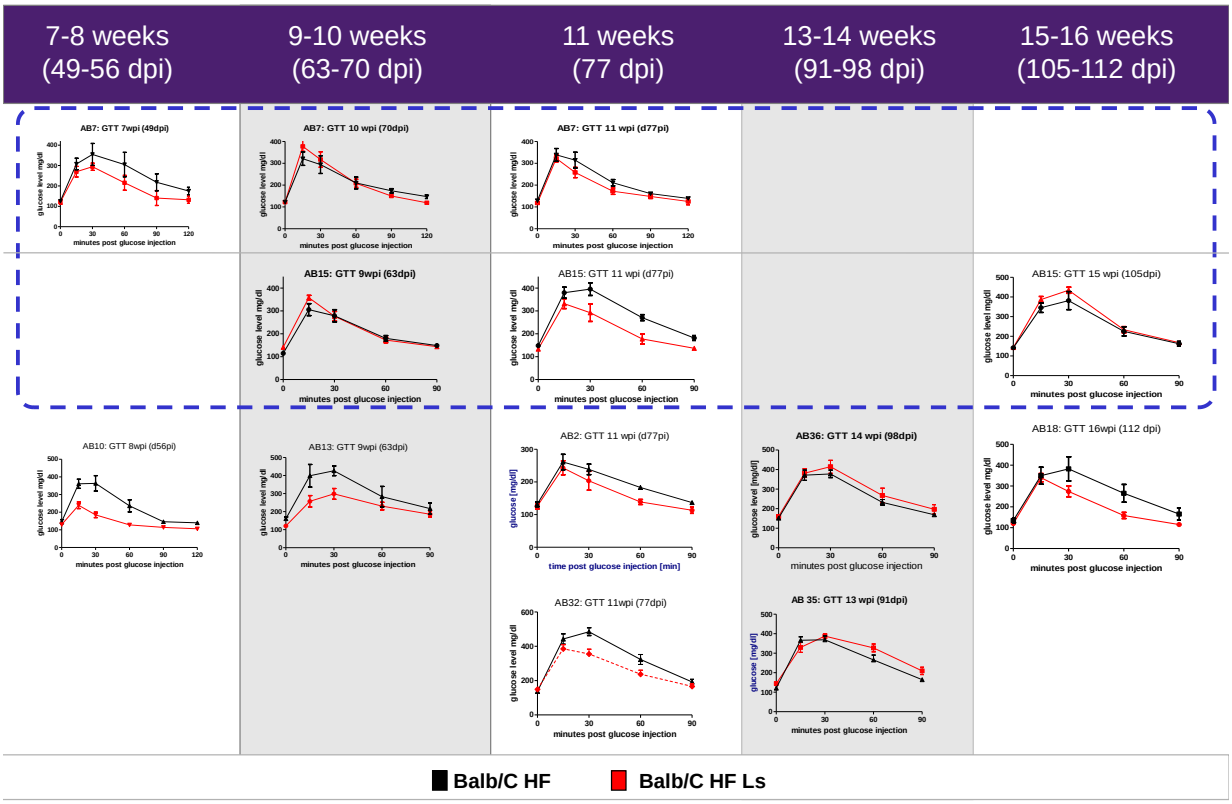

Figure 10. Glucose tolerance test (GTT) results of DIO mice at several time points of infection. Blood glucose levels over time are shown following i.p. glucose injection of *L.s*. infected and uninfected DIO mice at indicated time points of infection. The GTT curves of the top two rows were obtained from the same experiments. At least 5 mice per group were used in all experiments.

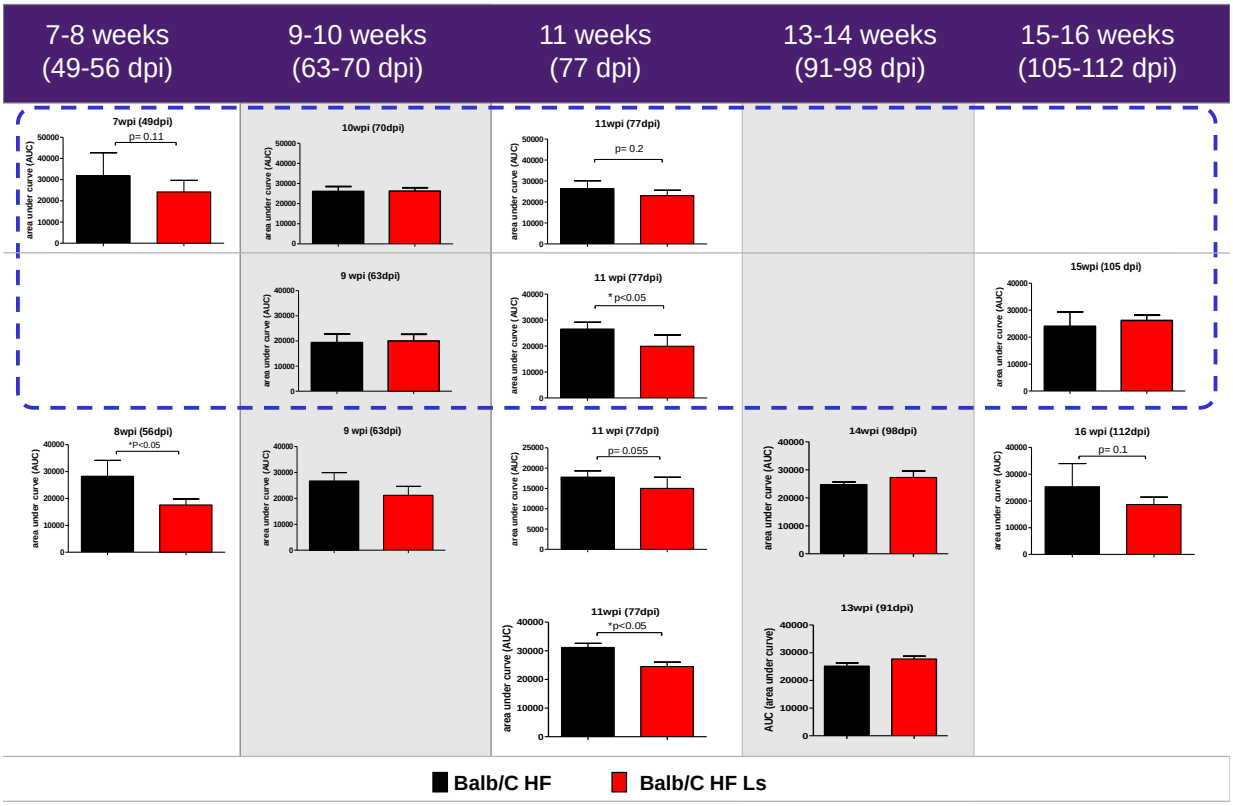

Figure 11. Improvement of glucose tolerance is dependent on the time point of *L.s. infection*. Area under the curve (AUC) obtained from glucose tolerance tests performed of *L.s.*-infected and uninfected DIO mice at indicated time points of infection. The AUCs of the top two rows were obtained from the same experiments. Statistical significance was determined using Mann-Whitney-U-test. Data are expressed as means ± SEM.

3.6 *L.s.* infection induces an anti-inflammatory immune respose, insulin signaling and reduces adipogenesis

Further investigation was performed to analyze expression of 84 genes using a PCR Array (SABioscience) from EAT of *L.s.*-infected animals and controls that received a HF diet as well as corresponding chow diet controls in order to obtain a broader view of the helminth-mediated modulation of the immune responses within the adipose tissue of DIO mice.

PCR array data showed that *L.s.* infection tended to promote insulin signaling in DIO mice as shown by a stronger expression of *Irs1* (p=0.18), a gene that codes for the synthesizing of the IRS-1 protein that plays a role in the insulin signaling cascade [167]. *Carcinoembryonic antigen-related cell adhesion molecule 1* (*Ceacam1*) was significantly upregulated in *L.s.*-infected DIO mice (p<0.05), suggesting an improved insulin signaling and glucose tolerance [168,169] (Fig. 12 and Table S1). In lipid metabolism, *L.s.* infection may promote ß-oxidation in mitochondria in EAT of DIO mice as a trend for an upregulated *Ppara* (p=0.19) expression was observed, while TG production and adipogenesis were suppressed as represented by a downregulated *glycerol-3-phosphate dehydrogenase-1* (*Gpd1*) (p<0.05) expression and a trend to a suppressed *Pparg* (p=0.09) as well as *CCAAT/enhancer binding protein alpha* (*Cebpa*) (p=0.18) gene expression (Fig. 12 and Table S1). This suppression of adipogenesis was not only shown in *L.s.*-infected DIO mice, but also in *L.s.*-Infected mice which received a chow diet (Fig. 12B and Table S2). In addition, *vascular endothelial growth factor* (*Vegf*) and *nitric oxide synthase 3* (*Nos3*) were weaker expressed in EAT of *L.s.*-infected DIO mice (p<0.05 and p=0.19), indicating that *L.s.* infection suppressed angiogenesis, restricted adipose tissue expansion, or reduced hypoxia in EAT, which results in a reduced angiogenesis (Fig. 12 and Table S1).

In line with previous FACS analysis of SVF from EAT which showed an increased recruitment of eosinophils, *L.s.* infection was accompanied with an increased leukocyte migration as highlighted by the upregulation of adhesion molecule genes including *Selectin-L (Sell)* (p<0.05) and *intercellular adhesion molecule-1* (*Icam1*) (p=0.17). This was further supported by a stronger trend in *Ccl5* expression (p=0.15), a chemoattractant chemokine that is involved in the migration of T cells and eosinophils from blood plasma into the tissue (Fig. 12).

In addition, *L.s.* infection in DIO mice led to an increased expression of *Cd28* (p=0.12), a co-stimulatory molecule expressed on T cells as well as *Ctla4* (p=0.14), a gene which codes for a protein receptor that induces tolerance [170] (Fig. 12 and Table S1). Although *Foxp3* as marker of regulatory T cells was not upregulated in EAT of *L.s.*-infected DIO mice, *L.s.*-infected animals that were fed with a chow diet had a

tendency of *Foxp3* upregulation (p=0.09) in EAT (Fig. 12B and Table S1). Furthermore, expression of *phosphoinositide-3-kinase, catalytic, delta polypeptide* (*Pik3cd*), a regulator of B1 function [171], tended to be increased in *L.s*.-infected DIO mice (p=0.18) (Fig. 12 and Table S1). This supports our previous FACS analyses of EAT that demonstrated an increased frequency of B1 cells in *L.s.* infection (Fig. 8-D). Moreover, PCR array data analyses indicates an increased anti-inflammatory response which was shown by a trend to a higher expression of *Il-10* (p=0.19) (Fig. 12 and Table S1). Accordingly, the inflammatory adipokine *Resistin* tended to be suppressed by *L.s.* infection (p=0.12). However, *L.s.* infection also tended to increase the inflammatory gene *Ifng* (p= 0.21) (Fig. 12 and Table S1).

In the fed state, a tendency of increased *phosphoenolpyruvate carboxykinase 1* (*Pck1*) (p=0.07) expression in adipocytes of *L.s.*-infected mice may indicate an effort to re-ester FFA to TG, which could restrict FFA release from adipocytes into the blood circulation [172]. In line with this, *glucose-6-phosphate dehydrogenase* (*G6pd*) expression tended to be suppressed by *L.s.* infection (p=0.06). This could increase insulin sensitivity, as overexpression of *G6pd* was previously shown to elevate FFA release and insulin resistance [173].

Although the majority of the results obtained from gene expression analysis in EAT of *L.s*.-infected DIO mice was in line with glucose tolerance improvement, the expression of a few genes were negatively correlated with glucose tolerance improvement. This included the observed downregulation of *dual specificity phosphatase-4* (*Dusp4*) ($p<0.05$) and the increased expression of the inflammatory cytokine *Ifng* (p=0.23), which was associated with HF diet-induced inflammation in two previous studies [174,175]

Most of these differences did not reach statistical significance due to the low sample size. Nevertheless, they indicate that *L.s.* infection may reduce inflammation in EAT, increased insulin signaling and ß-oxidation, while reducing adipogenesis in DIO mice (Fig. 13). Similarly, gene analysis in *L.s.*-infected mice with chow diet showed an up-regulation of genes-related to anti-inflammatory immune responses and a down-regulation of genes related to adipogenesis (Fig. 12B and Table S1).

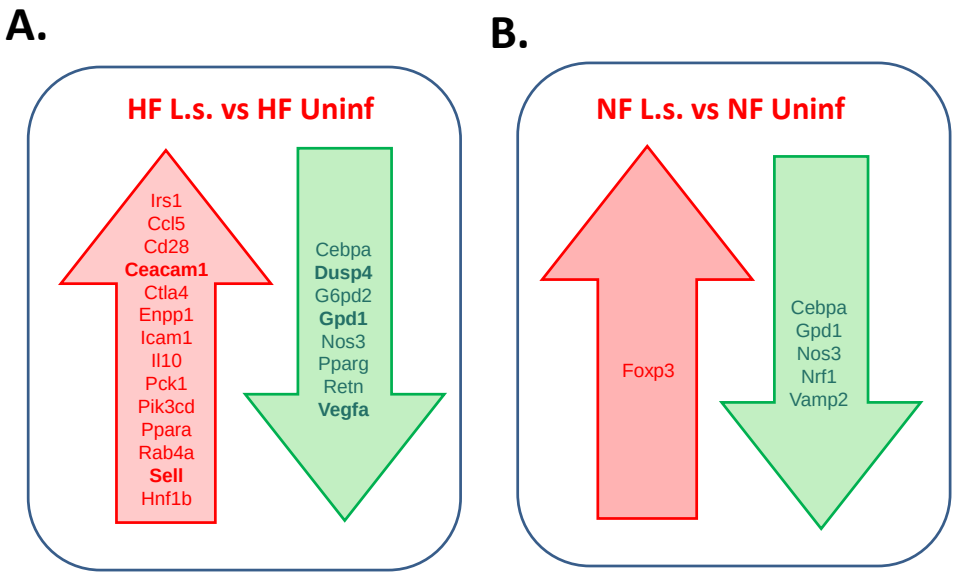

Figure 12. *L.s.* infection induces an anti-inflammatory immune response and reduces adipogenesis. RT^2 Profiler PCR array analysis of gene expression in EAT of (A) *L.s.*-infected (n=3) compared to uninfected BALB/c mice (n=3) maintained on high fat (HF) diet, and (B) *L.s.*-infected (n=3) compared to uninfected BALB/c mice (n=3) on a chow diet (NF). Red arrows indicate genes with up-regulated expression and green arrows represent down-regulated gene expression. Data illustrates genes that have fold change values > 1.3, $p<0.2$. Genes that are significantly different ($p<0.05$) are highlighted in bold.

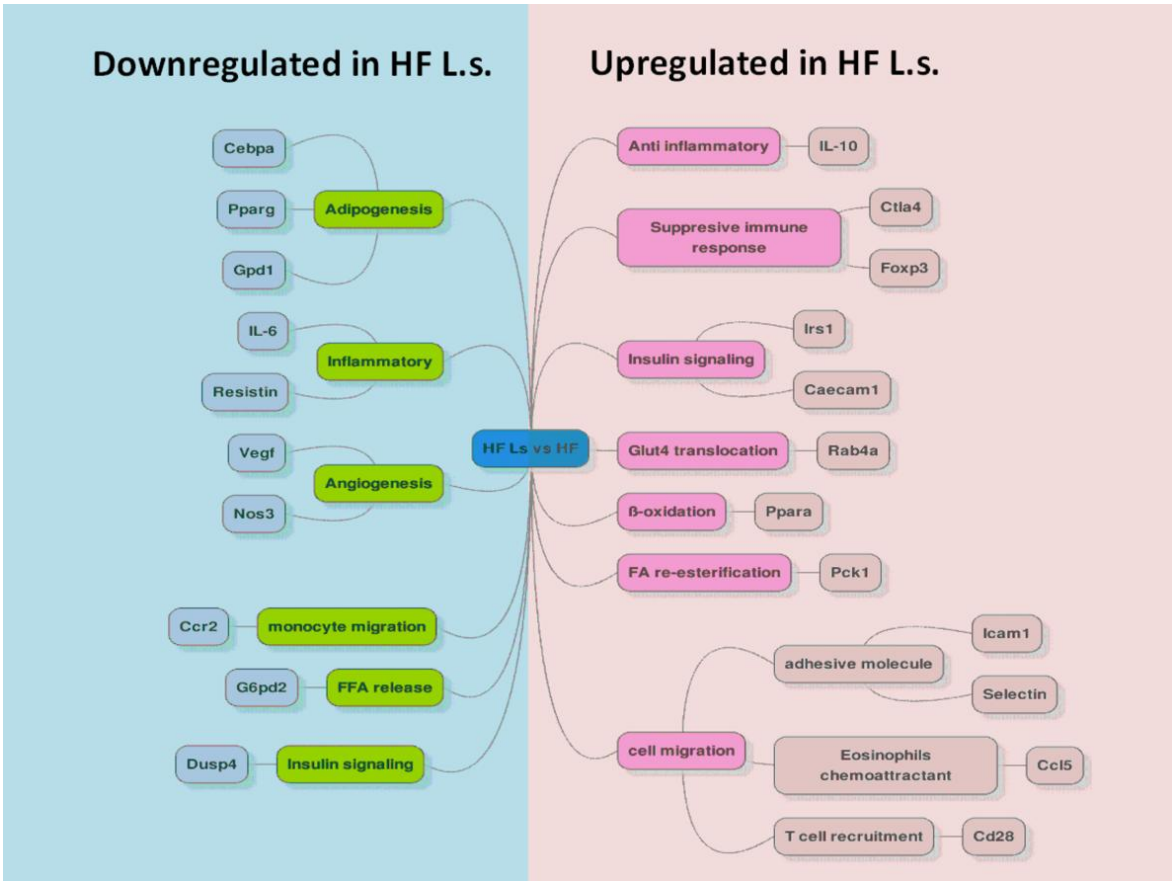

Figure 13. Analysis of gene expression in EAT of *L.s.*-infected (n=3) and uninfected BALB/c mice (n=3) maintained on high fat diet compared to uninfected BALB/c mice on high fat diet (n=3) based on genes function. Right diagram represents genes with up-regulated (red) expression, left diagram represents down-regulated (green) genes expression in *L.s.*-infected DIO mice compared to uninfected DIO mice controls. Data illustrate genes that have fold change values > 1.5, $p<0.2$ compared to BALB/c controls on a high fat diet.

3.7 *L.s.* antigen administration reduces adipogenesis in vitro

To confirm the finding of the qPCR array that suggested a suppressed adipogenesis in *L.s.*-infected mice, LsAg treatment of the 3T3-L1 pre-adipocyte cell line culture was performed to test the effect of helminth antigens on adipogenesis in vitro (Fig. 14A). After 8 days of treatment, LsAg-treated cells showed less mature adipocytes compared to untreated cells (Fig. 14B). Accordingly, absorbance of Oil Red O staining of lipid droplets ($p<0.05$; Fig. 14C) and TG levels ($p>0.05$; Fig. 14D) were lower in LsAg-treated than untreated cells. These results indicate that LsAg treatment suppresses adipocyte

maturation. Viability tests with MTT assay further demonstrated no difference amongst cell viability of PBS-treated control, LsAg-treated and troglitazone-treated cells, indicating that the reduced adipogenesis by LsAg treatment was not caused by a cell toxic effect.

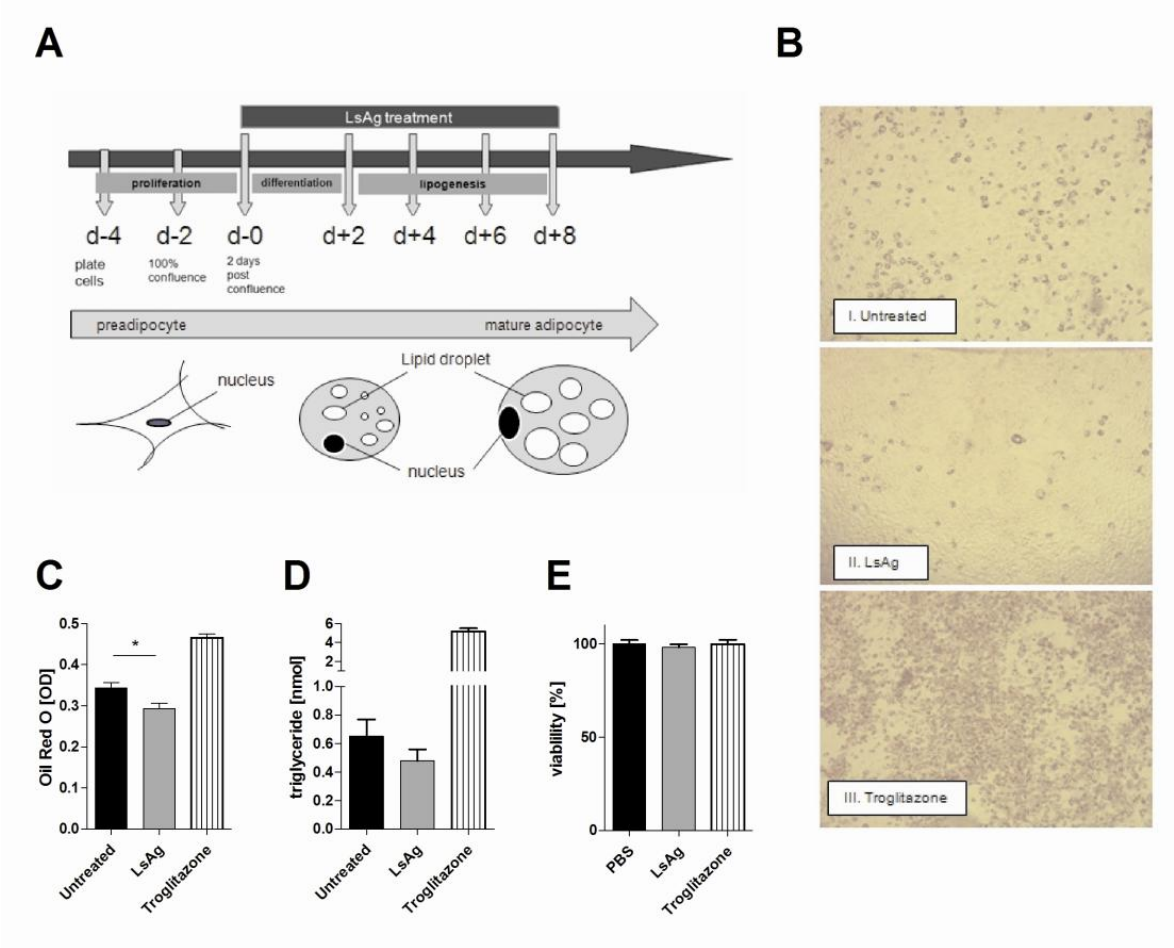

Figure 14. LsAg treatment suppresses adipogenesis in the 3T3-L1 adipose cell line. (A) LsAg treatment regimen during 3T3-L1 differentiation. 9 days post confluence, cells were stained with Oil Red O to identify mature adipocytes. (B) Representative pictures taken from Oil Red O stained cells that were either treated only with differentiation medium, cells treated with differentiation medium + LsAg, and cells treated with differentiation medium + troglitazone as positive control. (C) Absorbance of Oil Red O color intensity, (D) triglyceride levels of 3T3-L1 cell culture supernatant. (E) Cell viability after 2 days of LsAg and troglitazone treatment. Statistical significance was determined using Kruskal-Wallis followed by Dunn's multiple comparisons test. Data are expressed as means ± SEM. *p<0.05.

3.8 Daily LsAg administration for 2 weeks improves glucose tolerance in DIO mice

Since our previous finding showed an improvement of glucose tolerance in *L.s.*-infected DIO mice, we tested whether administration of crude extracts of *L.s.* (LsAg) and other helminth-derived products including ES-62, CPI, and ALT improve glucose tolerance in DIO mice. Daily i.p. injections of 2µg LsAg, ES-62, CPI, and ALT were administered to C57BL/6 mice started at 7 weeks on HF diet for 2 weeks. Glucose tolerance test was performed following the last day of administration.

Given that the earlier experiment in DIO mice with *L.s*. infection as well as 3T3-L1 cell line culture with LsAg treatment suggested an inhibition of adipogenesis, it was further investigated whether LsAg administration inhibits adipogenesis in vivo. For this purpose, whole body weight and fat tissue mass of mice were analyzed. Body weight developments among all groups showed no difference during the high fat diet, although CPI-treated animals had a tendency for a lower body weight compared to the other groups (Fig. 15A, B). Perirenal and EAT adipose tissue weights were not different among the groups (Fig. 15C, D). These findings revealed that two weeks of treatment with helminth-derived products of DIO mice did not induce weight loss (Fig 15A-E).

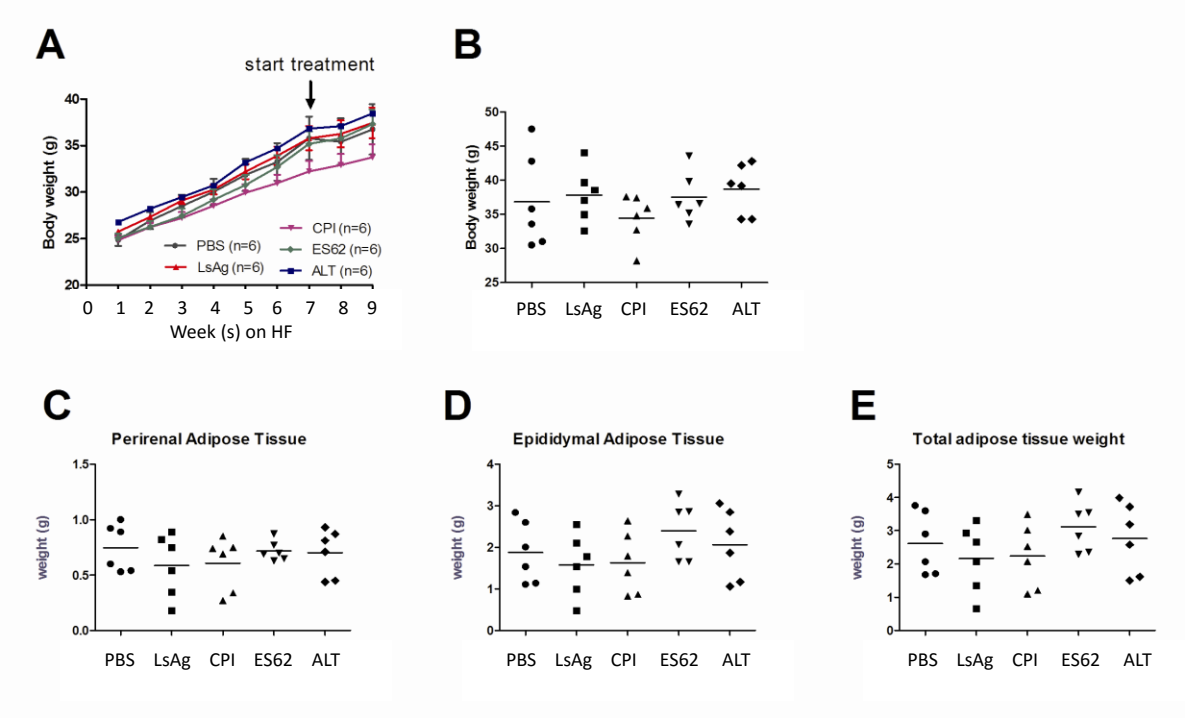

Figure 15. Two weeks of helminth-derived product administration does not induce weight loss in DIO mice. A) Body weight development during HF diet of mice that were treated daily for two weeks with PBS, LsAg, CPI, ES-62 and ALT started at 7 weeks on HF diet. B) Body weight after 9 weeks on HF diet. Comparison of C) perirenal adipose tissue, D) epididymal adipose tissue, E) total adipose tissue weight. Statistical significance was determined using Kruskal-Wallis followed by Dunn's multiple comparisons test. Data are expressed as means ± SEM.

While body weight among the groups were not different, blood glucose tolerance of *L.s.*-infected DIO mice was significantly improved compared to PBS-treated DIO controls and ES-62-treated DIO mice (Fig. 16A, B). In addition, CPI and ALT administration tended to improve glucose tolerance compared to PBS-treated controls, although this difference did not reach statistical significance. Despite the improvement of glucose tolerance by administration of LsAg, CPI and ALT, insulin tolerance of all treatment groups were not improved (Fig 16C, D).

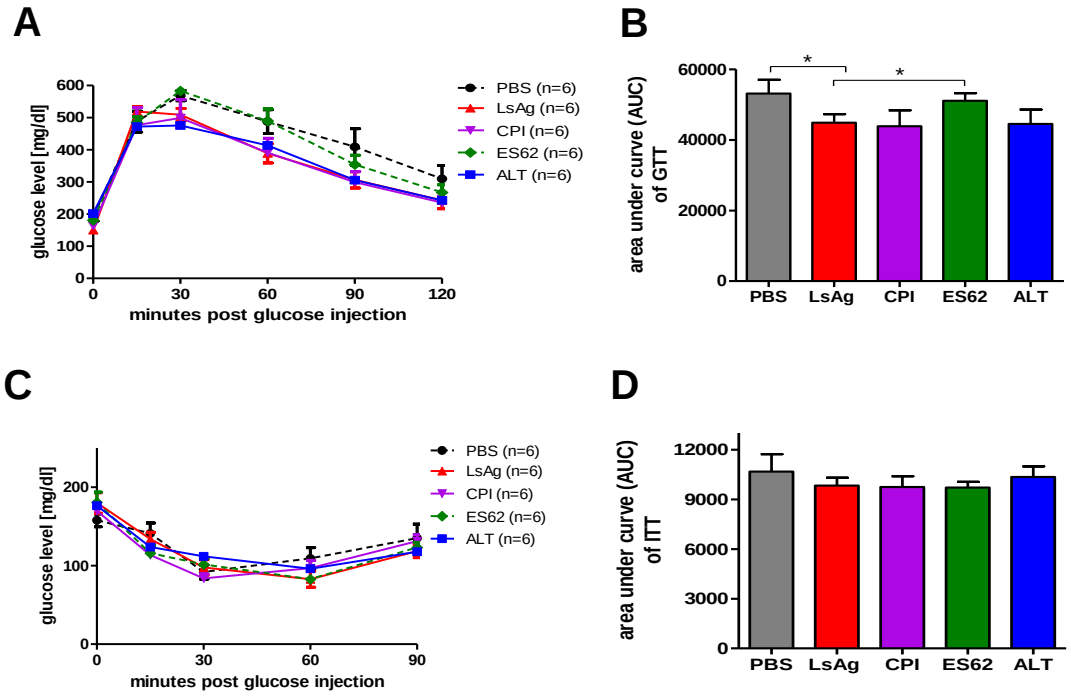

Figure 16. Two weeks of LsAg administration improves glucose tolerance in DIO mice. A) Blood glucose levels over time following i.p. glucose challenge in LsAg, CPI, ES-62, and ALT-treated mice and PBS-treated controls that received a HF diet for 9 weeks. B) Area under the curve obtained from the glucose tolerance test. C) Blood glucose levels over time following i.p. insulin challenge in LsAg-treated mice and PBS-treated controls that received a HF diet for 10 weeks. D) Area under the curve obtained from the insulin tolerance test. Statistical significance was determined using Kruskal-Wallis followed by Dunn's multiple comparisons test. Data are expressed as means ± SEM. *p<0.05.

3.9 Daily LsAg administration for 2 weeks increases the frequency of eosinophils and AAM in EAT

In line with the cellular composition of EAT in *L.s.*-infected mice, LsAg-treated mice demonstrated an increased frequency of eosinophils (Fig 17A), but no reduction of macrophage frequencies in SVF of EAT. However, although CPI and ALT administration improved glucose tolerance to some degree in DIO mice, they did not increase the frequency of eosinophils, indicating that glucose tolerance improvement in CPI and ALT administration are independent on eosinophils. Conversely, although ES-62 administration significantly increased the frequency of eosinophils (Fig. 17A) it

did not improve glucose tolerance in DIO mice. The frequency of neutrophils in EAT of DIO mice was not reduced by LsAg, CPI and ALT administration (Fig. 17B). Nevertheless, in ES-62-treated DIO mice, the frequency of neutrophils was significantly reduced (Fig.17B). CD4 frequencies of EAT in LsAg-treated DIO mice was significantly higher than in CPI-treated animals and tended to be increased compared to PBS treated DIO mice (Fig. 17C). The frequency of macrophages within EAT during HF diet among the groups were not different (Fig. 17D), suggesting that helminth antigen did not restrict macrophage infiltration during HF diet feeding. However, the frequency of CAM was reduced in all of the helminth antigen administrations, reaching statistical significance in the LsAg-treated DIO mice (Fig. 17E). In line with the increased frequency of eosinophils, AAM frequency was also increased in EAT of DIO mice that received LsAg and ES-62 administration compared to controls, indicating that eosinophils have a role in AAM polarization by LsAg and ES-62 administration. Although the eosinophil frequency was not increased in CPI-treated DIO mice, the frequency of AAM in that group was also increased compared to PBS control (Fig. 17F). The cell compositions in EAT indicate that each helminth-derived product (LsAg, CPI, and ALT) improve glucose tolerance via different mechanisms, and increases of eosinophils and AAM do not always a line with improved glucose tolerance as shown in ES-62-treated DIO mice.

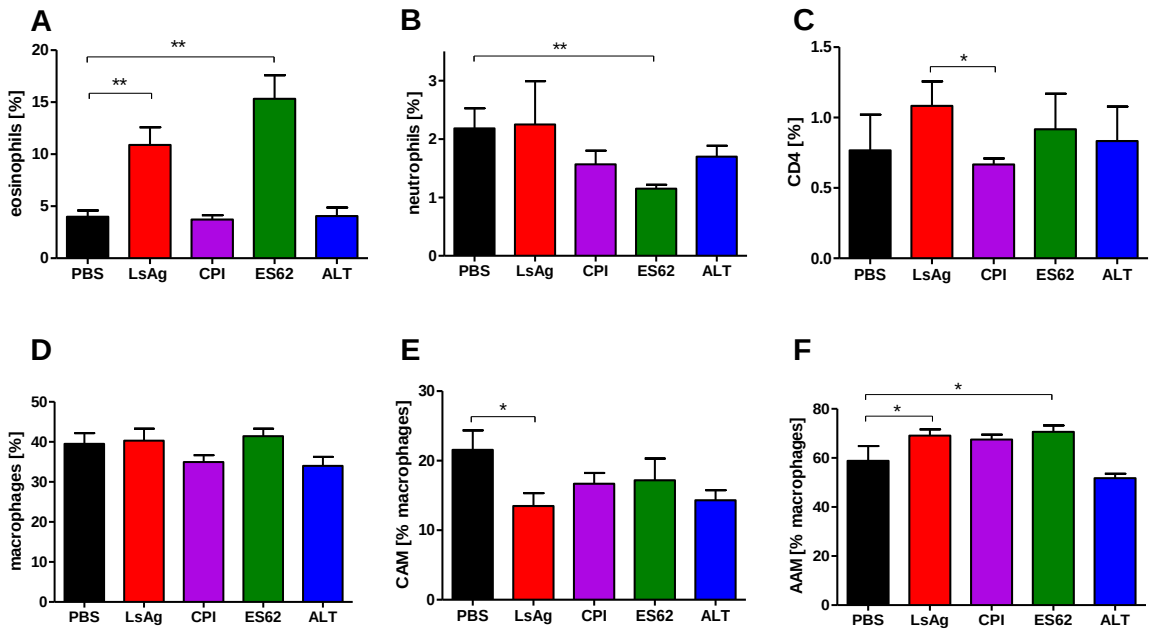

Figure 17. Impact of LsAg, CPI, ES-62, and ALT administration (n=6 per group) on the cellular composition within EAT during HF diet. Frequency of (A) eosinophils, (B) neutrophils, (C) CD4 T cells, (D) macrophages, (E) macrophages expressing CD11c (CAM), (F) macrophages expressing RELMα (AAM) within the SVF of EAT of DIO mice. Statistical significance was determined using Kruskal-Wallis followed by Dunn's multiple comparisons test. Data are expressed as means ± SEM. *p<0.05, **p<0.01.

Consistent with the increased frequency of AAM in EAT of LsAg-treated DIO mice, *Arginase 1* gene expression tended to be upregulated after 2 weeks of LsAg administration (Fig 18A) and parallel to the improvement of glucose tolerance, *Pparg* and *Glut4* expression tended to be increased in EAT of LsAg-treated DIO mice (Fig 18B,C). These initial findings suggest that LsAg administration improves glucose tolerance in DIO mice through induction of insulin signaling. While insulin signaling was improved by LsAg administration, anti-inflammatory *Il10* gene expression was not upregulated in DIO mice that were treated with all of the different helminth-derived products (Fig. 18D). Conversely, *Resistin* expression, an adipokine which is proposed to cause insulin resistance [176] was upregulated in all of the helminth-derived product administrations compared to PBS treated DIO control mice (Fig. 18E).

A recent study identified *transcriptional regulator interacting with the PHD-bromodomain 2 / SERTA domain-containing protein 2* (*Trip-Br2/Sertad2*), a protein that modulates fat storage through simultaneous regulation of lipolysis, thermogenesis and oxidative metabolism. The absence of *Trip-Br2/Sertad2* has been shown to protect mice from obesity-related insulin resistance, and was associated with increased thermogenesis and energy expenditure [177]. Interestingly, ALT and ES-62 administrations significantly suppressed expression of *Trip-Br2* in DIO mice, while LsAg administration had no effect (Fig. 18F), suggesting that both ALT and ES-62 may have an impact in energy expenditure.

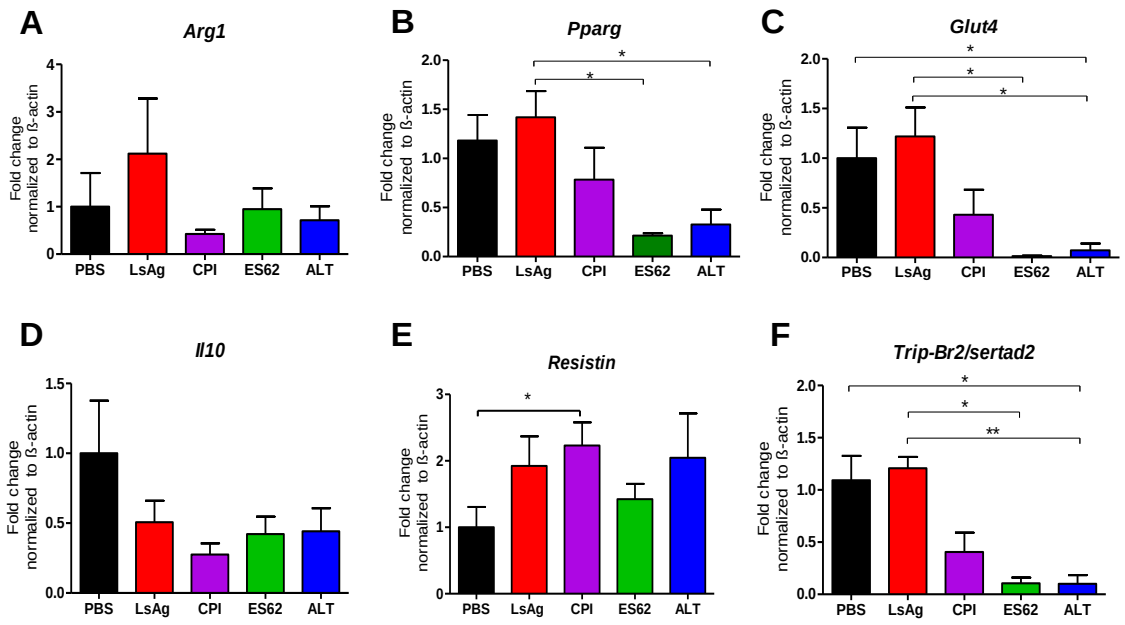

Figure 18. Relative gene expression of (A) *Arginase-1*, (B) *Pparg*, (C) *Glut4,* (D) *Il10,* (E) *Resistin* , and (F) *Trip-Br2/Sertad2* within EAT of helminth antigen or PBS-treated DIO mice. Statistical significance was determined using Kruskal-Wallis test followed by Dunn's multiple comparisons test. Data are expressed as means ± SEM. *p<0.05, **p<0.01.

3.10 Continuous administration of LsAg is required to improve glucose tolerance in DIO mice

Since LsAg administration showed the strongest improvement of glucose tolerance, further investigation was focused on LsAg administration and its impact on diet-induced insulin resistance. To investigate for how long LsAg administration maintains

the improved glucose tolerance in DIO mice and whether prolonged treatment with LsAg provides a better effect two repeat experiments were performed. A prolonged LsAg administration with three administrations per week for a total of 4 weeks failed to improve glucose tolerance in DIO mice compared to PBS controls and was associated with an increased body weight in the LsAg treated mice (Fig. 19A-C). In addition, glucose tolerance was also not improved when tested 2 weeks after the last LsAg injection (Fig. 19D-F). These findings suggest that a continuously administration of LsAg should be given to keep the beneficial effect on glucose tolerance.

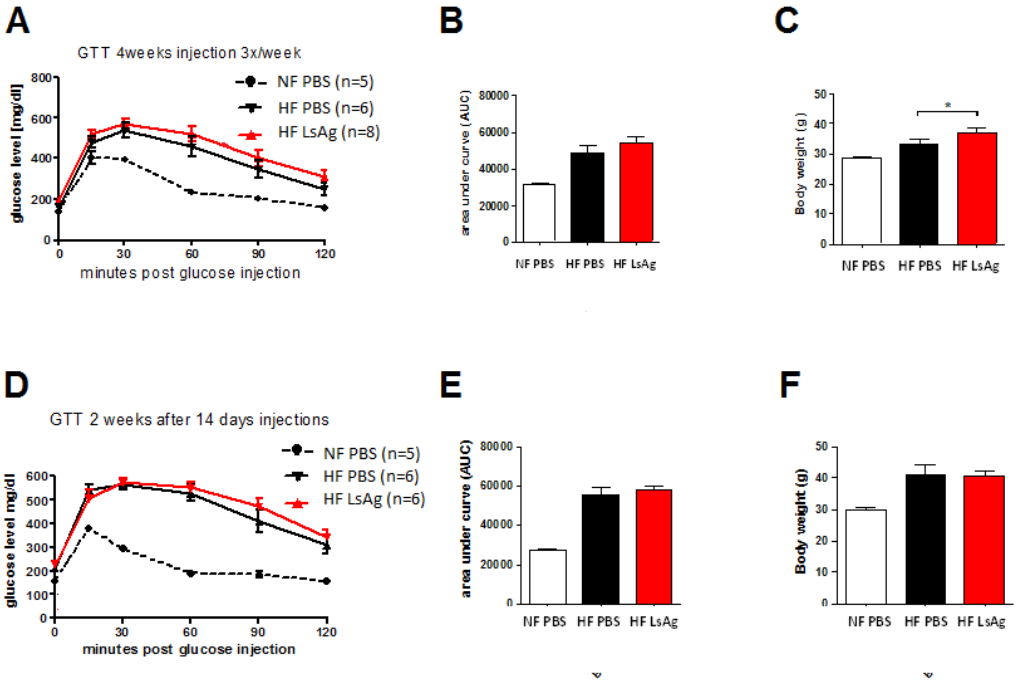

Figure 19. Discontinuous LsAg administration failed to improve glucose tolerance in DIO mice. (A) Blood glucose levels over time during a glucose tolerance test and (B) area under the curve of the glucose tolerance test. (C) Body weight of mice on HF diet after 4 weeks of injections with LsAg and PBS (3x per week). (D) Blood glucose levels over time during a glucose tolerance test and (E) area under the curve of the glucose tolerance test. (F) Body weight of mice on HF diet 2 weeks after 14 days of daily LsAg or PBS injection. Statistical significance was determined between HF diet groups using Mann-Whitney-U-test. Data are expressed as means ±SEM *$p < 0.05$.

Interestingly, a repeated round of daily i.p. LsAg injections of mice shown in Fig. 19D-F for another two weeks improved the glucose tolerance when tested four days after the last injection (Fig. 20A,B). These findings further confirm that continuous LsAg administration was required to improve glucose tolerance in DIO mice. Therefore, further experiments should test whether continuous release of LsAg by osmotic pumps provides a better protective effect against insulin resistance.

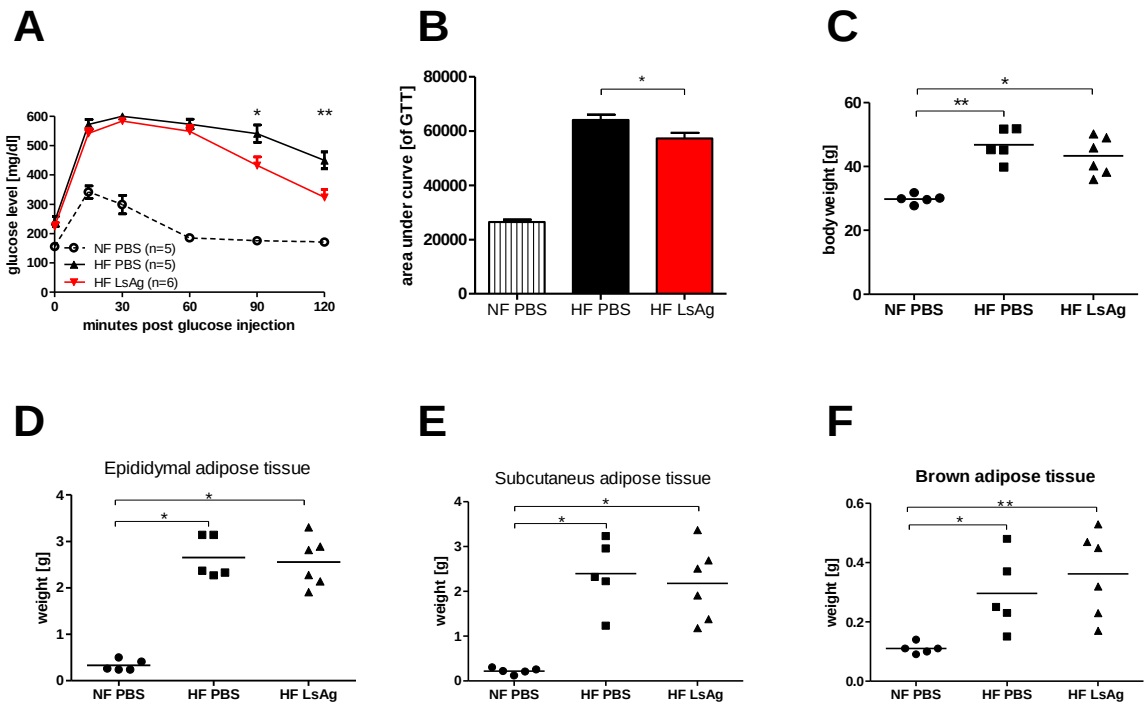

Figure 20. Repeated LsAg administration in DIO mice does not affect adipose tissue weight. (A) Blood glucose levels over time during a glucose tolerance test and (B) area under the curve of the glucose tolerance test from animals used for Fig. 19D-F, after two additional weeks of daily LsAg or PBS treatments. (C) Body weight development during HF and chow diet, (D) epididymal adipose tissue weight, (E) subcutaneous adipose tissue weight, as well as (F) brown adipose tissue weight. Statistical significance for (C-F) were determined using Kruskal-Wallis followed by Dunn's multiple comparisons test. For (A) and (B), statistical significance were determined between HF diet groups using Mann-Whitney-U-test. Data are expressed as means ±SEM *p < 0.05; **p < 0.01.

3.11 Repeated LsAg administration does not restrict adipogenesis

To confirm our findings in the previous experiment regarding the impact of LsAg administration on adipogenesis in vivo, the body weight and adipose tissue mass of DIO mice was analyzed after 2 weeks of LsAg administration. As shown in Fig. 20, there were no significant differences in body weight as well as epididymal, subcutaneous and brown adipose tissue weight between PBS- and LsAg-treated groups. This indicates and confirms our previous experiment that two weeks of LsAg administration are not sufficient to reduce adipogenesis in DIO mice (Fig. 20D-F).

It has been described that hypertrophy of adipocytes is correlated with inflammation-induced insulin resistance. Nevertheless, although LsAg administration improved glucose tolerance, adipocytes in both EAT and ScAT which were analyzed in LsAg- and PBS-treated DIO mice did not display a difference in diameter size (Fig. 21A-H), indicating that two weeks of LsAg administration does not suppress adipogenesis and fatty acid storage in adipocytes in vivo when administered after the development of glucose intolerance.

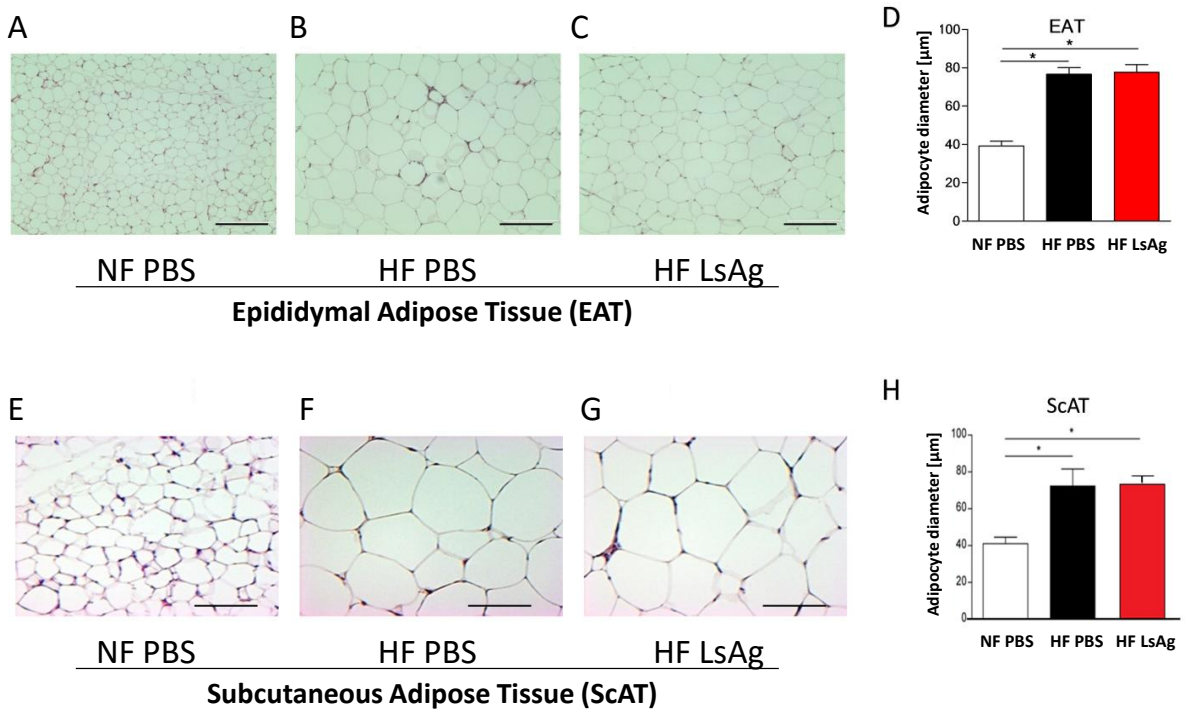

Figure 21. Two weeks of LsAg administration does impact adipocytes size. Structure of EAT of control mice on chow diet (A), PBS-treated DIO mice (B) and LsAg-treated DIO mice (C) as well as (D) epididymal adipocytes size. Structure of subcutaneous adipose tissue of control mice on chow diet (E), PBS-treated DIO mice (F) and LsAg-treated DIO mice (G) as well as (H) subcutaneous adipocyte size. For Fig. A-C the bar represents 200µm, for Fig. E-G the bar represent 100µm. Statistical significance was determined using Kruskal-Wallis followed by Dunn's multiple comparisons test. Data are expressed as means ± SEM.

Analyses of EAT revealed that the total number of leucocytes was increased in DIO mice and was not altered by two weeks of LsAg treatment (Fig. 22A). In line with our previous findings in *L.s.*-infected DIO mice and the first LsAg-treatment experiment in DIO mice, analysis of the cell composition of EAT by flow cytometry confirmed a significant higher frequency of eosinophils in LsAg-treated DIO mice compared to PBS-treated DIO controls (Fig. 22B). As expected, LsAg-treated DIO mice further had a higher frequency of RELMα+ macrophages, but less CD11c+ CAM compared to DIO control mice (Fig. 22C-E), suggesting that LsAg

administration improves glucose tolerance by increasing eosinophil and AAM frequencies in adipose tissue. Furthermore, CD4 T cell frequencies in LsAg-treated DIO mice were significantly higher compared with PBS-treated DIO controls (Fig. 22F). CD4 T cells were further assessed for FoxP3 positivity. Surprisingly, frequencies of CD4+FoxP3+ regulatory T-cells were higher in PBS-treated DIO controls compared to LsAg-treated mice (Fig. 22G). However, absolute numbers of CD4+FoxP3+ regulatory T-cells within EAT tended to be higher in LsAg-treated DIO mice ($p>0.05$; Fig. 22H), indicating that LsAg administration increases the recruitment of regulatory T-cells into the EAT of DIO mice.

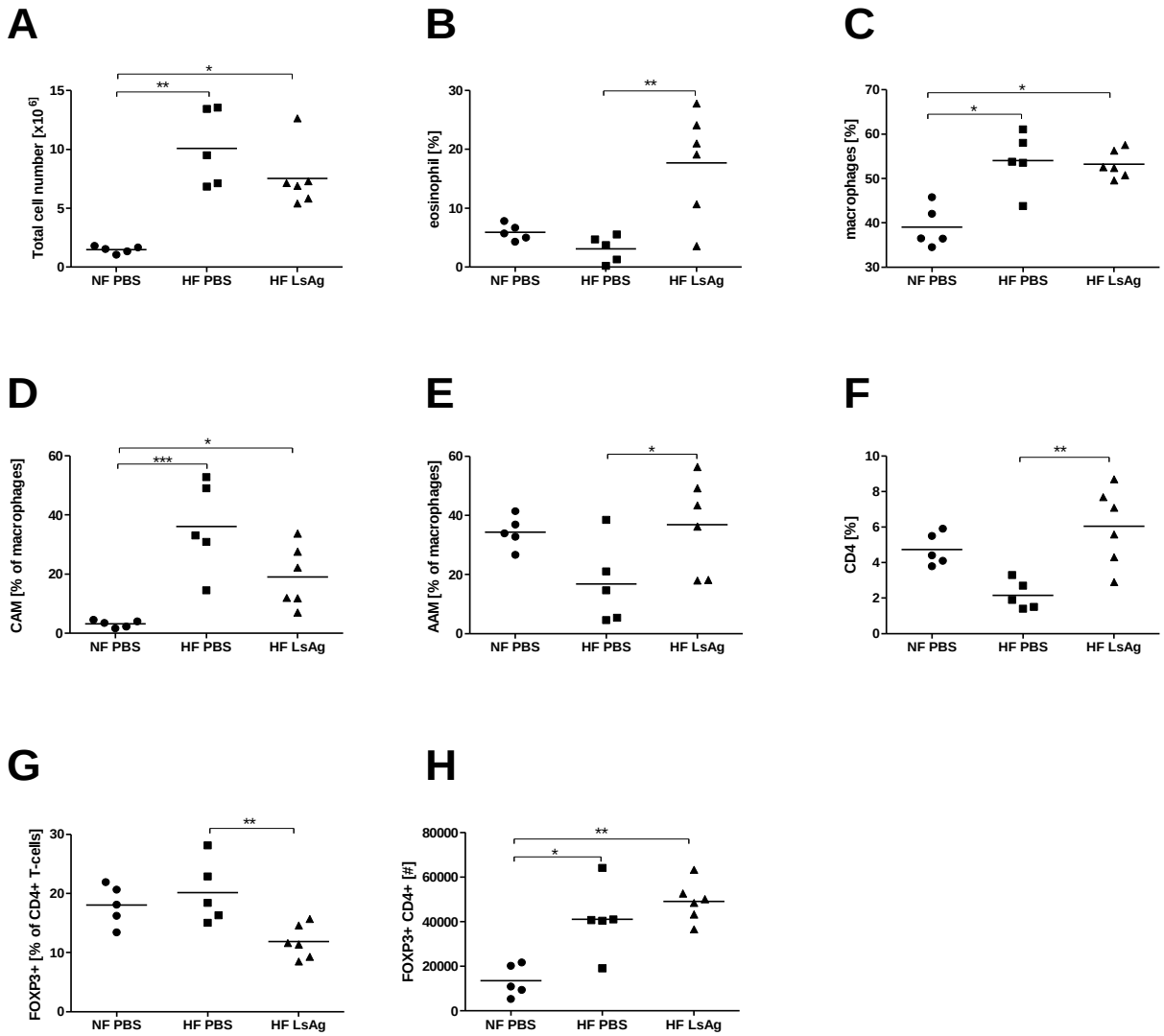

Figure 22. Repeated LsAg administration increases the frequency of eosinophils and alternatively activated macrophages within EAT. (A) Total number of leucocytes in EAT of LsAg- and PBS-treated DIO mice and PBS-treated chow diet controls. Frequency of (B) eosinophils, (C) macrophages, (D)

macrophages expressing CD11c (CAM), (E) macrophages expressing RELMα (AAM). (F) Frequency of CD4 T cells, (G) frequency of FoxP3+ CD4 T cells and (G) total number of CD4+ FoxP3+ T cells within EAT of LsAg- or PBS -treated DIO mice and chow diet controls. Statistical significance was determined using Kruskal-Wallis followed by Dunn's multiple comparisons test. Data are expressed as means ± SEM. *p<0.05, **p<0.01.

3.12 LsAg administration induces an anti-inflammatory immune response and promotes insulin signaling

To identify the impact of LsAg administration in DIO mice, particularly in mRNA levels, expression analysis of 84 genes in EAT of LsAg-treated mice (n=10) and PBS-treated controls (n=8) that received a HF diet, as well as corresponding chow diet controls were performed using a PCR Array (SABioscience). Gene expression data that had a fold change >1.3 are presented in Fig. 23 and Table S3.

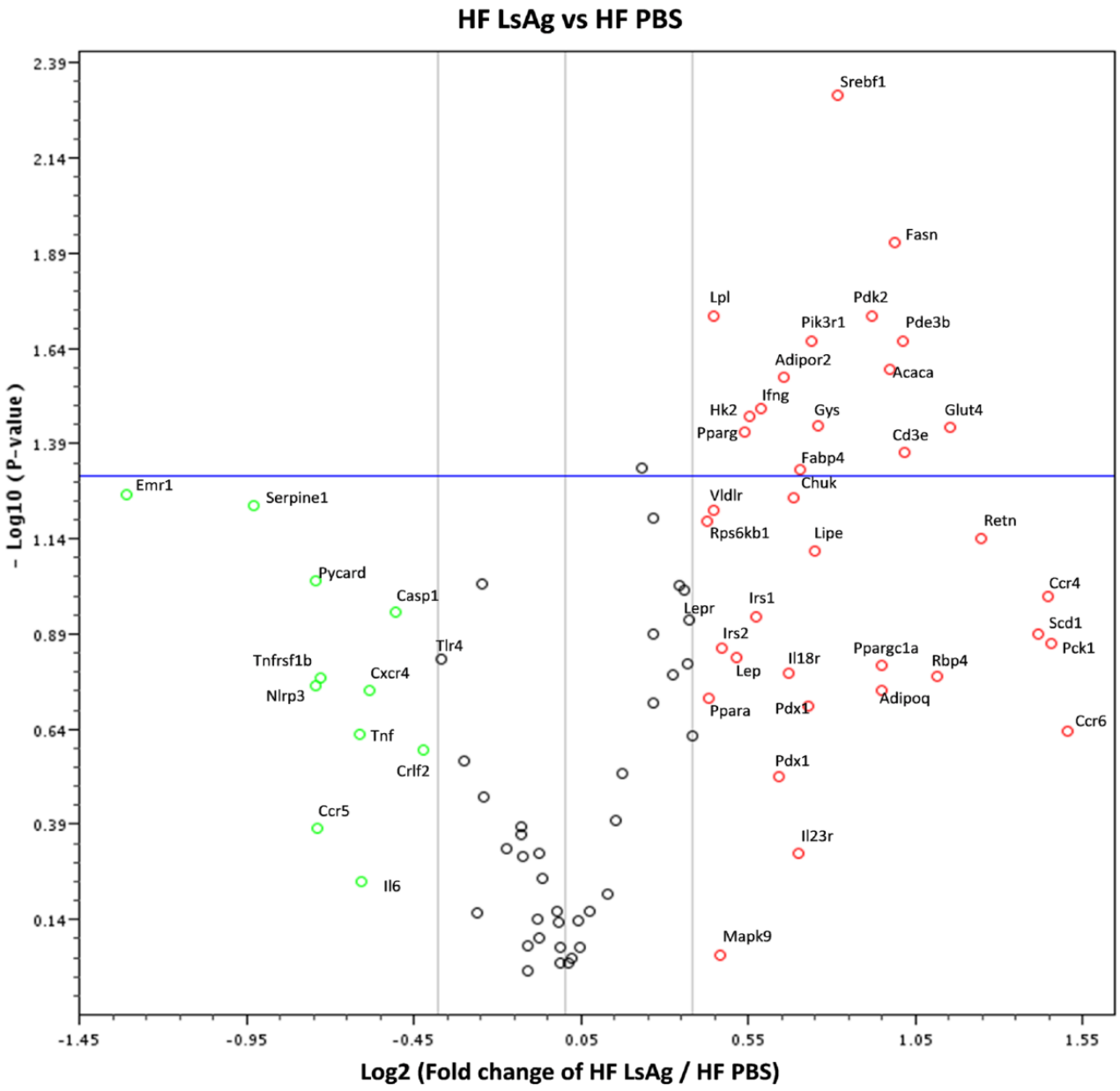

Figure 23. Volcano plot representing gene expression data from EAT of DIO mice which were treated with LsAg (n=10) compared to PBS-treated controls (n=8). The x axis represents the fold change (given in log2), whereas the y-axis represents the p-value (given in log10). The blue line represents p = 0.05 with points above the line having p < 0.05. Red circles have a fold change of more than 1.3, the green circles have a fold change of less than -1.3.

3.12.1 LsAg administration upregulates genes related to insulin signaling

In line with our previous finding that revealed an improvement of glucose tolerance in LsAg- treated mice, DIO mice that received i.p. LsAg injections had a significantly higher expression of genes-related to insulin signaling such as *solute carrier family 2 (facilitated glucose transporter), member 4* (*Slc2a4*) or *Glut4*, *phosphodiesterase 3B* (*Pde3b*)*, Phosphatidylinositol 3-kinase, regulatory subunit, polypeptide 1* (*Pik3r1*) and *hexokinase-2* (*Hk2*) compared to DIO mice that received PBS ($p<0.05$). Furthermore, there were tendencies of a higher expression of *Irs1* ($p=0.11$) and *Irs2* ($p=0.14$) in LsAg-treated DIO mice. These indicate that LsAg administration increased insulin signaling in EAT of DIO mice. Subsequently, LsAg administration had a tendency for an increased expression of *adiponectin* (*adipoq*) ($p=0.18$), an adiponectin coding gene, and increased expression of *adiponectin receptor-2* (*adipor2*, $p<0.05$) in EAT of DIO mice. Therefore, these may further support the improvement of insulin signaling in DIO mice that obtained LsAg treatment.

3.12.2 2 weeks of daily LsAg administration increases the expression of genes related to fatty acid uptake and energy anabolism

In accordance with the improved insulin signaling, the cell metabolism in LsAg-treated DIO mice exerted an anabolic state including lipogenesis and glycogenesis. Accordingly, upregulation of *sterol regulatory element binding transcription factor 1* (*Srebf1*) ($p<0.05$), *fatty acid synthase* (*Fasn*) ($p<0.01$), *acetyl-coenzyme A carboxylase alpha* (*Acaca*) ($p<0.05$) and *Pparg* ($p<0.05$), indicate an increased lipogenesis in adipocytes of DIO mice that received LsAg. Moreover, the tests revealed that expression of genes related to fatty acid uptake including *fatty acid binding protein 4* (*Fabp4*) and *Lpl* (both $p<0.05$), as well as *very low density lipoprotein receptor* (*Vldr*) ($p=0.06$) were increased in LsAg-treated DIO mice. Furthermore, array analysis indicated that the storage of excessive energy is not only generated as lipid formation, but also as glycogen as shown by *glycogen synthase* (*Gys*) upregulation in LsAg-treated DIO mice ($p<0.05$).

3.12.3 Inflammasome activation-induced apoptosis in EAT of LsAg-treated DIO mice is suppressed

In addition to the upregulation of genes related to insulin signaling and fatty acid uptake, we also found that expression of genes related to inflammatory immune responses tended to be downregulated in LsAg-treated mice. *Tumor necrosis factor receptor superfamily member 1B* (*Tnfrsf1b*) expression that encodes the membrane receptor for TNFα, tended to be suppressed in LsAg-treated DIO mice (p=0.17). Moreover, LsAg administration slightly suppressed inflammasome activation-induced apoptosis as were shown by downregulation of *NLR family, pyrin domain containing 3* (*Nlrp3*) (p=0.17), *PYD and CARD domain containing* (*Pycard*) (p=0.09), and *caspase-1* (*Casp1*) (p=0.11).

In line with the downregulation of genes involved in inflammatory responses and apoptosis, LsAg administration reduced macrophage recruitment into EAT as was highlighted by a downregulation of *epidermal growth factor module-containing mucin-like receptor 1* (*Emr1*) (*F4/80*) (p=0.056).

3.13 LsAg administration increases CD4 T cell recruitment in EAT and induces Th2 immune responses

Infiltration of CD4 T cells was increased in LsAg-treated mice as was shown by a stronger expression of *CD3 antigen, epsilon polypeptide* (*Cd3e*) ($p<0.05$) and confirmed our previous results on CD4+ T cells from flow cytometry. Furthermore, a trend to a higher expression of *chemokine (C-C motif) receptor type 4* (*Ccr4*) (p=0.10) in EAT of LsAg-treated DIO mice indicates an increased Th2 infiltration in EAT since *Ccr4* is highly expressed on the surface of Th2 cells, suggesting that LsAg administration induces a Th2 polarization.

Interestingly, DIO mice that received LsAg treatment showed a suppressed expression of genes related to atherothrombotic formation such as *serine (or cysteine) peptidase inhibitor, clade E, member 1* (*Serpine1*) (p=0.06) [29], suggesting that LsAg administration may provide a beneficial impact on cardiovascular disease prevention. Although most of gene expression analysis revealed an upregulation of genes related

to the improvement of insulin signaling, *Ifng* expression in LsAg-treated DIO mice was increased ($p<0.05$). In addition, array analysis also showed an upregulation of *pyruvate dehydrogenase kinase, isoenzyme 2* (*Pdk2*), which was previously associated with T2D [179]. With exception for these two genes, the findings of the array analysis indicate that LsAg administration suppresses apoptosis-induced inflammasome activation, promotes insulin signaling in EAT and increases glucose and fatty acid uptake into white adipocytes.

3.14 LsAg administration increases AAM polarization, regulatory T cells and type 2 immune responses within EAT

In order to obtain a better understanding regarding the underlying mechanism of improved glucose tolerance upon LsAg administration, several additional gene expression analyses were performed from EAT. In line with the previous FACS analysis of EAT that highlighted increased frequencies of F4/80+ RELMα+ AAM upon LsAg administration, the expression of *arginase-1* ($p<0.01$) (Fig. 24A), a gene expressed in AAM, was significantly upregulated in EAT of LsAg-treated DIO mice. This confirms that LsAg administration increases AAM polarization in EAT of DIO mice.

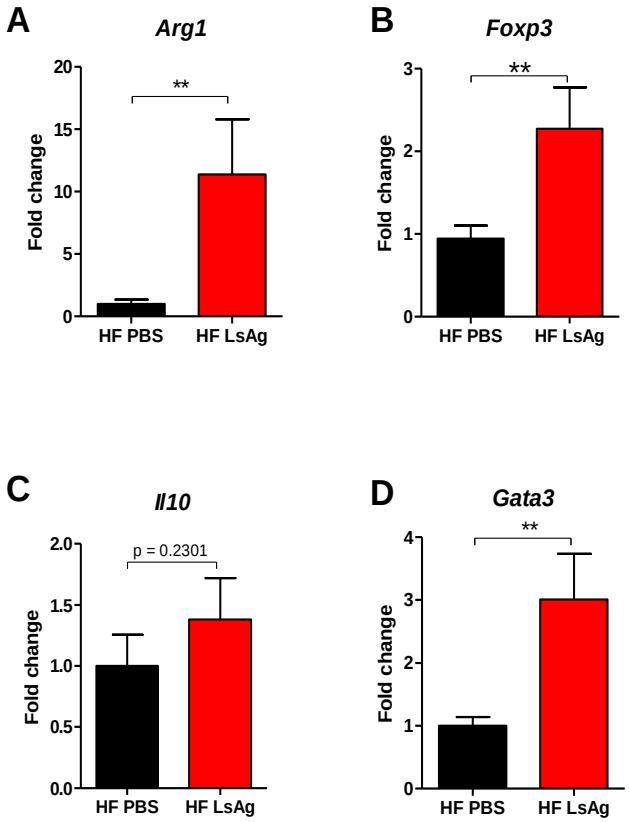

Figure 24. Daily LsAg administration for 2 weeks increases the expression of genes associated with type 2 immune responses in EAT of DIO mice. Gene expression of *Arg1* (*A*), *Foxp3* (*B*), *Il10,* and (*C*) *Gata3* (*D*). Gene expression is given as fold changes after normalization to *β-actin*. Statistical significance was determined using Mann-Whitney-U-test. Data are expressed as means ± SEM. *p < 0.05, **p <0.01.

As shown by our earlier data, FACS analysis of EAT revealed an increased CD4 frequency in LsAg-treated DIO mice. However it remained unclear whether LsAg increased CD4 regulatory T cell numbers in EAT since the frequency of CD4+FoxP3+ cells in LsAg-treated DIO mice was lower compared to PBS-treated controls although the absolute number showed the opposite. To confirm whether LsAg treatment increased regulatory T cells in EAT of DIO mice, *Foxp3* gene expression analysis was performed. *Foxp3* gene expression was significantly increased in EAT of LsAg-treated DIO mice compared to PBS-treated DIO controls ($p<0.01$, Fig. 24B), suggesting that

LsAg administration increased total numbers of regulatory T cells in EAT of DIO mice. Since regulatory T cells play an important role in maintaining glucose homeostasis in lean mice [64], this may contribute to the protective effect of LsAg treatment. However, analysis of *Il10* gene expression revealed that its expression by LsAg administration was not statistical significant (p=0.23, Fig. 24C).

Furthermore, in line with the tendency of an increased Th2 induction as was indicated by an increased expression of *Ccr4*, a significantly higher expression of the Th2 transcription factor GATA binding protein 3 (*Gata3*) [180] was observed (p<0.01, Fig. 24D). This result highlights that LsAg administration induces type 2 immune responses.

Collectively, data from PCR arrays and additional gene expression analyses suggest that LsAg administration induced type 2 immune responses, increased AAM and regulatory T cells as well as promoted insulin signaling in EAT, thus increasing glucose and FFA uptake into white adipocytes.

3.15 LsAg administration may induce browning of fat in EAT

Since LsAg administration induced an increase of eosinophils and AAM within EAT, further investigation was conducted to investigate whether LsAg treatment induced browning of EAT and ScAT of DIO mice. The PCR array analysis from EAT of DIO mice included genes that were related to browning of adipose tissue such as *Ucp1*, *Ppargc1a* and *Pparg*. Those PCR array results showed that *Pparg*, a gene which was reported to play a role in browning of adipose tissue [181] was upregulated in LsAg-treated DIO mice (p<0.05), whereas the increased expression of *Ppargc1a* (*Pgc1a*) in LsAg treated animals did not reach statistical significance (fold change = 1.93, p=0.156, Fig. 23 and Table S3) and no differences were observed for the expression of *Ucp1* in EAT of DIO mice that received LsAg or PBS administration (fold change =1.01, p=0.95). Since beige cells are more prominent in ScAT, gene expression analyses of *Pparg* and *Ucp1* were performed from ScAT. However, both *Pparg* (p=0.089) and *Ucp1* (p=0.331) expression was not significantly increased by LsAg treatment (Fig. 25A, B).

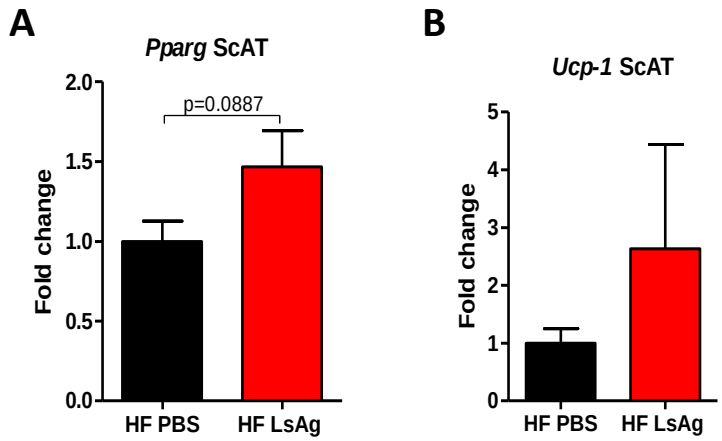

Figure 25. Gene expression levels in subcutaneous adipose tissue (ScAT) of DIO mice after 2 weeks of daily LsAg or PBS ip injection. Relative mRNA levels of (A) *Pparg*, and (B) *Ucp1* in ScAT after normalization to *ß-actin*. At least 5 samples per group were used for analysis. Statistical significance was determined using Mann-Whitney-U-test. Data are expressed as means ± SEM.

Given that browning of adipose tissue is enhanced during cold, cold exposure at 5°C was performed after 2 weeks of daily LsAg or PBS injection in DIO mice to investigate the impact of LsAg administration on browning of adipose tissue under cold induction. Development of hypothermia was reduced in LsAg-treated DIO mice compared to PBS-treated controls, and reaching statistical significance within the first 2 hours of cold exposure (Fig. 26A). Accordingly, *Ucp1* expression was significantly increased in EAT of LsAg-treated mice after 4h of cold exposure (Fig. 26B). Furthermore, an increased expression of *Gata3*, *Il4* and *Il5* (Fig. 26C-E) indicated the induction of type 2 immune responses in LsAg-treated DIO mice after 2 weeks of LsAg treatment. Moreover, as expected, *Arg1* expression was significantly upregulated in DIO that received LsAg treatment. These findings indicate that LsAg administrations induced browning of white adipose tissue under cold exposure via the induction of type 2 associated cytokines and AAM.

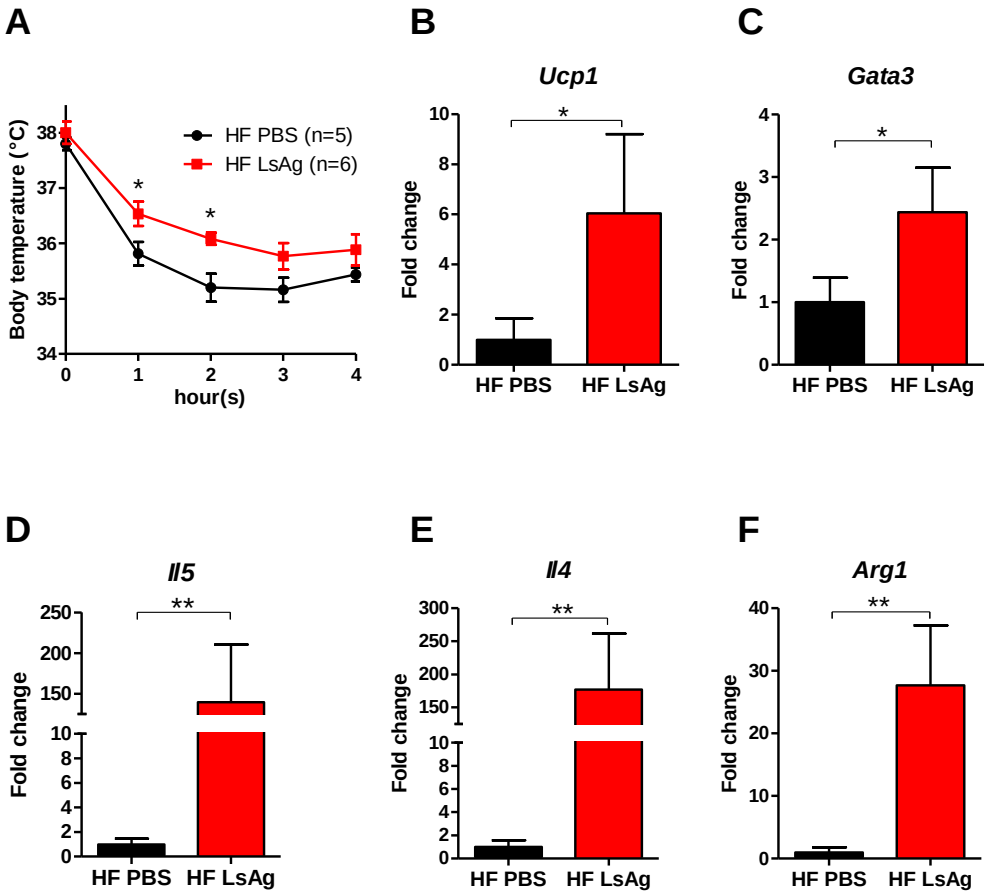

Figure 26. Two weeks of daily LsAg administration promotes thermogenesis and beiging of EAT of DIO mice under cold exposure. *A*) Body temperature kinetics during a cold exposure at 5°C of mice that received daily injections of LsAg or PBS for 14 days and were fed on a HF diet for a total of 4 weeks. Gene expression of (*B*) *Ucp1,* (*C*) *Gata3*, (*D*) *Il5*, (*E*) Il4, (*F*) *Arg1* in the EAT of those mice. Gene expression is given as fold change after normalization to *β-actin*. Statistical significance was determined using Mann-Whitney-U-test. Data are expressed as means ± SEM. *p < 0.05, **p <0.01.

4. Discussion

In this thesis, it was tested whether *L.s*. infection and filarial antigen administration have a beneficial impact on obesity-induced insulin resistance and the underlying mechanism was investigated. Numerous studies reported that chronic inflammation in obesity-induced insulin resistance is associated with increased frequencies of CAM and a reduction of AAM in visceral adipose tissue due to excessive expansion of adipose tissue [45,164,182]. On the other hand, filarial infection and its antigen induce regulatory immune response in their hosts via the induction of Tregs, AAM, anti-inflammatory cytokines, and induce a type 2 immune response that counter regulates type 1 immune responses. Several beneficial impacts and possible mechanisms of filarial infection and its antigen to counter insulin resistance due to chronic inflammation in visceral adipose tissue were investigated in this thesis.

4.1 High fat diet induces glucose intolerance in obese mice

As a storage organ, fat tissue has an almost unlimited capacity to store excessive energy. During HF diet, lipid droplet formation in the adipocytes continuously increases to store excessive energy and leads to lipid accumulation and adipocyte enlargement called hypertrophy [18]. As seen in mice that received long term HF diet, fat tissue in the whole body expands, especially in the subcutaneous and visceral adipose tissue, and increased body weight occurs. Gradual adipocyte hypertrophy and tissue expansion lead to a deficiency of oxygenation of cells due to an imbalance between the increase of oxygen demand and supply by blood innervations [20,183,184]. Overtime, adipocytes suffer from hypoxia and undergo oxidative stress which can initiate inflammatory cytokine production and apoptosis [19,20]. Released cytokines along with apoptotic cells induce infiltration of macrophages into the adipose tissue, augment inflammation by additional cytokine production and eventually alter cell composition in visceral adipose tissue. The chronic inflammation caused by CAM and adipocyte stress inhibit the insulin signaling cascade in the cells of the body ubiquitously [25,41,185]. Consequently, glucose in the circulation cannot be taken up into the cells, which leads to glucose intolerance upon glucose challenge. Accordingly, experiments of this thesis demonstrate that both body weight and

adipose tissue mass of mice that received a HF diet for at least 8 weeks were increased compared to mice with a normal chow diet. This was accompanied by larger diameters of adipocytes in both EAT and ScAT. Further analysis carried out by flowcytometry revealed an increased frequency of CAM within EAT of mice on HF diet, suggesting an increased recruitment of macrophages. Ultimately, glucose intolerance occurred in DIO mice as a consequence of inhibited insulin signaling due to chronic inflammation.

4.1.1 Changes of the cellular composition by *L.s.* infection and LsAg counter-regulate chronic inflammation in DIO mice

As presented in our study, both *L.s*. infection and helminth-derived products improve glucose tolerance. This beneficial effect was accompanied with an increased frequency of eosinophils, AAM, and a decreased frequency of B cells. Since AAM in adipose tissue maintain insulin sensitivity in lean mice [41,45,185], induction of AAM by helminth-induced type 2 immune responses could dampen obesity-induced insulin resistance.

L.s. is well known to induce systemic type 2 immune responses in mice [166,186] and results from this thesis demonstrate that *L.s*. infection and LsAg administration also increased the frequency of eosinophils and F4/80+ RELMα+ AAM within EAT of DIO mice. Those changes correlated with an improvement of glucose tolerance in both *L.s*.-infected and LsAg-treated DIO mice. This finding is therefore, in accordance with Wu et al. that showed an improvement of glucose tolerance in *N. brasiliensis*-infected DIO mice which was accompanied by increased numbers of eosinophils and AAM in EAT [44]. AAM are generated in vitro by exposure to IL-4 and IL-13 via the STAT6 signaling pathway [57,63]. In contrast to CAM, AAM express low levels of pro-inflammatory cytokines and generate high levels of anti-inflammatory cytokines like IL-10 [45]. Moreover, increased arginase production in AAM counters iNOS activity by several mechanisms, including competition for the substrate arginine that is required for NO production [61]. Therefore, increased AAM frequencies in EAT of obese mice are believed to suppress inflammatory responses thus promoting glucose tolerance. This is in line with findings from this thesis, as improved glucose tolerance

was accompanied by an upregulated *Il10* expression in EAT of *L.s.*-infected DIO mice as well as an upregulated *arginase1* expression in EAT of DIO mice that were treated with LsAg.

4.1.1.1 Eosinophils are indispensable for glucose tolerance improvement by *L.s.* infection

Wu et al. revealed that eosinophil-derived IL-4 was essential to maintain AAM in adipose tissue [44]. Eosinophil-produced IL-4 was also shown to have an important role for nutrient metabolism and insulin sensitivity via STAT6 signaling. Absence of STAT6, which is important for AAM polarization, impaired insulin signaling, while reactivation of STAT6 signaling via IL-4 improves insulin sensitivity by inhibiting the PPARα-induced nutrient catabolism and reduces adipose tissue inflammation [53]. In addition, IL-4 administration reduces adiposity in DIO mice by increasing beige fat mass and thermogenic capacity thus increasing energy expenditure [54]. IL-4 further increased AKT phosphorylation in liver and muscle thus improving insulin sensitivity [53,187]. Therefore, as a major source of IL-4, helminth-induced eosinophils may be indispensable for improvement of glucose tolerance in obese mice. In accordance, *L.s.*-infection failed to improve glucose tolerance in eosinophil-deficient dblGATA mice in this thesis. In the absence of eosinophils, *L.s.* infection did not lead to an increased frequency of AAM in EAT, suggesting that eosinophils are indeed required to improve glucose tolerance by sustaining AAM presence in adipose tissue of obese mice.

4.1.1.2 Glucose tolerance improvement by *L.s.* infection was associated with a reduction of B cell accumulation and an expanded B1-cells subset

The past decade revealed that chronic inflammation in adipose tissue does not only involve innate immunity, but also adaptive immunity. It was previously shown that total B cell numbers peak after 3–4 weeks after initiation of HF diet in visceral adipose tissue [46,71] and induces a class switch to IgG in B cells of the visceral adipose tissue, thus enhancing pro-inflammatory IgG2c production which promotes macrophage-mediated inflammation via a Fc-mediated process [46]. B cells isolated from adipose tissue also induced CD4+ and CD8+ T cell IFNγ and

CXCL8 production, whereas IL-10 release was decreased, which could further trigger the inflammatory process [188]. While increased B cell numbers promote insulin resistance in obese mice, mice lacking B cells are protected from insulin resistance and depletion of B cells improves insulin sensitivity in DIO mice [46]. Interestingly, the glucose tolerance improvement in our experiments was also accompanied with a lower number of B cells in SVF of EAT in *L.s.*-infected DIO mice compared to DIO controls. In line with the reduction of total B cell numbers in EAT, IgG2a levels were also reduced, which is comparable to a reduction of IgG2c in C57BL/6 mice [189]. This suggests that reduced B cell numbers in EAT of *L.s.*-infected mice diminish HF diet–induced inflammation. Furthermore, the B1 cell subset was significantly increased in *L.s*.-infected compared to uninfected DIO controls. Since B1 cells are a source of IL-10 [190,191], the expanded B1-cell subset may contribute to of the protective effect seen in *L.s.*-infected mice. Future studies should therefore assess whether B cells from *L.s.*-infected DIO mice are less pathogenic compared to B cells from DIO controls.

4.1.2 Glucose tolerance improvement by helminth infection could be elucidated by suppression of adipogenesis

As obesity is the major risk factor to develop insulin resistance, numerous studies were conducted to develop strategies to overcome obesity thus preventing the onset of metabolic syndrome, including diabetes. Interestingly, an epidemiological study in humans and experimental studies in animals reported a correlation between helminth infection and parameters related to obesity inhibition. Thus, people in a rural area in China with a history of schistosomiasis had a lower BMI (body mass index) compared to endemic controls that never suffered from schistosomiasis [98]. Indication that helminth infection may indeed inhibit obesity comes from animal studies with *N. brasiliensis*. Wu et al. (2011) found that *N. brasiliensis*-infected mice had a lower perigonadal (epididymal) adipose tissue weight [44]. Similarly, Yang et al. demonstrated a lower body weight development and less visceral fat pad mass in *N. brasiliensis*-infected mice that were fed on a HF diet compared to uninfected mice [192]. *N. brasiliensis* infection also induced weight loss in DIO mice after 14 weeks of

HF diet [192]. In their study, intestinal helminth infection impaired the glucose absorption of the intestine and led to a reduced body weight. As additional mechanism, *N. brasiliensis*-infection induced a type 2 immune response, which led to an activation of STAT6 signaling and reduced lipogenesis and thus adipose tissue mass [192]. However, to what level altered food intake or pathology contributed to these effects are not clear. Interestingly, suppression of adipogenesis was not only present in gastrointestinal helminth infections like *N. brasiliensis*, but was also induced by infection with *L.s.*, which resides in the pleural cavity. Our multiple genes expression analyses of EAT in DIO BALB/c mice showed a downregulation of genes related with adipogenesis such as *Pparg, Gpd1* and *Cebpa* in EAT of *L.s.*-infected mice, indicating that glucose tolerance improvement in *L.s*. infection might also be elucidated by suppression of adipogenesis although the body weight between those two groups was not significantly different. Consistent with the downregulation of several genes related with adipogenesis in *L.s.*-infected mice, in vitro experiments with the 3T3-L1 pre-adipocyte cell culture demonstrated that LsAg-treated cells have less mature adipocytes compared to untreated cells. The mechanism by which LsAg suppresses adipocyte maturation is not fully understood, but was not due to a toxic effect, as cell viability was not altered. One possible explanation is the induction of RELMα, since the addition of RELMα was reported to down-regulate adipocyte differentiation markers, including *Pparg, Cebpa, adipocyte Protein-2* (*aP2*)*, Adipoq,* and *Glycerol-3-phosphate dehydrogenase* (*Gpdh*) [193]. Nevertheless, daily LsAg administration for 2 weeks did not suppress adipogenesis in vivo although glucose tolerance in LsAg-treated DIO mice was improved, suggesting that suppression of adipogenesis is not the major protective effect.

4.1.3 The beneficial effect of *L.s.* infection on glucose tolerance improvement is dependent on the time point of infection

Data from several time points of *L.s*. infection indicated that at 7-8 weeks and 11 weeks post infection, glucose tolerance of *L.s*.-infected DIO were consistently improved, whereas 9-10 and more than 11 weeks post infection did not show such a protective effect. It is likely that the development of *L.s*. in its host is causing those

differences on the impact of glucose tolerance. Although adult worms have been reported to induce Th2 immune responses [186,194,195], microfilariae were reported to provoke Th1 immune responses [195]. Isolated spleen cells from microfilariae-injected mice produced high levels of IFNγ upon *Brugia malayi* antigen stimulation [195]. In *L.s.*-infected WT mice, microfilaremia starts around 8 weeks post infection and reaches its peak around 75 days post infection [166], and steadily decreases afterwards. Thus, those time points of peak microfilaremia correlated with an impaired protective effect on glucose tolerance. Stimulation of isolated pleural lavage cells from 60 dpi *L.s.*-infected WT mice with LsAg revealed high levels of IFNγ [166] and injection of *L.s.* microfilariae in naïve mice were previously shown to induce IFNγ, MIG and IL-12 [196]. Similarly, PCR array results from LsAg treated and *L.s.* infected DIO mice also indicated an increased IFNγ expression in EAT. Since IFNγ was reported to impair insulin signaling via activation of the JAK-STAT1 pathway [175], this may explain why *L.s.* infection did not improve glucose tolerance after 9 weeks of infection. Accordingly, treatment with filarial antigen preparations obtained from prepatent filariae may further improve its efficacy to treat insulin resistance.

4.2 The impacts of helminth-derived product administration on DIO mice

Data from this thesis demonstrate that glucose tolerance improvement in DIO mice was not only achieved by infections with living worms, but was also accomplished in obese mice after two weeks of daily LsAg, CPI as well as ALT administration, but not by treatment with ES-62. Similar to *L.s.* infection, LsAg, ES-62, and CPI administration increased the frequency of AAM in EAT. However, although ES-62 administration induced increased frequencies of eosinophils and AAM, it did not improve glucose tolerance in DIO mice. Nevertheless, since it mimicked the impact of LsAg in restoring the cell composition in EAT, further investigation should be performed with different dosage regimens to test their efficacy on glucose tolerance induction.

Although CPI administration did not increase the frequency of eosinophils, it improved glucose tolerance. Interestingly, EAT of CPI-treated mice contained increased frequencies of AAM in the absence of an increased number of eosinophils,

suggesting that glucose tolerance improvement by CPI administration may be produced by a different mechanism. Such a possible mechanism is the suppression of adiposity in CPI-treated mice since CPI-treated mice that received HF diet had a lower body weight and adipose tissue mass compared to the other groups.

Unlike ES-62, CPI, and LsAg-treated animals, ALT-treated DIO mice did neither show an increased frequency of eosinophils nor AAM within EAT. Nevertheless, ALT-treated DIO mice had a reduced frequency of macrophages and CAM within EAT, indicating that its administration restricted macrophage infiltration during HF diet.

4.2.1 Glucose tolerance improvement by both *L.s.* infection and LsAg administration is not mediated by increased IL-10 responses

Filarial infection and LsAg administration did not only induce AAM and eosinophils, but also regulatory T cells that are another hallmark of helminth infections [197]. Two weeks of LsAg administration increased the number of CD4+ FoxP3+ regulatory T cells in SVF of EAT, which was confirmed by upregulated *Foxp3* expression in EAT. Furthermore, *Foxp3* expression was increased in EAT of *L.s.*-infected DIO mice and *L.s.*-infected lean mice. As reported by Feuerer et al., along with AAM, regulatory T cells are a potential source of IL-10, an anti-inflammatory cytokine that was shown to improve insulin sensitivity [64]. Although potential IL-10 producing cells like AAM and CD4+ Foxp3+ were increased in our experiment, both IL-10 mRNA levels and Il-10 protein concentrations were not increased in EAT and serum of DIO mice treated with LsAg, suggesting that IL-10 is not essential for the improvement of glucose tolerance in this context.

4.2.2 LsAg administration upregulates *Pparg* expression in EAT of DIO mice

Although gene expression of adipogenesis markers were downregulated in *L.s.*-infected mice and in vitro LsAg-treated 3T3-L1 cells were less mature, we found no differences in body weight development, adipose tissue weights, and adipocytes size in DIO mice that received two weeks of LsAg administration. In contrast to the gene expression analysis in EAT of *L.s.*-infected mice, PPARγ, an adipogenesis marker was upregulated in EAT of LsAg-treated DIO mice, indicating that LsAg administration

improved glucose tolerance without inhibiting adipogenesis. A similar paradoxical effect of PPARγ in promoting adipogenesis and improving glucose homeostasis and insulin sensitivity was reported by numerous studies [198–201]. Several studies reported that transgenic mice with an increased PPARγ activity are protected from obesity-associated insulin resistance [202], whereas mice lacking PPARγ in fat, muscle, or liver are predisposed to develop insulin resistance [200,201,203,204]. Thiazolidinedione (TZDs), a high-affinity agonist for PPARγ, was also found to be an effective treatment for T2D as it directly reduces systemic insulin resistance of peripheral tissues [199,205]. In addition, PPARγ has been reported to mediate anti-inflammatory effects through inhibition of NFκB, activator protein-1 (AP1), and STAT transcription factors [206]. Taken together, although PPARγ promotes adipocyte differentiation and adipogenesis, PPARγ enhances insulin sensitivity and suppresses inflammation thus improving glucose tolerance in DIO mice. In this context, the upregulation of PPARγ in DIO mice that received LsAg administration is plausible to improve glucose tolerance.

4.2.3 Glucose tolerance improvement is associated with LsAg-induced type 2 immune responses

As has been shown in this thesis, a strong induction of type 2 immune response including upregulation of *Gata3*, *Il5 and IL4* expression in EAT of DIO mice which received LsAg administration was observed. In line with this, *Ccr4* expression, a Th2 marker tended to be increased after 2 weeks of LsAg administration. These confirm our earlier findings in FACS analysis that revealed an increase of type 2 associated cells including eosinophils and AAM in EAT of *L.s.*-infected and LsAg-treated DIO mice.

Th2-associated cytokines like IL-5 and IL-4 can be also provided by type 2 innate lymphoid cells (ILC2s), a new innate lymphoid subset, which also expresses GATA3 [207,208]. Upregulation of *Il5* and *Il4* in LsAg-treated DIO mice may therefore indicate an increase of either Th2 cells or ILC2s in EAT of DIO mice. Type 2 immune responses during LsAg administration may improve insulin sensitivity in DIO mice since overexpression of IL-5 has been reported to play a key role in maintaining

eosinophils and promoting AAM activation in visceral adipose tissue and to promote glucose tolerance in mice which received HF diet, whereas the absence of IL-5 or eosinophils impaired glucose tolerance in DIO mice [209]. This beneficial effect was predicted due to the increase of oxidative metabolism and suppression of inflammation, which will reduce adiposity and promote insulin sensitivity [53].

4.2.4 Increase of energy expenditure by LsAg administration may improve glucose tolerance in DIO mice

The biology of brown adipose tissue has received growing attention over the last few years to counter obesity and its related diseases. In contrast to white adipose tissue which functions as storage of lipid excess, the main function of brown adipose tissue is the dissipation of chemical energy in the form of heat, thus increasing energy expenditure [155]. Surprisingly, a number of studies have identified another type of adipocytes that expresses high levels of mitochondrial uncoupling protein-1 (UCP-1) which is induced by "browning" of white adipose tissue by chronic cold exposure and β-adrenergic stimulation [210,211]. These "brown-like" cells are also called "beige" or "brite" cells and are distributed within the white adipose tissue [212,213]. Absence of beige cells in adipo- *PRD1-BF-1-RIZ1 homologous domain containing protein-16* (PRDM16) KO mice led to an increased susceptibility to obesity and metabolic dysfunctions including hepatic insulin resistance [214]. Since beige cells possess the capacity to burn energy from fat by producing heat, browning of white adipose tissue may be a novel target to increase energy expenditure, thus combating obesity and T2D.

Interestingly, recent studies demonstrated that browning of white adipose tissue correlated with AAM and eosinophils [54,55]. Upon eosinophil-derived IL-4 release, adipose tissue macrophages develop an AAM polarization [44], release catecholamines, activate β-adrenergic signaling and drive thermogenesis [54,56]. In accordance, LsAg administration in DIO mice increased eosinophils, AAM, and induced type 2 immune responses. Upon cold exposure, LsAg-treated DIO mice developed better body temperature tolerance. Increased expression of *Ucp1* in these mice further indicates that LsAg administration promotes beiging of white

adipose tissue by providing high number of eosinophils and AAM, thereby inducing thermogenesis and increasing energy expenditure in DIO mice. Since PPARγ agonist was also reported to induce browning of white adipose tissue via stabilization of PRDM16 protein [181], the upregulation of *Pparg* expression in EAT of LsAg-treated DIO mice also supports an increased energy expenditure in those mice. In addition to reduced adiposity, lipid ß-oxidation for thermogenesis could enhance utilization of fatty acids, thereby increasing FFA uptake into the cells, thus reducing FFA levels in the circulation. This may attenuate lipotoxicity-induced insulin resistance.

4.2.5 Array analysis revealed an improved insulin signaling and fatty acid uptake in EAT of LsAg-treated DIO mice

Although LsAg administration did not suppress adiposity, PCR array analysis of EAT from LsAg-treated DIO mice indicated a suppression of inflammatory responses as was shown by a slight downregulation of *Tnfrsf1b* expression. Since TNFα signaling induces insulin resistance, lower expression of *Tnfrsf1b* may help to maintain insulin sensitivity in LsAg treated mice. Insulin sensitivity improvement upon LsAg administration in obese mice further correlated with a significantly higher expression of *Pik3r*, which encodes the p50α, p55α, and p85α regulatory subunits of phosphatidylinositol 3 kinases (PI3Ks), and has a key role for insulin signaling by activating AKT [215,216]. Activated AKT in turn phosphorylates PDE3B, which further promotes expression of *Slac2a4* (*Glut4*) and promotes glucose uptake into the cells [217]. In addition, increased expression of the *Adipor2* in EAT of LsAg-treated DIO mice can enhance insulin signaling to promote GLUT4 translocation by binding with adiponectin [218].

Increased expression of genes correlated to insulin signaling in LsAg-treated DIO mice as highlighted above may therefore maintain insulin's function in cell metabolism. As an anabolic hormone, the binding of insulin with its receptor in induces in the fed state glucose and fatty acid uptake to store excessive energy intake in the form of glycogen and lipid. Consequently, lipogenesis and glycogenesis were more stimulated in LsAg-treated compared to PBS-treated DIO mice as was shown by a higher expression of *Srebf1*, *Fasn*, and *Acaca* which contribute to fatty

acid synthesis as well as *Gys,* which plays a role in glycogenesis. In addition to the enhanced glucose uptake, insulin signaling increased fatty acid uptake into the cells as indicated by upregulated expression of *Fabp4* and *Lpl* as well as *vldlr*. Accordingly, both body weight and adipocytes size in EAT of LsAg-treated DIO were not different compared to PBS-treated DIO, suggesting that there is no suppression of lipogenesis upon LsAg administration. These findings suggest that LsAg administration improves insulin sensitivity without suppression of adiposity.

Given that the inflammasome activation by FFA leads to lipotoxicity and results in apoptosis of adipocytes which triggers additional inflammatory responses [219], increased FFA uptake by adipocytes upon LsAg administration may restrict inflammasome-induced apoptosis by reducing FFA in the circulation. A tendency of lower expression of *Nlrp3*, *Pycard* as well as *Casp1* upon LsAg administration supports this hypothesis. Therefore, LsAg administration may avoid adipocyte stress and apoptosis which may ultimately result in less inflammatory cytokine production and macrophage recruitment. Accordingly, a lower macrophage infiltration was shown by FACS analysis and lower expression of *Emr1* (*F4/80*) by PCR array. Suppressive inflammatory immune responses in turn maintain insulin sensitivity in EAT. Although some genes related to inflammation were suppressed upon LsAg treatment, we also found that *Ifng* expression was significantly increased in adipose tissue of LsAg-treated mice. This increased *Ifng* expression could be due to endosymbiotic *Wolbachia* bacteria that are found in most human pathogenic filariae as well as *L.s.* [114,220] and increased IFNγ levels were previously associated with the release of the microfilarial stage [195,196]. Elevated *Ifng* expression within EAT of LsAg-treated mice may attenuate the beneficial effect of LsAg administration. Therefore, further studies regarding the effect of LsAg from *Wolbachia*-depleted worms should be conducted to reduced pro-inflammatory responses caused by *Wolbachia*.

In general, we found an association between the improvement of glucose tolerance in both *L.s.*-infected DIO mice and LsAg-treated DIO mice with an increased number of eosinophils and AAM which was accompanied by increased type 2 immune

responses and expression of genes linked to insulin signaling. Continuity of LsAg administration was needed to ameliorate glucose tolerance in DIO mice as long as HF diet continued.

4.3 Conclusion

In conclusion, this thesis demonstrates that both *L.s.* infection and LsAg treatment of DIO mice improves glucose tolerance and leads to an increased number of eosinophils, AAM and CD4+ Foxp3+ regulatory T cells within the EAT. Eosinophils are required to mediate the protective effect in *L.s.*-infected DIO mice and additional protective mechanisms may include the suppression of adipogenesis. In contrast, LsAg administration improves glucose tolerance without suppression of adipogenesis. Gene expression analysis highlighted that LsAg administration promotes insulin signaling in EAT of DIO mice. This exerts uptake of glucose via GLUT4 and fatty acids via the LPL and VLDL receptor from the circulation into the cells. Insulin signaling and uptake of fatty acid in turn reduced TG levels in the blood thus preventing lipotoxicity-induced insulin resistance in other tissues.

Type 2 immune responses, along with increased frequencies of eosinophils and AAM in EAT of DIO mice indicated a browning of white adipose tissue upon cold exposure, thus promoting energy expenditure. In addition, increased energy expenditure may increase the utilization of FFA to reduce lipotoxicity-induced insulin resistance. Therefore, LsAg administration is a promising therapy against obesity and its related diseases. These findings suggest that filariae induce several protective mechanisms that should be pursued in order to develop new strategies to ameliorate insulin resistance in human T2D.

4.4 Outlook

- Elevated *Ifng* expression during LsAg administration could be due to lipoproteins from *Wolbachia*, which could reduce the beneficial impact of LsAg. Further studies should be conducted to investigate whether *Wolbachia*-depleted LsAg further improves insulin sensitivity in HF diet-induced insulin resistant mice.

- Since our experiments demonstrated that the beneficial impact of LsAg administration is no longer present several days after the treatment is stopped, a modified therapy consistent of a long term treatment and continuous slow release of LsAg should be tried, e.g. via the implantation of osmotic pumps.

- Future experiments should include the analysis of mice in metabolic cages to obtain a better picture of the metabolic changes.

- Studies regarding the impact of LsAg administration on liver and muscle tissue are required to obtain better understanding how LsAg affects energy metabolism.

References

1. Alberti KG, Zimmet PZ. Definition, diagnosis and classification of diabetes mellitus and its complications. Part 1: diagnosis and classification of diabetes mellitus provisional report of a WHO consultation. Diabet Med. 1998;15: 539–53. doi:10.1002/(SICI)1096-9136(199807)15:7<539::AID-DIA668>3.0.CO;2-S

2. International Diabetes Federation. IDF Diabetes Atlas 6th Edition. 2013.

3. Larsson SC, Orsini N, Wolk A. Diabetes mellitus and risk of colorectal cancer: a meta-analysis. J Natl Cancer Inst. 2005;97: 1679–87. doi:10.1093/jnci/dji375

4. Ott A, Stolk RP, van Harskamp F, Pols HAP, Hofman A, Breteler MMB. Diabetes mellitus and the risk of dementia: The Rotterdam Study. Neurology. 1999;53: 1937–1937. doi:10.1212/WNL.53.9.1937

5. International Diabetes Federation. IDF Diabetes Atlas 6th edn. 2014 update. Brussels, Belgium; 2014.

6. International Diabetes Federation. What is diabetes. IDF Diabetes Atlas 6th ed. 6th ed. 2013. pp. 19–27.

7. Donath MY, Shoelson SE. Type 2 diabetes as an inflammatory disease. Nat Rev Immunol. Nature Publishing Group; 2011;11: 98–107. doi:10.1038/nri2925

8. Weyer C, Bogardus C, Mott DM, Pratley RE. The natural history of insulin secretory dysfunction and insulin resistance in the pathogenesis of type 2 diabetes mellitus. J Clin Invest. 1999;104: 787–94. doi:10.1172/JCI7231

9. Lim EL, Hollingsworth KG, Aribisala BS, Chen MJ, Mathers JC, Taylor R. Reversal of type 2 diabetes: normalisation of beta cell function in association with decreased pancreas and liver triacylglycerol. Diabetologia. 2011;54: 2506–14. doi:10.1007/s00125-011-2204-7

10. Sonksen P, Sonksen J. Insulin: understanding its action in health and disease. Br J Anaesth. 2000;85: 69–79.

11. Tirone TA, Brunicardi FC. Overview of glucose regulation. World J Surg. 2001;25: 461–7. doi:10.1007/s002680020338

12. Cushman SW, Wardzala LJ. Potential mechanism of insulin action on glucose transport in the isolated rat adipose cell. Apparent translocation of intracellular transport systems to the plasma membrane. J Biol Chem. 1980;255: 4758–62.

13. Kusari AB, Byon J, Bandyopadhyay D, Kenner KA, Kusari J. Insulin-induced mitogen-activated protein (MAP) kinase phosphatase-1 (MKP-1) attenuates insulin-stimulated MAP kinase activity: a mechanism for the feedback inhibition of insulin signaling. Mol Endocrinol. 1997;11: 1532–43. doi:10.1210/mend.11.10.9998

14. Thorens B, Mueckler M. Glucose transporters in the 21st Century. Am J Physiol Endocrinol Metab. 2010;298: E141–5. doi:10.1152/ajpendo.00712.2009

15. Choi SH, Ginsberg HN. Increased very low density lipoprotein (VLDL) secretion, hepatic steatosis, and insulin resistance. Trends Endocrinol Metab. 2011;22: 353–63. doi:10.1016/j.tem.2011.04.007

16. Choi SM, Tucker DF, Gross DN, Easton RM, DiPilato LM, Dean AS, et al. Insulin regulates adipocyte lipolysis via an Akt-independent signaling pathway. Mol Cell Biol. 2010;30: 5009–20. doi:10.1128/MCB.00797-10

17. Slawik M, Vidal-Puig AJ. Adipose tissue expandability and the metabolic syndrome. Genes Nutr. 2007;2: 41–5. doi:10.1007/s12263-007-0014-9

18. Brook CG, Lloyd JK, Wolf OH. Relation between age of onset of obesity and size and number of adipose cells. Br Med J. 1972;2: 25–7.

19. Trayhurn P. Hypoxia and adipose tissue function and dysfunction in obesity. Physiol Rev. 2013;93: 1–21. doi:10.1152/physrev.00017.2012

20. Hosogai N, Fukuhara A, Oshima K, Miyata Y, Tanaka S, Segawa K, et al. Adipose tissue hypoxia in obesity and its impact on adipocytokine dysregulation. Diabetes. 2007;56: 901–11. doi:10.2337/db06-0911

21. Cipolletta D, Kolodin D, Benoist C, Mathis D. Tissular T(regs): a unique population of adipose-tissue-resident Foxp3+CD4+ T cells that impacts organismal metabolism. Semin Immunol. Elsevier Ltd; 2011;23: 431–7. doi:10.1016/j.smim.2011.06.002

22. Wang P, Mariman E, Renes J, Keijer J. The secretory function of adipocytes in the physiology of white adipose tissue. J Cell Physiol. 2008;216: 3–13. doi:10.1002/jcp.21386

23. Scherer PE. Adipose tissue: from lipid storage compartment to endocrine organ. Diabetes. 2006;55: 1537–45. doi:10.2337/db06-0263

24. Halberg N, Wernstedt-Asterholm I, Scherer PE. The adipocyte as an endocrine cell. Endocrinol Metab Clin North Am. 2008;37: 753–68, x–xi. doi:10.1016/j.ecl.2008.07.002

25. Hotamisligil GS, Shargill NS, Spiegelman BM. Adipose expression of tumor necrosis factor-alpha: direct role in obesity-linked insulin resistance. Science. 1993;259: 87–91.

26. Kershaw EE, Flier JS. Adipose tissue as an endocrine organ. J Clin Endocrinol Metab. 2004;89: 2548–56. doi:10.1210/jc.2004-0395

27. Ye J. Emerging role of adipose tissue hypoxia in obesity and insulin resistance. Int J Obes (Lond). 2009;33: 54–66. doi:10.1038/ijo.2008.229

28. Yuan M, Konstantopoulos N, Lee J, Hansen L, Li ZW, Karin M, et al. Reversal of obesity- and diet-induced insulin resistance with salicylates or targeted disruption of Ikkbeta. Science. 2001;293: 1673–7. doi:10.1126/science.1061620

29. Gao Z, Hwang D, Bataille F, Lefevre M, York D, Quon MJ, et al. Serine phosphorylation of insulin receptor substrate 1 by inhibitor kappa B kinase complex. J Biol Chem. 2002;277: 48115–21. doi:10.1074/jbc.M209459200

30. Aguirre V. The c-Jun NH2-terminal Kinase Promotes Insulin Resistance during Association with Insulin Receptor Substrate-1 and Phosphorylation of Ser307. J Biol Chem. 2000;275: 9047–9054. doi:10.1074/jbc.275.12.9047

31. Gao Z, He Q, Peng B, Chiao PJ, Ye J. Regulation of nuclear translocation of HDAC3 by IkappaBalpha is required for tumor necrosis factor inhibition of peroxisome proliferator-activated receptor gamma function. J Biol Chem. 2006;281: 4540–7. doi:10.1074/jbc.M507784200

32. Ye J. Regulation of PPARgamma function by TNF-alpha. Biochem Biophys Res Commun. 2008;374: 405–8. doi:10.1016/j.bbrc.2008.07.068

33. Zhang J, Gao Z, Yin J, Quon MJ, Ye J. S6K directly phosphorylates IRS-1 on Ser-270 to promote insulin resistance in response to TNF-(alpha) signaling through IKK2. J Biol Chem. 2008;283: 35375–82. doi:10.1074/jbc.M806480200

34. Rui L, Aguirre V, Kim JK, Shulman GI, Lee A, Corbould A, et al. Insulin/IGF-1 and TNF-alpha stimulate phosphorylation of IRS-1 at inhibitory Ser307 via distinct pathways. J Clin Invest. 2001;107: 181–9. doi:10.1172/JCI10934

35. Ye J. Mechanisms of insulin resistance in obesity. Front Med. 2013;7: 14–24. doi:10.1007/s11684-013-0262-6

36. Johnston AM, Pirola L, Van Obberghen E. Molecular mechanisms of insulin receptor substrate protein-mediated modulation of insulin signalling. FEBS Lett. 2003;546: 32–36. doi:10.1016/S0014-5793(03)00438-1

37. Odegaard JI, Chawla A. Alternative macrophage activation and metabolism. Annu Rev Pathol. 2011;6: 275–97. doi:10.1146/annurev-pathol-011110-130138

38. Ginsberg HN, Zhang Y-L, Hernandez-Ono A. Regulation of Plasma Triglycerides in Insulin Resistance and Diabetes. Arch Med Res. 2005;36: 232–240. doi:10.1016/j.arcmed.2005.01.005

39. Zhang L, Keung W, Samokhvalov V, Wang W, Lopaschuk GD. Role of fatty acid uptake and fatty acid beta-oxidation in mediating insulin resistance in heart and skeletal muscle. Biochim Biophys Acta. 2010;1801: 1–22. doi:10.1016/j.bbalip.2009.09.014

40. Badin P-M, Vila IK, Louche K, Mairal A, Marques M-A, Bourlier V, et al. High-fat diet-mediated lipotoxicity and insulin resistance is related to impaired lipase expression in mouse skeletal muscle. Endocrinology. Endocrine Society Chevy Chase, MD; 2013;154: 1444–53. doi:10.1210/en.2012-2029

41. Chawla A, Nguyen KD, Goh YPS. Macrophage-mediated inflammation in metabolic disease. Nat Rev Immunol. Nature Publishing Group; 2011;11: 738–49. doi:10.1038/nri3071

42. Hotamisligil GS. Inflammation and metabolic disorders. Nature. 2006;444: 860–7. doi:10.1038/nature05485

43. Shi H, Kokoeva M V, Inouye K, Tzameli I, Yin H, Flier JS. TLR4 links innate immunity and fatty acid-induced insulin resistance. J Clin Invest. 2006;116: 3015–25. doi:10.1172/JCI28898

44. Wu D, Molofsky AB, Liang H-E, Ricardo-Gonzalez RR, Jouihan H a, Bando JK, et al. Eosinophils sustain adipose alternatively activated macrophages associated with glucose homeostasis. Science. 2011;332: 243–7. doi:10.1126/science.1201475

45. Lumeng CN, Bodzin JL, Saltiel AR. Obesity induces a phenotypic switch in adipose tissue macrophage polarization. J Clin Invest. 2007;117: 175–84. doi:10.1172/JCI29881

46. Winer D a, Winer S, Shen L, Wadia PP, Yantha J, Paltser G, et al. B cells promote insulin resistance through modulation of T cells and production of pathogenic IgG antibodies. Nat Med. 2011;17: 610–617. doi:10.1038/nm.2353

47. Winer S, Winer D a. The adaptive immune system as a fundamental regulator of adipose tissue inflammation and insulin resistance. Nature Publishing Group; 2012;90: 755–62. doi:10.1038/icb.2011.110

48. Rosenberg HF, Dyer KD, Foster PS. Eosinophils: changing perspectives in health and disease. Nat Rev Immunol. Nature Publishing Group, a division of Macmillan Publishers Limited. All Rights Reserved.; 2013;13: 9–22. doi:10.1038/nri3341

49. Kita H. Eosinophils: multifaceted biological properties and roles in health and disease. Immunol Rev. 2011;242: 161–77. doi:10.1111/j.1600-065X.2011.01026.x

50. Meeusen EN., Balic A. Do Eosinophils have a Role in the Killing of Helminth Parasites? Parasitol Today. 2000;16: 95–101. doi:10.1016/S0169-4758(99)01607-5

51. L. Makepeace B, Martin C, D. Turner J, Specht S. Granulocytes in Helminth Infection - Who is Calling the Shots? Curr Med Chem. 2012;19: 1567–1586. doi:10.2174/092986712799828337

52. Specht S, Saeftel M, Arndt M, Endl E, Dubben B, Lee NA, et al. Lack of eosinophil peroxidase or major basic protein impairs defense against murine filarial infection. Infect Immun. 2006;74: 5236–43. doi:10.1128/IAI.00329-06

53. Ricardo-Gonzalez RR, Red Eagle A, Odegaard JI, Jouihan H, Morel CR, Heredia JE, et al. IL-4/STAT6 immune axis regulates peripheral nutrient metabolism and insulin sensitivity. Proc Natl Acad Sci U S A. 2010;107: 22617–22. doi:10.1073/pnas.1009152108

54. Qiu Y, Nguyen KD, Odegaard JI, Cui X, Tian X, Locksley RM, et al. Eosinophils and type 2 cytokine signaling in macrophages orchestrate development of functional beige fat. Cell. Elsevier Inc.; 2014;157: 1292–308. doi:10.1016/j.cell.2014.03.066

55. Nguyen KD, Qiu Y, Cui X, Goh YPS, Mwangi J, David T, et al. Alternatively activated macrophages produce catecholamines to sustain adaptive thermogenesis. Nature. Nature Publishing Group; 2011;480: 104–8. doi:10.1038/nature10653

56. Rao RR, Long JZ, White JP, Svensson KJ, Lou J, Lokurkar I, et al. Meteorin-like Is a Hormone that Regulates Immune-Adipose Interactions to Increase Beige Fat Thermogenesis. Cell. Elsevier Inc.; 2014;157: 1279–91. doi:10.1016/j.cell.2014.03.065

57. Gordon S. Alternative activation of macrophages. Nat Rev Immunol. 2003;3: 23–35. doi:10.1038/nri978

58. Mosser DM. The many faces of macrophage activation. J Leukoc Biol. 2003;73: 209–212. doi:10.1189/jlb.0602325

59. Olefsky JM, Glass CK. Macrophages, inflammation, and insulin resistance. Annual review of physiology. 2010. doi:10.1146/annurev-physiol-021909-135846

60. Kreider T, Anthony RM, Jr JFU, Gause WC. Alternatively activated macrophages in helminth infections. 2007; 1–6. doi:10.1016/j.coi.2007.07.002

61. Bronte V, Zanovello P. Regulation of immune responses by L-arginine metabolism. Nat Rev Immunol. 2005;5: 641–654. doi:10.1038/nri1668

62. Gordon S, Taylor PR. Monocyte and macrophage heterogeneity. Nat Rev Immunol. 2005;5: 953–64. doi:10.1038/nri1733

63. Vats D, Mukundan L, Odegaard JI, Zhang L, Smith KL, Morel CR, et al. Oxidative metabolism and PGC-1beta attenuate macrophage-mediated inflammation. Cell Metab. 2006;4: 13–24. doi:10.1016/j.cmet.2006.05.011

64. Feuerer M, Herrero L, Cipolletta D, Naaz A, Wong J, Nayer A, et al. Lean, but not obese, fat is enriched for a unique population of regulatory T cells that affect metabolic parameters. Nat Med. 2009;15: 930–9. doi:10.1038/nm.2002

65. Sakaguchi S, Yamaguchi T, Nomura T, Ono M. Regulatory T cells and immune tolerance. Cell. 2008;133: 775–87. doi:10.1016/j.cell.2008.05.009

66. Zheng Y, Rudensky AY. Foxp3 in control of the regulatory T cell lineage. Nat Immunol. 2007;8: 457–62. doi:10.1038/ni1455

67. Maloy KJ, Salaun L, Cahill R, Dougan G, Saunders NJ, Powrie F. CD4+CD25+ TR Cells Suppress Innate Immune Pathology Through Cytokine-dependent Mechanisms. J Exp Med. 2002;197: 111–119. doi:10.1084/jem.20021345

68. Murphy TJ, Ni Choileain N, Zang Y, Mannick JA, Lederer JA. CD4+CD25+ regulatory T cells control innate immune reactivity after injury. J Immunol. 2005;174: 2957–63.

69. Nguyen LT, Jacobs J, Mathis D, Benoist C. Where FoxP3-dependent regulatory T cells impinge on the development of inflammatory arthritis. Arthritis Rheum. 2007;56: 509–20. doi:10.1002/art.22272

70. Winer S, Chan Y, Paltser G, Truong D, Tsui H, Bahrami J, et al. Normalization of obesity-associated insulin resistance through immunotherapy. Nat Med. 2009;15: 921–9. doi:10.1038/nm.2001

71. Duffaut C, Galitzky J, Lafontan M, Bouloumié A. Unexpected trafficking of immune cells within the adipose tissue during the onset of obesity. Biochem Biophys Res Commun. 2009;384: 482–5. doi:10.1016/j.bbrc.2009.05.002

72. Allman D, Pillai S. Peripheral B cell subsets. Curr Opin Immunol. 2008;20: 149–57. doi:10.1016/j.coi.2008.03.014

73. Haas KM, Poe JC, Steeber DA, Tedder TF. B-1a and B-1b cells exhibit distinct developmental requirements and have unique functional roles in innate and adaptive immunity to S. pneumoniae. Immunity. 2005;23: 7–18. doi:10.1016/j.immuni.2005.04.011

74. Mauri C, Bosma A. Immune regulatory function of B cells. Annu Rev Immunol. 2012;30: 221–41. doi:10.1146/annurev-immunol-020711-074934

75. Cooper PJ. Interactions between helminth parasites and allergy. Curr Opin Allergy Clin Immunol. 2009;9: 29–37. doi:10.1097/ACI.0b013e32831f44a6

76. Rujeni N, Nausch N, Bourke CD, Midzi N, Mduluza T, Taylor DW, et al. Atopy is inversely related to schistosome infection intensity: a comparative study in Zimbabwean villages with distinct levels of Schistosoma haematobium infection. Int Arch Allergy Immunol. 2012;158: 288–98. doi:10.1159/000332949

77. Van den Biggelaar AH, van Ree R, Rodrigues LC, Lell B, Deelder AM, Kremsner PG, et al. Decreased atopy in children infected with Schistosoma haematobium: a role for parasite-induced interleukin-10. Lancet. 2000;356: 1723–7. doi:10.1016/S0140-6736(00)03206-2

78. Araujo MI, de Carvalho EM. Human schistosomiasis decreases immune responses to allergens and clinical manifestations of asthma. Chem Immunol Allergy. 2006;90: 29–44. doi:10.1159/000088879

79. Araujo MI, Lopes AA, Medeiros M, Cruz AA, Sousa-Atta L, Solé D, et al. Inverse association between skin response to aeroallergens and Schistosoma mansoni infection. Int Arch Allergy Immunol. 2000;123: 145–8. doi:24433

80. Medeiros M, Figueiredo JP, Almeida MC, Matos MA, Araújo MI, Cruz AA, et al. Schistosoma mansoni infection is associated with a reduced course of asthma. J Allergy Clin Immunol. 2003;111: 947–51.

81. Flohr C, Tuyen LN, Quinnell RJ, Lewis S, Minh TT, Campbell J, et al. Reduced helminth burden increases allergen skin sensitization but not clinical allergy: a randomized, double-blind, placebo-controlled trial in Vietnam. Clin Exp Allergy. 2010;40: 131–42. doi:10.1111/j.1365-2222.2009.03346.x

82. Van den Biggelaar AHJ, Rodrigues LC, van Ree R, van der Zee JS, Hoeksma-Kruize YCM, Souverijn JHM, et al. Long-term treatment of intestinal helminths increases mite skin-test reactivity in Gabonese schoolchildren. J Infect Dis. 2004;189: 892–900. doi:10.1086/381767

83. Elliott AM, Ndibazza J, Mpairwe H, Muhangi L, Webb EL, Kizito D, et al. Treatment with anthelminthics during pregnancy: what gains and what risks for the mother and child? Parasitology. Cambridge University Press; 2011;138: 1499–507. doi:10.1017/S0031182011001053

84. Mpairwe H, Webb EL, Muhangi L, Ndibazza J, Akishule D, Nampijja M, et al. Anthelminthic treatment during pregnancy is associated with increased risk of infantile eczema: randomised-controlled trial results. Pediatr Allergy Immunol. 2011;22: 305–12. doi:10.1111/j.1399-3038.2010.01122.x

85. Endara P, Vaca M, Chico ME, Erazo S, Oviedo G, Quinzo I, et al. Long-term periodic anthelmintic treatments are associated with increased allergen skin reactivity. Clin Exp Allergy. 2010;40: 1669–77. doi:10.1111/j.1365-2222.2010.03559.x

86. Flohr C, Tuyen LN, Lewis S, Quinnell R, Minh TT, Liem HT, et al. Poor sanitation and helminth infection protect against skin sensitization in Vietnamese children: A cross-sectional study. J Allergy Clin Immunol. 2006;118: 1305–11. doi:10.1016/j.jaci.2006.08.035

87. Zaccone P, Fehervari Z, Phillips JM, Dunne DW, Cooke a. Parasitic worms and inflammatory diseases. Parasite Immunol. 2006;28: 515–23. doi:10.1111/j.1365-3024.2006.00879.x

88. Fleming JO, Cook TD. Multiple sclerosis and the hygiene hypothesis. Neurology. 2006;67: 2085–6. doi:10.1212/01.wnl.0000247663.40297.2d

89. Correale J, Farez M. Association between parasite infection and immune responses in multiple sclerosis. Ann Neurol. 2007;61: 97–108. doi:10.1002/ana.21067

90. Elliott DE, Summers RW, Weinstock J V. Helminths as governors of immune-mediated inflammation. Int J Parasitol. 2007;37: 457–64. doi:10.1016/j.ijpara.2006.12.009

91. Correale J, Farez M. Helminth antigens modulate immune responses in cells from multiple sclerosis patients through TLR2-dependent mechanisms. J Immunol. 2009;183: 5999–6012. doi:10.4049/jimmunol.0900897

92. Hübner MP, Stocker JT, Mitre E. Inhibition of type 1 diabetes in filaria-infected non-obese diabetic mice is associated with a T helper type 2 shift and induction of FoxP3+ regulatory T cells. Immunology. 2009;127: 512–22. doi:10.1111/j.1365-2567.2008.02958.x

93. Hübner MP, Shi Y, Torrero MN, Mueller E, Larson D, Soloviova K, et al. Helminth protection against autoimmune diabetes in nonobese diabetic mice is independent of a type 2 immune shift and requires TGF-β. J Immunol. 2012;188: 559–68. doi:10.4049/jimmunol.1100335

94. Cooke A, Tonks P, Jones FM, O'Shea H, Hutchings P, Fulford AJ, et al. Infection with Schistosoma mansoni prevents insulin dependent diabetes mellitus in non-obese diabetic mice. Parasite Immunol. 1999;21: 169–76.

95. Zaccone P, Burton O, Miller N, Jones FM, Dunne DW, Cooke A. Schistosoma mansoni egg antigens induce Treg that participate in diabetes prevention in NOD mice. Eur J Immunol. 2009;39: 1098–107. doi:10.1002/eji.200838871

96. Zaccone P, Fehérvári Z, Jones FM, Sidobre S, Kronenberg M, Dunne DW, et al. Schistosoma mansoni antigens modulate the activity of the innate immune response and prevent onset of type 1 diabetes. Eur J Immunol. 2003;33: 1439–49. doi:10.1002/eji.200323910

97. Aravindhan V, Mohan V, Surendar J, Muralidhara Rao M, Pavankumar N, Deepa M, et al. Decreased prevalence of lymphatic filariasis among diabetic subjects associated with a diminished pro-inflammatory cytokine response (CURES 83). PLoS Negl Trop Dis. 2010;4: e707. doi:10.1371/journal.pntd.0000707

98. Chen Y, Lu J, Huang Y, Wang T, Xu Y, Xu M, et al. Association of Previous Schistosome Infection With Diabetes and Metabolic Syndrome: A Cross-Sectional Study in Rural China. J

Clin Endocrinol Metab. Endocrine Society Chevy Chase, MD; 2012;98: 1–5. doi:10.1210/jc.2012-2517

99. Wiria AE, Hamid F, Wammes LJ, Prasetyani MA, Dekkers OM, May L, et al. Infection with Soil-Transmitted Helminths Is Associated with Increased Insulin Sensitivity. PLoS One. Public Library of Science; 2015;10: e0127746. doi:10.1371/journal.pone.0127746

100. Yang Z, Grinchuk V, Smith A, Qin B, Bohl J a., Sun R, et al. Parasitic nematode-induced modulation of body weight and associated metabolic dysfunction in mouse models of obesity. Infect Immun. 2013;81: 1905–1914. doi:10.1128/IAI.00053-13

101. Bhargava P, Li C, Stanya KJ, Jacobi D, Dai L, Liu S, et al. Immunomodulatory glycan LNFPIII alleviates hepatosteatosis and insulin resistance through direct and indirect control of metabolic pathways. Nat Med. Nature Publishing Group; 2012; 1–9. doi:10.1038/nm.2962

102. Hussaarts L, García-Tardón N, van Beek L, Heemskerk MM, Haeberlein S, van der Zon GC, et al. Chronic helminth infection and helminth-derived egg antigens promote adipose tissue M2 macrophages and improve insulin sensitivity in obese mice. FASEB J. 2015;29: 3027–39. doi:10.1096/fj.14-266239

103. Hotez PJ, Brindley PJ, Bethony JM, King CH, Pearce EJ, Jacobson J. Helminth infections: the great neglected tropical diseases. J Clin Invest. 2008;118: 1311. doi:10.1172/JCI34261.The

104. Hotez PJ, Molyneux DH, Fenwick A, Kumaresan J, Sachs SE, Sachs JD, et al. Control of neglected tropical diseases. N Engl J Med. 2007;357: 1018–27. doi:10.1056/NEJMra064142

105. McSorley HJ, Maizels RM. Helminth infections and host immune regulation. Clin Microbiol Rev. 2012;25: 585–608. doi:10.1128/CMR.05040-11

106. Wiria AE, Djuardi Y, Supali T, Sartono E, Yazdanbakhsh M. Helminth infection in populations undergoing epidemiological transition: a friend or foe? Semin Immunopathol. 2012;34: 889–901. doi:10.1007/s00281-012-0358-0

107. Maizels RM, Yazdanbakhsh M. T-cell regulation in helminth parasite infections: implications for inflammatory diseases. Chem Immunol Allergy. 2008;94: 112–23. doi:10.1159/000154944

108. Hussaarts L, van der Vlugt LEPM, Yazdanbakhsh M, Smits HH. Regulatory B-cell induction by helminths: implications for allergic disease. J Allergy Clin Immunol. 2011;128: 733–9. doi:10.1016/j.jaci.2011.05.012

109. Anthony RM, Urban JF, Alem F, Hamed HA, Rozo CT, Boucher J-L, et al. Memory T(H)2 cells induce alternatively activated macrophages to mediate protection against nematode parasites. Nat Med. 2006;12: 955–60. doi:10.1038/nm1451

110. Liu Q, Kreider T, Bowdridge S, Liu Z, Song Y, Gaydo AG, et al. B cells have distinct roles in host protection against different nematode parasites. J Immunol. 2010;184: 5213–23. doi:10.4049/jimmunol.0902879

111. Herbert DR, Yang J-Q, Hogan SP, Groschwitz K, Khodoun M, Munitz A, et al. Intestinal epithelial cell secretion of RELM-beta protects against gastrointestinal worm infection. J Exp Med. 2009;206: 2947–57. doi:10.1084/jem.20091268

112. Zhao A, McDermott J, Urban JF, Gause W, Madden KB, Yeung KA, et al. Dependence of IL-4, IL-13, and nematode-induced alterations in murine small intestinal smooth muscle contractility on Stat6 and enteric nerves. J Immunol. 2003;171: 948–54.

113. Maizels RM, Balic A, Gomez-Escobar N, Nair M, Taylor MD, Allen JE. Helminth parasites--masters of regulation. Immunol Rev. 2004;201: 89–116. doi:10.1111/j.0105-2896.2004.00191.x

114. Hoerauf A, Satoguina J, Saeftel M, Specht S. Immunomodulation by filarial nematodes. Parasite Immunol. 2005;27: 417–29. doi:10.1111/j.1365-3024.2005.00792.x

115. Allen JE, Sutherland TE. Host protective roles of type 2 immunity: parasite killing and tissue repair, flip sides of the same coin. Semin Immunol. 2014;26: 329–40. doi:10.1016/j.smim.2014.06.003

116. Anthony RM, Rutitzky LI, Urban JF, Stadecker MJ, Gause WC. Protective immune mechanisms in helminth infection. Nat Rev Immunol. 2007;7: 975–87. doi:10.1038/nri2199

117. Kanda H, Tateya S, Tamori Y, Kotani K, Hiasa K, Kitazawa R, et al. MCP-1 contributes to macrophage infiltration into adipose tissue, insulin resistance, and hepatic steatosis in obesity. J Clin Invest. 2006;116: 1494–505. doi:10.1172/JCI26498

118. McNeil KS, Knox DP, Proudfoot L. Anti-inflammatory responses and oxidative stress in Nippostrongylus brasiliensis-induced pulmonary inflammation. Parasite Immunol. 2002;24: 15–22.

119. Loke P, Gallagher I, Nair MG, Zang X, Brombacher F, Mohrs M, et al. Alternative activation is an innate response to injury that requires CD4+ T cells to be sustained during chronic infection. J Immunol. 2007;179: 3926–36.

120. Specht and Hoerauf. Immunity to Parasitic Immunity to Parasitic Edited by. In: Lamb TJ, editor. Chicester: John Wiley & Son, Ltd; 2012. pp. 201–230.

121. Allen JE, Loke P. Divergent roles for macrophages in lymphatic filariasis. Parasite Immunol. 2001;23: 345–52.

122. Allen JE, Maizels RM. Diversity and dialogue in immunity to helminths. Nat Rev Immunol. 2011;11: 375–88. doi:10.1038/nri2992

123. Seno H, Miyoshi H, Brown SL, Geske MJ, Colonna M, Stappenbeck TS. Efficient colonic mucosal wound repair requires Trem2 signaling. Proc Natl Acad Sci U S A. 2009;106: 256–61. doi:10.1073/pnas.0803343106

124. Taylor MD, Harris A, Nair MG, Maizels RM, Allen JE. F4/80+ Alternatively Activated Macrophages Control CD4+ T Cell Hyporesponsiveness at Sites Peripheral to Filarial Infection. J Immunol. American Association of Immunologists; 2006;176: 6918–6927. doi:10.4049/jimmunol.176.11.6918

125. Herbert DR, Hölscher C, Mohrs M, Arendse B, Schwegmann A, Radwanska M, et al. Alternative macrophage activation is essential for survival during schistosomiasis and

downmodulates T helper 1 responses and immunopathology. Immunity. 2004;20: 623–635. doi:10.1016/S1074-7613(04)00107-4

126. Espinoza-Jiménez A, Peón AN, Terrazas LI. Alternatively Activated Macrophages in Types 1 and 2 Diabetes. Mediators Inflamm. 2012;2012: 1–10. doi:10.1155/2012/815953

127. Donnelly S, O'Neill SM, Sekiya M, Mulcahy G, Dalton JP. Thioredoxin peroxidase secreted by Fasciola hepatica induces the alternative activation of macrophages. Infect Immun. 2005;73: 166–73. doi:10.1128/IAI.73.1.166-173.2005

128. Robinson MW, Dalton JP, Donnelly S. Helminth pathogen cathepsin proteases: it's a family affair. Trends Biochem Sci. 2008;33: 601–8. doi:10.1016/j.tibs.2008.09.001

129. Zaccone P, Burton OT, Gibbs S, Miller N, Jones FM, Dunne DW, et al. Immune modulation by Schistosoma mansoni antigens in NOD mice: effects on both innate and adaptive immune systems. J Biomed Biotechnol. 2010;2010: 795210. doi:10.1155/2010/795210

130. Atochina O, Da'dara AA, Walker M, Harn DA. The immunomodulatory glycan LNFPIII initiates alternative activation of murine macrophages in vivo. Immunology. 2008;125: 111–21. doi:10.1111/j.1365-2567.2008.02826.x

131. Mclaren DJ, Worms MJ, Laurence BR, Simpson MG. Micro-organisms in filarial larvae (Nematoda). Trans R Soc Trop Med Hyg. 1975;69: 509–514. doi:10.1016/0035-9203(75)90110-8

132. Taylor M., Hoerauf A. Wolbachia Bacteria of Filarial Nematodes. Parasitol Today. 1999;15: 437–442. doi:10.1016/S0169-4758(99)01533-1

133. Desjardins CA, Cerqueira GC, Goldberg JM, Dunning Hotopp JC, Haas BJ, Zucker J, et al. Genomics of Loa loa, a Wolbachia-free filarial parasite of humans. Nat Genet. Nature Publishing Group, a division of Macmillan Publishers Limited. All Rights Reserved.; 2013;45: 495–500. doi:10.1038/ng.2585

134. Landmann F, Voronin D, Sullivan W, Taylor MJ. Anti-filarial activity of antibiotic therapy is due to extensive apoptosis after Wolbachia depletion from filarial nematodes. PLoS Pathog. 2011;7: e1002351. doi:10.1371/journal.ppat.1002351

135. Hoerauf A. Filariasis: new drugs and new opportunities for lymphatic filariasis and onchocerciasis. Curr Opin Infect Dis. 2008;21: 673–81. doi:10.1097/QCO.0b013e328315cde7

136. Brattig NW, Büttner DW, Hoerauf A. Neutrophil accumulation around Onchocerca worms and chemotaxis of neutrophils are dependent on Wolbachia endobacteria. Microbes Infect. 2001;3: 439–46.

137. Pfarr KM, Hoerauf AM. Antibiotics which target the Wolbachia endosymbionts of filarial parasites: a new strategy for control of filariasis and amelioration of pathology. Mini Rev Med Chem. 2006;6: 203–10.

138. Turner JD, Langley RS, Johnston KL, Gentil K, Ford L, Wu B, et al. Wolbachia lipoprotein stimulates innate and adaptive immunity through Toll-like receptors 2 and 6 to induce

disease manifestations of filariasis. J Biol Chem. 2009;284: 22364–78. doi:10.1074/jbc.M901528200

139. Taylor MJ, Cross HF, Ford L, Makunde WH, Prasad GB, Bilo K. Wolbachia bacteria in filarial immunity and disease. Parasite Immunol. 2001;23: 401–9.

140. Pathak M, Verma M, Srivastava M, Misra-Bhattacharya S. Wolbachia endosymbiont of Brugia malayi elicits a T helper type 17-mediated pro-inflammatory immune response through Wolbachia surface protein. Immunology. 2015;144: 231–44. doi:10.1111/imm.12364

141. Pfarr KM, Debrah AY, Specht S, Hoerauf A. Filariasis and lymphoedema. Parasite Immunol. 2009;31: 664–72. doi:10.1111/j.1365-3024.2009.01133.x

142. Hewitson JP, Grainger JR, Maizels RM. Helminth immunoregulation: the role of parasite secreted proteins in modulating host immunity. Mol Biochem Parasitol. 2009;167: 1–11. doi:10.1016/j.molbiopara.2009.04.008

143. Maizels RM, Hewitson JP, Smith KA. Susceptibility and immunity to helminth parasites. Curr Opin Immunol. 2012;24: 459–66. doi:10.1016/j.coi.2012.06.003

144. Goodridge HS, Marshall F a., Else KJ, Houston KM, Egan C, Al-Riyami L, et al. Immunomodulation via Novel Use of TLR4 by the Filarial Nematode Phosphorylcholine-Containing Secreted Product, ES-62. J Immunol. 2004;174: 284–293. doi:10.4049/jimmunol.174.1.284

145. Goodridge HS, Marshall F a, Else KJ, Houston KM, Egan C, Al-Riyami L, et al. Immunomodulation via novel use of TLR4 by the filarial nematode phosphorylcholine-containing secreted product, ES-62. J Immunol. 2005;174: 284–93.

146. Harnett W, Harnett MM. Helminth-derived immunomodulators: can understanding the worm produce the pill? Nat Rev Immunol. Nature Publishing Group; 2010;10: 278–84. doi:10.1038/nri2730

147. Hartmann S, Lucius R. Modulation of host immune responses by nematode cystatins. Int J Parasitol. 2003;33: 1291–302.

148. Schnoeller C, Rausch S, Pillai S, Avagyan A, Wittig BM, Loddenkemper C, et al. A helminth immunomodulator reduces allergic and inflammatory responses by induction of IL-10-producing macrophages. J Immunol. 2008;180: 4265–72.

149. Hoffmann W, Petit G, Schulz-Key H, Taylor D, Bain O, Le Goff L. Litomosoides sigmodontis in mice: reappraisal of an old model for filarial research. Parasitol Today. 2000;16: 387–9.

150. Babu S, Porte P, Klei TR, Shultz LD, Rajan T V. Host NK cells are required for the growth of the human filarial parasite Brugia malayi in mice. J Immunol. 1998;161: 1428–32.

151. Folkard S, Taylor M, Butcher G, Bianco A. Protective responses against skin-dwelling microfilariae of Onchocerca lienalis in severe combined immunodeficient mice. Infect Immun. 1997;65: 2846–2851.

152. Le Goff L, Martin C, Oswald IP, Vuong PN, Petit G, Ungeheuer MN, et al. Parasitology and immunology of mice vaccinated with irradiated Litomosoides sigmodontis larvae. Parasitology. 2000;120 (Pt 3: 271–80.

153. Babayan S, Ungeheuer M-N, Martin C, Attout T, Belnoue E, Snounou G, et al. Resistance and susceptibility to filarial infection with Litomosoides sigmodontis are associated with early differences in parasite development and in localized immune reactions. Infect Immun. 2003;71: 6820–9.

154. Hübner MP, Torrero MN, McCall JW, Mitre E. Litomosoides sigmodontis: a simple method to infect mice with L3 larvae obtained from the pleural space of recently infected jirds (Meriones unguiculatus). Exp Parasitol. 2009;123: 95–8. doi:10.1016/j.exppara.2009.05.009

155. Kajimura S, Saito M. A New Era in Brown Adipose Tissue Biology: Molecular Control of Brown Fat Development and Energy Homeostasis. Annu Rev Physiol. 2013; 1–25. doi:10.1146/annurev-physiol-021113-170252

156. Townsend KL, Tseng Y-H. Brown fat fuel utilization and thermogenesis. Trends Endocrinol Metab. Elsevier Ltd; 2014;25: 168–77. doi:10.1016/j.tem.2013.12.004

157. Bartelt A, Heeren J. Adipose tissue browning and metabolic health. Nat Rev Endocrinol. Nature Publishing Group; 2014;10: 24–36. doi:10.1038/nrendo.2013.204

158. Lee M-W, Odegaard JI, Mukundan L, Qiu Y, Molofsky AB, Nussbaum JC, et al. Activated Type 2 Innate Lymphoid Cells Regulate Beige Fat Biogenesis. Cell. 2014; doi:10.1016/j.cell.2014.12.011

159. Ayala JE, Samuel VT, Morton GJ, Obici S, Croniger CM, Shulman GI, et al. Standard operating procedures for describing and performing metabolic tests of glucose homeostasis in mice. Dis Model Mech. 2010;3: 525–34. doi:10.1242/dmm.006239

160. Miinalainen IJ, Schmitz W, Huotari A, Autio KJ, Soininen R, Ver Loren van Themaat E, et al. Mitochondrial 2,4-dienoyl-CoA reductase deficiency in mice results in severe hypoglycemia with stress intolerance and unimpaired ketogenesis. PLoS Genet. 2009;5: e1000543. doi:10.1371/journal.pgen.1000543

161. Volkmann L, Bain O, Saeftel M, Specht S, Fischer K, Brombacher F, et al. Murine filariasis: interleukin 4 and interleukin 5 lead to containment of different worm developmental stages. Med Microbiol Immunol. 2003;192: 23–31. doi:10.1007/s00430-002-0155-9

162. Xu H, Barnes GT, Yang Q, Tan G, Yang D, Chou CJ, et al. Chronic inflammation in fat plays a crucial role in the development of obesity-related insulin resistance. J Clin Invest. 2003;112: 1821–30. doi:10.1172/JCI19451

163. McSorley HJ, Hewitson JP, Maizels RM. Immunomodulation by helminth parasites: defining mechanisms and mediators. Int J Parasitol. 2013;43: 301–10. doi:10.1016/j.ijpara.2012.11.011

164. Weisberg SP, McCann D, Desai M, Rosenbaum M, Leibel RL, Ferrante AW. Obesity is associated with macrophage accumulation in adipose tissue. J Clin Invest. 2003;112: 1796–808. doi:10.1172/JCI19246

165. Murano I, Barbatelli G, Parisani V, Latini C, Muzzonigro G, Castellucci M, et al. Dead adipocytes, detected as crown-like structures, are prevalent in visceral fat depots of genetically obese mice. J Lipid Res. 2008;49: 1562–8. doi:10.1194/jlr.M800019-JLR200

166. Ajendra J, Specht S, Neumann A-L, Gondorf F, Schmidt D, Gentil K, et al. ST2 deficiency does not impair type 2 immune responses during chronic filarial infection but leads to an increased microfilaremia due to an impaired splenic microfilarial clearance. PLoS One. 2014;9: e93072. doi:10.1371/journal.pone.0093072

167. Sun XJ, Rothenberg P, Kahn CR, Backer JM, Araki E, Wilden P a, et al. Structure of the insulin receptor substrate IRS-1 defines a unique signal transduction protein. Nature. 1991;352: 73–77. doi:10.1038/352073a0

168. Xu E, Dubois M-J, Leung N, Charbonneau A, Turbide C, Avramoglu RK, et al. Targeted disruption of carcinoembryonic antigen-related cell adhesion molecule 1 promotes diet-induced hepatic steatosis and insulin resistance. Endocrinology. 2009;150: 3503–12. doi:10.1210/en.2008-1439

169. DeAngelis AM, Heinrich G, Dai T, Bowman TA, Patel PR, Lee SJ, et al. Carcinoembryonic antigen-related cell adhesion molecule 1: a link between insulin and lipid metabolism. Diabetes. 2008;57: 2296–303. doi:10.2337/db08-0379

170. Lee KM, Chuang E, Griffin M, Khattri R, Hong DK, Zhang W, et al. Molecular basis of T cell inactivation by CTLA-4. Science. 1998;282: 2263–2266. doi:10.1126/science.282.5397.2263

171. Durand C a, Hartvigsen K, Fogelstrand L, Kim S, Iritani S, Vanhaesebroeck B, et al. Phosphoinositide 3-kinase p110 delta regulates natural antibody production, marginal zone and B-1 B cell function, and autoantibody responses. J Immunol. 2009;183: 5673–5684. doi:10.4049/jimmunol.0900432

172. Beale EG, Hammer RE, Antoine B, Forest C. Disregulated glyceroneogenesis: PCK1 as a candidate diabetes and obesity gene. Trends Endocrinol Metab. 2004;15: 129–35. doi:10.1016/j.tem.2004.02.006

173. Park J, Rho HK, Kim KH, Choe SS, Lee YS, Kim JB. Overexpression of glucose-6-phosphate dehydrogenase is associated with lipid dysregulation and insulin resistance in obesity. Mol Cell Biol. 2005;25: 5146–57. doi:10.1128/MCB.25.12.5146-5157.2005

174. Jiao H, Tang P, Zhang Y. MAP kinase phosphatase 2 regulates macrophage-adipocyte interaction. PLoS One. 2015;10: e0120755. doi:10.1371/journal.pone.0120755

175. McGillicuddy FC, Chiquoine EH, Hinkle CC, Kim RJ, Shah R, Roche HM, et al. Interferon gamma attenuates insulin signaling, lipid storage, and differentiation in human adipocytes via activation of the JAK/STAT pathway. J Biol Chem. 2009;284: 31936–44. doi:10.1074/jbc.M109.061655

176. Bełtowski J. Adiponectin and resistin--new hormones of white adipose tissue. Med Sci Monit. 2003;9: RA55–61.

177. Liew CW, Boucher J, Cheong JK, Vernochet C, Koh H-J, Mallol C, et al. Ablation of TRIP-Br2, a regulator of fat lipolysis, thermogenesis and oxidative metabolism, prevents diet-induced obesity and insulin resistance. Nat Med. 2013; doi:10.1038/nm.3056

178. Alessi M-C, Juhan-Vague I. PAI-1 and the metabolic syndrome: links, causes, and consequences. Arterioscler Thromb Vasc Biol. 2006;26: 2200–7. doi:10.1161/01.ATV.0000242905.41404.68

179. Jeoung NH, Harris RA. Knocking out PDK2 and PDK4 lowers fasting blood glucose levels, increases insulin sensitivity, and greatly improves glucose tolerance. FASEB J. 2007;21: LB35–d–36.

180. Zhou M, Ouyang W. The function role of GATA-3 in Th1 and Th2 differentiation. Immunol Res. 2003;28: 25–37. doi:10.1385/IR:28:1:25

181. Ohno H, Shinoda K, Spiegelman BM, Kajimura S. PPARγ agonists induce a white-to-brown fat conversion through stabilization of PRDM16 protein. Cell Metab. 2012;15: 395–404. doi:10.1016/j.cmet.2012.01.019

182. Odegaard JI, Ricardo-Gonzalez RR, Goforth MH, Morel CR, Subramanian V, Mukundan L, et al. Macrophage-specific PPARgamma controls alternative activation and improves insulin resistance. Nature. 2007;447: 1116–20. doi:10.1038/nature05894

183. Trayhurn P, Introduction I. Hypoxia and Adipose Tissue Function and Dysfunction in Obesity. 2013; 1–21. doi:10.1152/physrev.00017.2012

184. Hosogai N, Fukuhara A, Oshima K, Miyata Y, Tanaka S, Furukawa S, et al. Adipose Tissue Hypoxia in Obesity and Its Impact on. 2007;56: 901–911. doi:10.2337/db06-0911

185. Hotamisligil GS. Inflammatory pathways and insulin action. Int J Obes Relat Metab Disord. 2003;27 Suppl 3: S53–5. doi:10.1038/sj.ijo.0802502

186. Maréchal P, Le Goff L, Hoffman W, Rapp J, Oswald IP, Ombrouck C, et al. Immune response to the filaria Litomosoides sigmodontis in susceptible and resistant mice. Parasite Immunol. 1997;19: 273–9.

187. Chang Y-H, Ho K-T, Lu S-H, Huang C-N, Shiau M-Y. Regulation of glucose/lipid metabolism and insulin sensitivity by interleukin-4. Int J Obes (Lond). Macmillan Publishers Limited; 2012;36: 993–8. doi:10.1038/ijo.2011.168

188. Jagannathan M, McDonnell M, Liang Y, Hasturk H, Hetzel J, Rubin D, et al. Toll-like receptors regulate B cell cytokine production in patients with diabetes. Diabetologia. 2010;53: 1461–71. doi:10.1007/s00125-010-1730-z

189. Martin RM, Brady JL, Lew AM. The need for IgG2c specific antiserum when isotyping antibodies from C57BL/6 and NOD mice. J Immunol Methods. 1998;212: 187–92.

190. O'Garra A, Chang R, Go N, Hastings R, Haughton G, Howard M. Ly-1 B (B-1) cells are the main source of B cell-derived interleukin 10. Eur J Immunol. 1992;22: 711–7. doi:10.1002/eji.1830220314

191. Griffin DO, Rothstein TL. Human “orchestrator” CD11b(+) B1 cells spontaneously secrete interleukin-10 and regulate T-cell activity. Mol Med. 2012;18: 1003–8. doi:10.2119/molmed.2012.00203

192. Yang Z, Grinchuk V, Smith A, Qin B, Bohl J a., Sun R, et al. Parasitic nematode-induced modulation of body weight and associated metabolic dysfunction in mouse models of obesity. Infect Immun. 2013;81: 1905–14. doi:10.1128/IAI.00053-13

193. Blagoev B, Kratchmarova I, Nielsen MM, Fernandez MM, Voldby J, Andersen JS, et al. Inhibition of adipocyte differentiation by resistin-like molecule alpha. Biochemical characterization of its oligomeric nature. J Biol Chem. 2002;277: 42011–6. doi:10.1074/jbc.M206975200

194. Pesce JT, Ramalingam TR, Wilson MS, Mentink-Kane MM, Thompson RW, Cheever AW, et al. Retnla (relmalpha/fizz1) suppresses helminth-induced Th2-type immunity. PLoS Pathog. 2009;5: e1000393. doi:10.1371/journal.ppat.1000393

195. Lawrence RA, Allen JE, Osborne J, Maizels RM. Adult and microfilarial stages of the filarial parasite Brugia malayi stimulate contrasting cytokine and Ig isotype responses in BALB/c mice. J Immunol. 1994;153: 1216–24.

196. Hübner MP, Pasche B, Kalaydjiev S, Soboslay PT, Lengeling A, Schulz-Key H, et al. Microfilariae of the filarial nematode Litomosoides sigmodontis exacerbate the course of lipopolysaccharide-induced sepsis in mice. Infect Immun. 2008;76: 1668–77. doi:10.1128/IAI.01042-07

197. Doetze A, Satoguina J, Burchard G, Rau T, Löliger C, Fleischer B, et al. Antigen-specific cellular hyporesponsiveness in a chronic human helminth infection is mediated by T(h)3/T(r)1-type cytokines IL-10 and transforming growth factor-beta but not by a T(h)1 to T(h)2 shift. Int Immunol. 2000;12: 623–630. doi:10.1093/intimm/12.5.623

198. Lehrke M, Lazar M a. The many faces of PPARgamma. Cell. 2005;123: 993–9. doi:10.1016/j.cell.2005.11.026

199. Lehmann JM, Moore LB, Smith-Oliver TA, Wilkison WO, Willson TM, Kliewer SA. An Antidiabetic Thiazolidinedione Is a High Affinity Ligand for Peroxisome Proliferator-activated Receptor (PPAR). J Biol Chem. 1995;270: 12953–12956. doi:10.1074/jbc.270.22.12953

200. Hevener AL, He W, Barak Y, Le J, Bandyopadhyay G, Olson P, et al. Muscle-specific Pparg deletion causes insulin resistance. Nat Med. 2003;9: 1491–7. doi:10.1038/nm956

201. Norris AW, Chen L, Fisher SJ, Szanto I, Ristow M, Jozsi AC, et al. Muscle-specific PPARgamma-deficient mice develop increased adiposity and insulin resistance but respond to thiazolidinediones. J Clin Invest. 2003;112: 608–18. doi:10.1172/JCI17305

202. Rangwala SM, Rhoades B, Shapiro JS, Rich AS, Kim JK, Shulman GI, et al. Genetic modulation of PPARgamma phosphorylation regulates insulin sensitivity. Dev Cell. 2003;5: 657–63.

203. He W, Barak Y, Hevener A, Olson P, Liao D, Le J, et al. Adipose-specific peroxisome proliferator-activated receptor gamma knockout causes insulin resistance in fat and liver but not in muscle. Proc Natl Acad Sci U S A. 2003;100: 15712–7. doi:10.1073/pnas.2536828100

204. Matsusue K, Haluzik M, Lambert G, Yim S-H, Gavrilova O, Ward JM, et al. Liver-specific disruption of PPARgamma in leptin-deficient mice improves fatty liver but aggravates diabetic phenotypes. J Clin Invest. 2003;111: 737–47. doi:10.1172/JCI17223

205. Nolan, J.J., Ludvik, B., Beerdsen, P., Joyce, M., and Olefsky J. Improvement in Glucose Tolerance and Insulin Resistance in Obese Subjects Treated with Troglitazone — NEJM. N Engl J Med. 1994;331: 1188–1193.

206. Welch JS, Ricote M, Akiyama TE, Gonzalez FJ, Glass CK. PPARgamma and PPARdelta negatively regulate specific subsets of lipopolysaccharide and IFN-gamma target genes in macrophages. Proc Natl Acad Sci U S A. 2003;100: 6712–7. doi:10.1073/pnas.1031789100

207. Moro K, Yamada T, Tanabe M, Takeuchi T, Ikawa T, Kawamoto H, et al. Innate production of T(H)2 cytokines by adipose tissue-associated c-Kit(+)Sca-1(+) lymphoid cells. Nature. Nature Publishing Group; 2010;463: 540–544. doi:10.1038/nature08636

208. Neill DR, Wong SH, Bellosi A, Flynn RJ, Daly M, Langford TK a, et al. Nuocytes represent a new innate effector leukocyte that mediates type-2 immunity. Nature. Nature Publishing Group; 2010;464: 1367–1370. doi:10.1038/nature08900

209. Molofsky AB, Nussbaum JC, Liang H, Dyken SJ Van, Cheng LE, Mohapatra A, et al. Innate lymphoid type 2 cells sustain visceral adipose tissue eosinophils and alternatively activated macrophages. J Exp Med. 2013;210: 535–49. doi:10.1084/jem.20121964

210. Cousin B, Cinti S, Morroni M, Raimbault S, Ricquier D, Pénicaud L, et al. Occurrence of brown adipocytes in rat white adipose tissue: molecular and morphological characterization. J Cell Sci. 1992;103 (Pt 4: 931–42.

211. Xue B, Coulter A, Rim JS, Koza RA, Kozak LP. Transcriptional synergy and the regulation of Ucp1 during brown adipocyte induction in white fat depots. Mol Cell Biol. 2005;25: 8311–22. doi:10.1128/MCB.25.18.8311-8322.2005

212. Ishibashi J, Seale P. Medicine. Beige can be slimming. Science. 2010;328: 1113–4. doi:10.1126/science.1190816

213. Seale P, Bjork B, Yang W, Kajimura S, Chin S, Kuang S, et al. PRDM16 controls a brown fat/skeletal muscle switch. Nature. Macmillan Publishers Limited. 2008;454: 961–7. doi:10.1038/nature07182

214. Cohen P, Levy JD, Zhang Y, Frontini A, Kolodin DP, Svensson KJ, et al. Ablation of PRDM16 and beige adipose causes metabolic dysfunction and a subcutaneous to visceral fat switch. Cell. 2014;156: 304–16. doi:10.1016/j.cell.2013.12.021

215. Thauvin-Robinet C, Auclair M, Duplomb L, Caron-Debarle M, Avila M, St-Onge J, et al. PIK3R1 mutations cause syndromic insulin resistance with lipoatrophy. Am J Hum Genet. 2013;93: 141–9. doi:10.1016/j.ajhg.2013.05.019

216. Downward J. Signal transduction. A target for PI(3) kinase. Nature. 1995;376: 553–4. doi:10.1038/376553a0

217. Zmuda-Trzebiatowska E, Oknianska A, Manganiello V, Degerman E. Role of PDE3B in insulin-induced glucose uptake, GLUT-4 translocation and lipogenesis in primary rat adipocytes. Cell Signal. 2006;18: 382–390. doi:10.1016/j.cellsig.2005.05.007

218. Ceddia RB, Somwar R, Maida A, Fang X, Bikopoulos G, Sweeney G. Globular adiponectin increases GLUT4 translocation and glucose uptake but reduces glycogen synthesis in rat skeletal muscle cells. Diabetologia. 2005;48: 132–9. doi:10.1007/s00125-004-1609-y

219. Wen H, Gris D, Lei Y, Jha S, Zhang L, Huang MT-H, et al. Fatty acid-induced NLRP3-ASC inflammasome activation interferes with insulin signaling. Nat Immunol. Nature Publishing Group; 2011;12: 408–15. doi:10.1038/ni.2022

220. Hoerauf A, Nissen-Pähle K, Schmetz C, Henkle-Dührsen K, Blaxter ML, Büttner DW, et al. Tetracycline therapy targets intracellular bacteria in the filarial nematode Litomosoides sigmodontis and results in filarial infertility. J Clin Invest. 1999;103: 11–8. doi:10.1172/JCI4768

5. Appendix

5.1 Table S1. Comparison of diabetes-related gene expression between *L.s.*-infected DIO (n=3) and uninfected DIO mice (n=3). The table lists fold changes for genes that exhibit at least a 1.5-fold change when EAT of *L.s.*-infected DIO mice is compared to EAT of uninfected DIO mice. Red fold changes indicate upregulated genes compared to controls, while blue fold changes highlight downregulated genes compared to controls. Statistical significant differences ($p < 0.05$) are shown in red color.

Gene Symbol	Fold Change HF *L.s* / HF Uninf.	t-Test p value
Ace	1.839	0.286823
Ccl5	4.4144	0.14551
Cd28	2.9259	0.116235
Ceacam1	3.1143	0.046104
Ctla4	21.0472	0.136601
Dpp4	2.0594	0.278991
Enpp1	2.0452	0.091382
Foxp3	1.7	0.458718
Glp1r	5.0358	0.270648
Icam1	2.0264	0.168345
Ifng	117.9656	0.214471
Il10	3.4396	0.190844
Il12b	2.4947	0.247776
Inppl1	14.5091	0.165306
Ins1	1.5286	0.43024
Irs1	1.6345	0.183127
Pck1	1.5716	0.070911
Pfkfb3	1.797	0.630151
Pik3cd	1.7681	0.177571
Ppara	1.5972	0.196131
Rab4a	2.0642	0.355155
Sell	3.4795	0.013394
Hnf1b	31.245	0.372507
Tnf	1.9349	0.225582
Adra1a	-1.7026	0.124435
Ccr2	-1.6258	0.600397
Cebpa	-1.9378	0.184165
Dusp4	-2.9508	0.042055
G6pc	-1.6561	0.332967
G6pd2	-2.8768	0.067003

Gpd1	-2.3968	0.04047
Hnf4a	-1.9112	0.407527
Igfbp5	-3.0549	0.086491
Il6	-5.9564	0.464393
Nos3	-2.0015	0.190899
Pparg	-1.7956	0.093176
Retn	-3.3507	0.128151
Serpine1	-3.6497	0.269378
Stxbp1	-7.5568	0.682317
Vamp3	-1.9786	0.151319
Vegfa	-1.8503	0.034739

5.2 Table S2. Comparison of diabetes-related gene expression between *L.s.*-infected mice (n=3) and uninfected mice (n=3) with normal chow diet. The table lists fold changes for genes that exhibit at least a 1.5-fold change when EAT of *L.s.*-infected and uninfected mice are compared. Red fold changes indicate upregulated genes compared to controls, while blue fold changes highlight downregulated genes compared to controls. Statistical significant differences ($p < 0.05$) are shown in red color

Genes	**Fold Change** NF *L.s.* / NF Uninf.	**t-Test p value**
Ccl5	4.9895	0.33484
Foxp3	10.3548	0.097135
Gcg	2.3223	0.131485
Hmox1	12.314	0.506217
Icam1	2.1768	0.295093
Ifng	8.9728	0.27438
Il10	2.559	0.342021
Il6	2.8723	0.395458
Retn	3.361	0.659846
Sell	2.1124	0.378368
Srebf1	2.879	0.818365
Tnf	3.3378	0.290015
Tnfrsf1a	16.2859	0.740888
Ace	-3.0478	0.054201
Acly	-1.9244	0.810571
Adrb3	-1.8291	0.507211
Agt	-1.6485	0.970347
Akt2	-1.622	0.529489

Aqp2	-1.8675	0.290219
Cebpa	-1.6523	0.718491
Dpp4	-3.148	0.07046
Foxc2	-1.6108	0.861539
G6pc	-4.9398	0.338341
G6pd2	-2.8968	0.278797
Gcgr	-1.7264	0.586311
Gpd1	-1.9786	0.977361
Gsk3b	-1.8418	0.25342
Hnf4a	-2.5867	0.189191
Igfbp5	-3.3275	0.063823
Irs1	-1.6371	0.342047
Nos3	-8.2885	0.886111
Nrf1	-9.0701	0.078861
Pck1	-2.2106	0.431709
Pik3r1	-2.0201	0.500968
Ppara	-2.1255	0.476968
Pparg	-2.2415	0.30708
Ppargc1a	-1.6108	0.583102
Pygl	-1.8461	0.358524
Serpine1	-3.3045	0.321022
Sod2	-1.6071	0.218434
Trib3	-1.6034	0.370869
Vamp2	-1.7627	0.178702
Vapa	-1.5169	0.260782

5.3 Table S3. Comparison of diabetes-related gene expression between LsAg-treated (n=10) and PBS-treated (n=8) mice receiving a high fat diet. Displayed are fold-changes and p-values of genes expressed in EAT derived from LsAg-treated DIO mice in comparison to PBS-treated DIO controls (cut off 1.3 fold change). Upregulated genes are indicated in red, downregulated genes are presented in blue. P-values < 0.05 are presented in red.

Gene Symbol	Fold Regulation	p-value
Srebf1	1.7578	0.004987
Fasn	1.9762	0.012098
Pdk2	1.8898	0.018928
Lpl	1.3601	0.019036
Pde3b	2.0122	0.021991
Pik3r1	1.6676	0.022137
Acaca	1.9585	0.026172
Adipor2	1.5754	0.027524

Ifng	1.4993	0.033234
Hk2	1.4661	0.034874
Gys1	1.6865	0.036739
Slc2a4	2.2199	0.037317
Pparg	1.4492	0.038214
Cd3e	2.0234	0.043157
Fabp4	1.627	0.04822
Chuk	1.6055	0.056951
Vldlr	1.3599	0.061409
Rps6kb1	1.3412	0.065711
Retn	2.371	0.072863
Lipe	1.68	0.078575
Ccr4	2.7193	0.103747
Irs1	1.4835	0.116958
Scd1	2.6624	0.13008
Pck1	2.7401	0.136777
Irs2	1.3837	0.14121
Lep	1.4241	0.149471
Ppargc1a	1.9275	0.156765
Il18r1	1.5867	0.163892
Rbp4	2.1641	0.168106
Adipoq	1.9242	0.183023
Ppara	1.3482	0.191082
Acacb	1.6558	0.201308
Ccr6	2.8333	0.232769
Pdx1	1.5559	0.307193
Il23r	1.6194	0.490008
Mapk9	1.3777	0.903007
Emr1	-2.482	0.05594
Serpine1	-1.9053	0.059855
Pycard	-1.6754	0.09398
Casp1	-1.4184	0.113289
Tnfrsf1b	-1.6609	0.168709
Nlrp3	-1.6737	0.176981
Cxcr4	-1.4974	0.183075
Tnf	-1.5294	0.237718
Crlf2	-1.34	0.26139
Ccr5	-1.6716	0.421126
Il6	-1.5268	0.580275

5.4 Table S4. The list of primer sequences used in experiment

Gene	Forward ('5---3')	Reverse ('5---3')
mouse Arginase 1	CCTATGTGTCATTTGGGTGGA	CAGGAGAAAGGACACAGGTTG
mouse Foxp3	TCTTGCCAAGCTGGAAGACT	GGGGTTCAAGGAAGAAGAGG
mouse IL-10	GGTTGCCAAGCCTTATCGGA	ACCTGCTCCACTGCCTTGCT
mouse IL-5	AGCACAGTGGTGAAAGAGACCTT	TCCAATGCATAGCTGGTGATT
mouse IL-4	ACAGGAGAAGGGACGCCAT	GAAGCCCTACAGACGAGCTCA
mouse Gata3	GTCATCCCTGAGCCACATCT	AGGGCTCTGCCTCTCTAACC
mouse Ucp1	CTGCCAGGACAGTACCCAAG	TCAGCTGTTCAAAGCACACA
mouse β-Actin	AGAGGGAAATCGTGCGTGAC	CAATAGTGATGACCTGGCGGT

List of abbreviations

AAM	alternatively activated macrophages
Acaca	Acetyl-Coenzyme A carboxylase alpha
Adipoq	adiponectin
Adipor	Adiponectin receptor
ALT	abundant larval transcript
AP1	activator protein 1
aP2	adipocyte Protein-2
APC	antigen–presenting cells
arg1	Arginase1
AUC	area under the curve
BSA	bovine serum albumin
B2M	beta-2-microglobulin
Cebpa	CCAAT/enhancer binding protein alpha
CAM	classically activated macrophages
cAMP	cyclic Adenosine Monophosphate
Ca	calsium
Casp1	Caspase1
CCL	chemokine (C-C motif) ligand
Ccr4	Chemokine (C-C motif) receptor 4
Cd	cluster of differentiation
Cd3e	CD3 antigen, epsilon polypeptide
cDNA	complementary DNA
Ceacam1	Carcinoembryonic antigen-related cell adhesion molecule 1
CPI	cysteine proteinase inhibitor
Ctla4	cytotoxic T-lymphocyte-associated protein 4
Cxcr4	C–X–C chemokine receptor type 4
DEC	diethyl carbamazine
DIO	diet-induced obese
DMEM	Dulbecco's Modified Eagle Medium
DMSO	Dimethyl sulfoxide
DNA	Deoxyribonucleic Acid
dNTP	Deoxynucleotide
dpi	days post infection
DSS	Dextran sulfate sodium
Dusp4	dual specificity phosphatase 4
EAT	Epididymal adipose tissue
EDTA	Ethylenediaminetetraacetic acid
ELISA	Enzyme-linked immunosorbent assay
Emr1	epidermal growth factor module-containing mucin-like receptor 1
Enpp1	Ectonucleotide pyrophosphatase/phosphodiesterase 1
EPO	eosinophil peroxidase

ER	endoplasmic reticulum
ES	Excretory secretory
Fabp4	Fatty acid binding protein 4
FACS	Fluorescence-Activated Cell Sorter
Fasn	Fatty acid synthase
Fc	fragment crystallizable
FFA	Free fatty acid
Fig.	Figure
FITC	Fluorescein isothiocyanate
Foxp3	forkhead–winged-helix transcription factor-3
FSC	Forward scatter
GAPDH	Glyceraldehyde 3-phosphate dehydrogenase
Gata3	GATA binding protein 3
GITR	glucocorticoid-induced TNF receptor
Glut4	Glucose transporter type 4
Gpd1	glycerol-3-phosphate dehydrogenase-1
Gpdh	Glycerol-3-phosphate dehydrogenase
GTT	Glucose tolerance test
Gys	Glycogen synthase 1
G6pd	Glucose-6-phosphate dehydrogenase
Hb	hemoglobin
HEPES	N-2-Hydroxyethylpiperazine-N'-2-Ethanesulfonic Acid
HF	high fat
Hk2	Hexokinase-2
HOMAIR	homeostatic model assessment for insulin resistance
HRP	horseradish peroxidase
i.p	intra peritoneal
Icam1	intercellular adhesion molecule 1
IDF	International Diabetes Federation
Ifng	Interferon gamma
IKKβ	IκBα kinase β
IL-4Rα	IL-4 receptor-alpha
ILC2	type 2 innate lymphoid cells
iNOS	inducible nitric oxide synthase
Irs1	Insulin receptor substrate 1
Irs2	Insulin receptor substrate 2
iTreg	inducible Treg
ITT	Insulin tolerance test
L	Larvae
L.s	*Litomosoides sigmodontis*
Lpl	Lipoprotein lipase
LsAg	Litomosoides sigmodontis antigen
M	molar
MBP	major basic protein
MCP	monocyte chemotactic protein
mf	microfilariae

Mg	magnesium
MHC	major histocompatibility complex
mM	mili molar
MS	Multiple sclerosis
µl	micro liter
µm	micro meter
Nlrp3	NLR family, pyrin domain containing 3
nm	nano meter
NO	nitric oxide
NOD	non obese diabetic
Nos3	nitric oxide synthase 3
Nrf1	nuclear factor (erythroid-derived 2)-like 1
O. bacoti	*Ornithonyssus bacoti*
OD	optical density
PAI	Plasminogen activator Inhibitor
PBS	Phosphat Buffer Saline
Pck1	phosphoenolpyruvate carboxykinase 1
PCR	polymerase chain reaction
Pde3b	phosphodiesterase 3B
Pdk2	Pyruvate dehydrogenase kinase, isoenzyme 2
PE	phycoerythrin
PGC-1β	peroxisome proliferator-activated receptor gamma coactivator 1β
PI3Ks	phosphatidylinositol 3 kinases
Pik3cd	phosphoinositide-3-kinase, catalytic, delta polypeptide
Pik3r1	Phosphatidylinositol 3-kinase, regulatory subunit, polypeptide 1 (p85 alpha)
Ppara	Peroxisome Proliferator-Activated Receptor Alpha
Pparg	Peroxisome proliferator activated receptor gamma
PRDM16	PRD1-BF-1-RIZ1 homologous domain containing protein-16
Pycard	PYD and CARD domain containing
qPCR	quantitative real-time polymerase chain reaction
RELMα	Resistin-like molecule α
RNA	ribonucleic acid
ROS	reactive oxygen species
rpm	rotations per minute
RQI	RNA quality indicator
RT	room temperature
ScAT	Subcutaneous adipose tissue
SEA	soluble egg antigen
Sell	Selectin L
Serpine1	Serine (or cysteine) peptidase inhibitor, clade E, member 1
Slc2a4	Solute carrier family 2 (facilitated glucose transporter), member 4
Srebf1	Sterol regulatory element binding transcription factor 1
SSC	Side scatter
ß-islet	beta islet
STAT6	signal transducer and activator of transcription 6

STH	Soil-transmitted helminth
SVF	stromal vascular fraction
SWA	soluble worm antigen
T1D	type 1 diabetes
T2D	type 2 diabetes
TG	Triglyceride
TGF-ß	transforming growth factor beta
Tlr	Toll-like receptor
TMB	tetramethylbenzidine
Tnfrsf1b	tumor necrosis factor receptor superfamily member 1B
Uninf.	uninfected
Vamp2	vesicle-associated membrane protein 2
VAT	Visceral adipose tissue
Vegf	Vascular endothelial growth factor
VLDL	very low density lipoproteins
Vldlr	Very low density lipoprotein receptor
w/v	weight per volume ratio
wpi	weeks post infection
WT	wild type
#	number/count
˚C	degree celcius

Acknowledgements

I would like to express my deepest gratitude to Prof. Dr. Achim Hoerauf (Director: Institute for Medical Microbiology, Immunology and Parasitology (IMMIP)), Bonn, for giving me the opportunity to work on this project, and to my group leader Dr. Marc Hübner for his full support and direction during my studies.

I would like to thank Prof. Dr. Sven Burgdorf (co-supervisor), PD Dr. Gerhild van Echten-Deckert and Prof. Dr. Dorothea Barthels for being in the committee board for my thesis defense.

I would also like to express my deepest appreciation to Dr. Fabian Gondorf, Jesuthas Ajendra, Benedikt Buerfent, Khaldoun Aslan, Ajeng Pratiwi, David Schmidt, Anna-Lena Neumann and Dr. Surendar Jayagopi for their assistance during my experiments. I am grateful to PD Dr. Sabine Specht, Dr. Laura Layland, Dr. Kenneth Pfarr, Dr. Beatrix Schumak, Dr. Tomabu Ajobimey, Kwame Kwarteng, Dr. Muhsin Gani, Dr. Christian Lentz, Stefan Frohberger, Alexandra Ehrens, Wiebke Stamminger, Bettina Dubben, Marianne Koschel and Martina Fendler for their support and advice. I am also thankful to all the other members from the AG Specht, AG Pfarr, AG Layland, AG Schumak and AG Adjobimey as well as colleagues at IMMIP.

I would like to thank Prof. Dr. Alexander Pfeifer and Dr. Linda S. Hoffmann (Institute of Pharmacology and Toxicology Uniklinikum Bonn) for collaboration in this project.

I am also immensely grateful to my family and my colleagues in the Faculty of Medicine Universitas Padjadjaran Bandung Indonesia for their morale support during my studies.

Finally, I would like to thank DAAD (Germany Academic Exchange Service) for financial support during my stay in Germany and to the BONFOR Forschungsforderprogramm and Marie Curie Actions of the European Union’s Seventh Framework Programme for funding this research project.